The Thesis Committee for Calvin M. Eberle
Certifies that this is the approved version of the following thesis:

An Investigation Into Surfactant Stabilized, Non-Aqueous and Semi-Aqueous Foam for Enhanced Oil Recovery

APPROVED BY
SUPERVISING COMMITTEE:

Supervisor:

Quoc P. Nguyen

Nhut M. Nguyen

An Investigation Into Surfactant Stabilized, Non-Aqueous and Semi-Aqueous Foam for Enhanced Oil Recovery

by

Calvin M. Eberle

Thesis

Presented to the Faculty of the Graduate School of

The University of Texas at Austin

in Partial Fulfillment

of the Requirements

for the Degree of

Master of Science in Engineering

The University of Texas at Austin

August 2017

Dedication

To my family and friends, without whom, this thesis would never have been completed.

Acknowledgements

I would like to thank and acknowledge Dr. Quoc P. Nguyen for his guidance and insight throughout this project. I would also like to thank Dr. Nhut M. Nguyen for passing on all of his experience in the lab and for enduring my constant requests for new equipment. I would like to give additional praise to all of the members of the team who contributed to this work in some way: Greg, Lee, Connor, Heather, Taylor, Andres, Stephan, Ben, Ye, Marilena, Brandon, Hanwei, Alolika, Oualid, Eric, Galang, Litan, Neha, Vence, Litan, and Vu.

Abstract

An Investigation Into Surfactant Stabilized, Non-Aqueous and Semi-Aqueous Foam for Enhanced Oil Recovery

Calvin M. Eberle, MSE

The University of Texas at Austin, 2017

Supervisor: Quoc P. Nguyen

Foam serves as an important role in enhanced oil recovery processes involving gas injection since it hinders flow and acts as a mobility control agent. Significant work has been presented for the utilization of water as the continuous, external phase of the foam, but opportunity exists in using a non-aqueous compound instead.

Y-grade, a raw blend of NGLs, has been becoming more available with the increase in wet gas, shale plays over the last decade. Coinjecting or alternating the injection of nitrogen and y-grade with a foam stabilizing additive, such as a surfactant, may provide a recovery scheme with both a strong displacement efficiency due to the miscible nature of the y-grade with oil and a strong sweep efficiency due to the mobility control provided by the y-grade-based foam.

The foaming ability of y-grade was investigated by using pentane as a stand-in since it is the lightest alkane that is still readily a liquid at room conditions. Thirty-eight additives spanning a wide range of chemical properties were evaluated for their potential

to generate and stabilize the non-aqueous foam. In addition, both water and non-aqueous liquids were investigated to see if they would increase the foaming potential of the y-grade or pentane by being mixed as a secondary component.

Concurrently, a procedure and experimental assembly was created to blend a synthetic y-grade containing ethane through octane. This synthetic y-grade was used to validate the assumptions made in the pentane screening tests by further blending in nitrogen, water, and other additives into pressurized visual cells for observation. In addition, the y-grade was used in a coreflood as a base case for a planned series of tests for y-grade-based foam within a porous media for oil recovery purposes.

Table of Contents

List of Tables

List of Figures

Chapter 1: Introduction

The chapter provides background information about the use of foam-assisted enhanced oil recovery (EOR) methods in addition to the potential of using novel, non-aqueous foam in future operations. The chapter continues with an outline for the research objectives of the conducted work as well as outlines for subsequent chapters.

1.1 Overview

Foam serves several important roles within petroleum engineering operations to increase ultimate recovery from a field and decrease recovery time within a single well. Immiscible gas injection into a reservoir is a well-established EOR technique, but it typically suffers from poor sweep efficiency due to the injected gas phase having a much higher mobility than the water and oil already present within the reservoir. The low viscosity of the injected gas means that the gas will finger through the reservoir and leave large pockets of oil untouched. However, an alternating injection of gas and water with surfactant will generate foam under the proper conditions which will serve to reduce the relative mobility of the gas phase and lead to a better sweep efficiency especially close to the injection wellbore. The injection rates, surfactant concentration, and salinity of the water phase all play an important role in the generation of strong foam, and how these parameters affect recovery is still an active area of research.

While foam with water as the continuous, external phase has already proven to be an effective means of mobility control for immiscible gas injection, the novel idea of replacing the injected water with a liquid that would be miscible with the oil present within the reservoir has some theoretical advantages. First, using a coinjection or alternating injection strategy of nitrogen gas and some light, miscible liquid would allow the liquid phase to interact with the oil in place similar to a high-pressure CO_2 flood. The oil in place would expand due to the presence of the injected hydrocarbons, and the displacement efficiency of the system would be increased compared to a water-nitrogen injection. Secondly, the presence of nitrogen and some stabilizing additive such as a

surfactant would reduce the amount of light hydrocarbon liquid that would need to be injected and produce the benefits of a better sweep efficiency associated with a foam flood. Finally, the oil phase combining with the injected hydrocarbon phase may increase the stability of the foam allowing for further propagation of the foam into the reservoir which is not always the case with water-based foams.

1.2 RESEARCH OBJECTIVES

The goal of this work is to investigate the foaming abilities of a y-grade-nitrogen system that might be used for EOR purposes. In order to do so, potential foam-enhancing additives need to be examined to determine the most effective type of additive as well as optimum additive concentration. Secondary objectives included reducing or eliminating the presence of water within the system to create a completely non-aqueous foam, building experimental assemblies to create a synthetic y-grade blend in-house, and investigating the properties of non-aqueous compounds that may be added to the y-grade solution that would improve the foaming potential.

1.3 DESCRIPTION OF CHAPTERS

Chapter 2: This chapter is a literature review of the fundamentals of enhanced oil recovery, conventional nitrogen flooding without foam, the principles governing the generation and stabilization of bulk foam, and the flow of foam through a porous media.

Chapter 3: To produce foam with a solution of alkanes with a relatively low average molecular weight, 38 additives were tested with pentane, pentane plus deionized (DI) water, and diesel fuel. Pentane was used as a stand in for y-grade since pentane largely remains a liquid under room temperature and pressure unlike y-grade which evaporates quickly. Adding a bit of DI water to the pentane provided further insight into how a y-grade based foam could be stabilized. Our research objective stated that water should be minimized or removed entirely to create a completely non-aqueous foam. Since diesel fuel can readily create foam without the addition of supporting additives such as surfactants, an investigation of which additive would further enhance diesel fuel's

foaming potential could possibly lead to a method to produce more stable y-grade based foam.

Chapter 4: Results from the pentane screening process indicated that it would be highly unlikely for y-grade to produce a stable foam with any of the additives to which we had access. However, the positive results from the diesel fuel screening led to further investigation into what compound within the diesel fuel might be the cause of high foaming potential. Several substances were tested in a similar manner to the previous screening experiment, but only the six best additives were investigated for each compound. It was believed that if a specific compound was identified as having a very high foaming potential with one or more of the six select additives, this compound could be mixed with y-grade or pentane to increase their foaming ability.

Chapter 5: Once the solvents and additives that had high foaming potential were identified, they needed to be combined with pentane to see if they would still yield positive results. The product was a mixture with pentane as the primary component, some secondary component with a high foaming potential, and an additive, such as surfactant, to allow foam generation and stabilization. The volume fraction of these secondary compounds was then reduced as much as possible to see how low the volume fraction could be taken to still allow stable foam to be created. Since the main goal of this research project was to create a y-grade-based foam, reducing the amount of all components that were not y-grade was necessary.

Chapter 6: While the two previous chapters largely focused on completely non-aqueous foam, positive results from the pentane plus water screening process indicated that a very stable foam could be generated if water and certain surfactants were present within the system. Since water would naturally be present within the reservoir, it was prudent to see if it might be utilized to create a strong, stable foam. Several tests were performed including analysis to minimize water fraction and surfactant concentration, a test to see how salinity might inhibit foaming potential, and a cloud-point test on one of the nonionic surfactants that stabilized the semi-aqueous foam.

Chapter 7: While the properties of the 38 additives and many possible secondary components were being explored, work was being done to create an assembly that would allow for the synthesis of a y-grade blend within the laboratory. Having the ability to create a synthetic y-grade instead of ordering it from a third-party allowed to significantly cut down on the lead time for the y-grade to be available, and users had the ability to change the blend's composition if needed. To ensure an accurate synthesis of the y-grade, phase behavior analysis of the full y-grade mixture and of each component was performed, and an intensive set up was created.

Chapter 8: Once the y-grade was properly synthesized, it needed to be blended with a foam-stabilizing additive, pure nitrogen, and any foam-enhancing secondary component. The ratio of y-grade, additive, secondary component, and nitrogen to each other would be the same in any eventual corefloods, so this could be thought of as a static test of the blend's ability to create bulk foam outside of a porous media. If foam could be generated here, the high-shear environment of an N_2-y-grade injection would likely also produce stable foam. A new set up was designed and constructed to combine the required components in a high-pressure visual cell to see if any stable foam was generated.

Chapter 9: The high foaming potential of pentane-based foam seen in test vials needed to be translated into flow inhibition within a porous media. To test the ability of the foam inside a porous media, a coreflood was performed with pure y-grade displacing crude oil from a limestone core sample. This coreflood would serve as the base case in a future series of tests designed to see how the presence of non-aqueous foam can increase the pressure drop observed across the core and, hopefully, increasing oil recovery.

Chapter 10: This chapter summarizes the conclusions reached throughout the entire project. In addition, recommendations on future work are given that would allow this technology to be further explored.

Chapter 2: Literature Review

A review of relevant literature on the topics relating to non-aqueous and semi-aqueous foam injection is presented here. Topics include the conventional use of nitrogen floods without the presence of foam through the lens of EOR, the principles of bulk foam used highly within this project, the fundamentals of foam in porous media since using foam for EOR was the ultimate goal.

2.1 Fundamentals of Enhanced Oil Recovery

Enhanced oil recovery can roughly be defined as the injection of materials not present within the reservoir at initial conditions. This definition must be interpreted liberally because in some thermal techniques such as steam injection or solvent methods such as CO_2 flooding, some amount of water or CO_2 is usually present within the reservoir, but the phase or quantity being injected is what matters. Waterflooding has sometimes been categorized as an EOR technique, but is often excluded since water is already present within the reservoir in considerable quantities, and excluding the process draws a more distinct line between secondary and tertiary recovery phases (Egbogah 1985).

The effectiveness of any EOR process is dictated by its recovery efficiency, E_R, which is simply a ratio of how much oil was recovered to the amount of oil in place when the process began.

$$E_R = \frac{Amount\ of\ oil\ displaced}{Oil\ in\ place}$$

Since it is not possible to produce more oil than there actually is within the reservoir, this number is always between 0 and 1. This appears as a simple concept, but the equation can be broken down further into having E_R being a function of displacement efficiency, E_D, and sweep efficiency, E_S (Lake 2014).

$$E_R = E_D E_S$$

These two terms can be used to explain why some EOR processes perform better in certain environment than others and how there is no perfect EOR technique since an increase in one efficiency usually leads to a decrease in the other.

Displacement efficiency is a ratio of the amount of oil displaced to the amount of oil that was contacted by the displacing fluid.

$$E_D = \frac{Amount\ of\ oil\ displaced}{Amount\ of\ oil\ contacted\ by\ displacing\ fluid}$$

Displacement efficiency is always between 0 and 1 as any injection will result in some oil being contacted and displaced, but the displacing fluid will never be able to mobilize all of the oil that it contacts within the reservoir since some is lost to residual oil. This value can be more accurately described in relation to irreducible water saturation and residual oil saturation.

$$E_D = \frac{1 - S_{or} - S_{wi}}{1 - S_{wi}}$$

Where

$$S_{or} = saturation\ of\ residual\ oil$$

$$S_{wi} = saturation\ of\ irriducible\ water$$

This equation states that to increase the displacement efficiency of a process, the amount of oil that is leftover because it is unobtainable must be lowered.

The displacement efficiency depends upon the ratio of viscous forces to capillary forces within the fluids, which is the capillary number, N_c (Sam Saren 1992).

$$N_c = \frac{u_{Inj} * \mu_{Inj}}{\sigma}$$

Where

$$u_{inj} = superficial\ velocity\ of\ injected\ fluid$$

$$\mu_{inj} = dynamic\ viscosity\ of\ injected\ fluid$$

$$\sigma = Interfacial\ tension\ (IFT)\ between\ injected\ and\ displaced\ fluids$$

Other definitions exist for capillary number that include buoyancy effects and multiphase flow, but this is the simplest that is applicable in high level evaluations. Having the viscous forces dominate over the capillary forces is preferred for oil recovery, so higher capillary numbers are better. Thus, processes that can quickly inject a rather viscous fluid with low IFT will be most successful. Unfortunately, the velocity and viscosity term often negate each other as viscous fluids cannot be injected at high velocities, so the IFT term is the driving factor for a high capillary number. The capillary number has also been shown to be effected by the pore size distribution of the reservoir, wettability, and whether the conventional reservoir is sandstone or carbonate (Sam Sarem 1992).

The second term to calculate overall recovery efficiency is volumetric sweep efficiency, E_S.

$$E_S = \frac{Amount\ of\ oil\ contacted\ by\ displacing\ fluid}{Oil\ in\ place}$$

This term can further be broken down into the product of vertical sweep efficiency which is heavily dependent upon the layering of the reservoir and areal sweep efficiency dependent on large heterogeneities such as faults within the reservoir.

Like displacement efficiency, the sweep efficiency is always between 0 and 1 since it is not physically possible to contact more oil than is present within the reservoir. Similarly, displacement efficiency and capillary number can be characterized by the mobility ratio, M, between the injected and displaced fluids.

$$M = \frac{k_{rel,Inj} * \mu_{dis}}{k_{rel,dis} * \mu_{Inj}}$$

Where

$$k_{rel,Inj} = relative\ permeability\ of\ the\ injected\ fluid$$

$$k_{rel,dis} = relative\ permeability\ of\ the\ injected\ fluid$$

$$\mu_{dis} = displaced\ fluid\ viscosity$$

$$\mu_{Inj} = injected\ fluid\ viscosity$$

This function takes into account the rock properties and saturation of each phase through the relative permeabilities and the viscous forces of each of the displaced and injected fluid.

For a high oil recovery, a piston-like displacement works the best since the maximum amount of displaced fluid will be reached before the displacing fluid breaks through at a production well. Mobility ratios greater than one will exhibit instability and viscous fingering which will cause the displacing fluid to preferentially flow to already contacted zones. A mobility ratio less than zero will yield a much better sweep of the reservoir. A visual representation of areal sweep efficiency is shown in Figure 2.1.

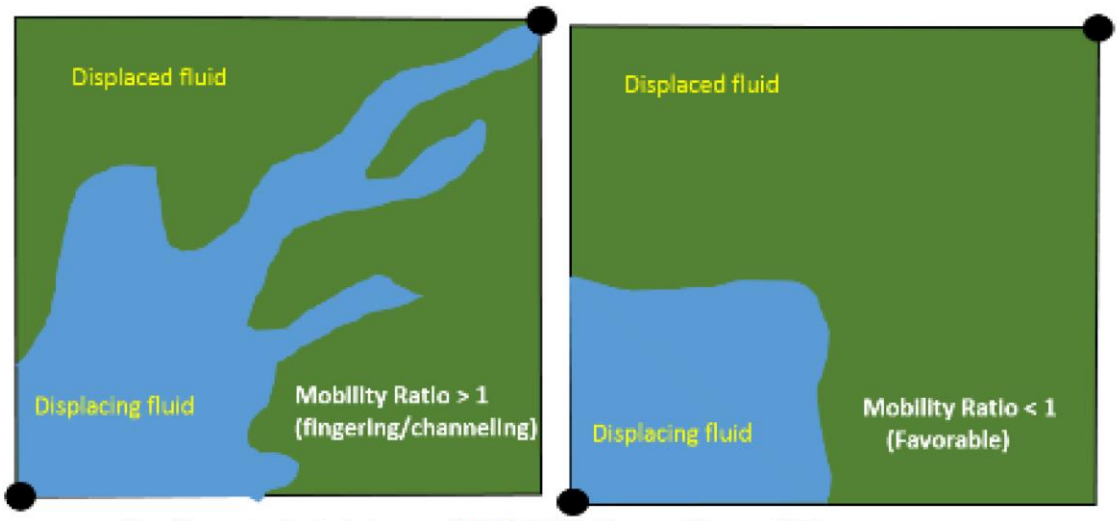

http://large.stanford.edu/courses/2015/ph240/aldousary1/images/f2big.png

Figure 2.1: Visualization of sweep efficiency

Since both displacement and sweep efficiency are less than unity, multiplying the two numbers together yields an even lower result meaning that a process that has a very good displacement efficiency can still be hampered by a poor sweep and vice versa. The relationship between these two efficiencies characterized by capillary number and mobility ratio will become apparent.

2.2 CONVENTIONAL NITROGEN INJECTION

Injecting nitrogen into a petroleum reservoir is a common and well-established method of EOR. Like every type of gas injection, the nitrogen flood can be characterized as either miscible where the nitrogen readily interacts with the oil in place or as immiscible where the nitrogen and oil phases remain relatively separate. Whether a nitrogen flood is miscible or immiscible is determined by if the gas is being injected below or above the minimum miscibility pressure (MMP) (Al-Anazi 2007). The MMP of an injected fluid is dependent upon the composition and saturation of the reservoir fluids and the temperature of the reservoir.

Below the MMP, nitrogen is immiscible with the reservoir fluids, and this method of EOR is limited in its usage due to nitrogen's poor performance. Injecting nitrogen below the MMP mimics a waterflood where the immiscible fluid is used for pressure maintenance and to drive a limited amount of oil towards producing wells. Examples do exist of immiscible nitrogen being used in conjunction with traditional waterfloods, but these processes are typically done as a last resort if CO_2 or natural gas is not available (Slack 1981).

Above the MMP, the injected nitrogen is considered to be miscible with the oil in place and represents a much more effective EOR method. In miscible gas processes, recovery is increased due to the lighter components within the oil phase being transferred or vaporized to the gas phase or the gas being condensed into the liquid phase. Several contacts between the injected gas and the reservoir oil is often observed leading to multiple oil banks of different compositions depending upon which lighter components have already been stripped from the oil. No discrete interface between the injected and reservoir fluids is observed (Glaso 1990). Miscible gas processes are able to increase recovery by swelling the oil to mobilize isolated pockets of residual oil, decreasing the viscosity of the oil phase if the miscible gas dissolves into the liquid, or through a vaporization drive where the lighter components of the oil are transferred to the gas phase and mobilized. In most reservoirs, the MMP of nitrogen for the reservoir fluids is too

high to allow for miscibility which restricts the usage of miscible nitrogen floods to offshore and high pressure applications (Heucke 2015).

Nitrogen floods can be related back to the two guiding principles for EOR: capillary number and mobility ratio. For an effective EOR process, capillary number should be high while mobility ratio is ideally less than 0. Nitrogen has a very low viscosity compared to other commonly injected fluids such as water, and the IFT between nitrogen and oil tends to be high especially at conditions far below MMP, because of these two factors, the capillary number is low and contacted oil is not easily displaced. The low velocity of nitrogen also leads to a high mobility ratio and uneven displacement occurs where the nitrogen does not create an effective, piston-like sweep of the reservoir. Overall, the recovery efficiency of a nitrogen flood is low. Foam, however, can solve these problems.

2.3 PRINCIPLES OF BULK FOAM

Outside of a porous media, foam is most familiar as a bulk phase of many bubbles stacked together. This bulk phase is a colloidal dispersion where gas, forming an internal phase, is most often dispersed within a liquid, the continuous, external phase. Figure 2.2 shows a 2-D example of bulk foam as one would see with in the head of beer or in soapy water (Schramm 1994). Free gas and liquid lie above and below the bulk foam phase which is comprised of both fluids. The gas bubbles are surrounded by the liquid phase situated into thin films which meet at 120 degrees. The entirety of the thin film region and the two interfaces on either side of the thin film is referred as a lamella. The lamellae meet at a plateau border at their ends. The thickness and stability of the lamella is what allows for a stable, long lasting foam.

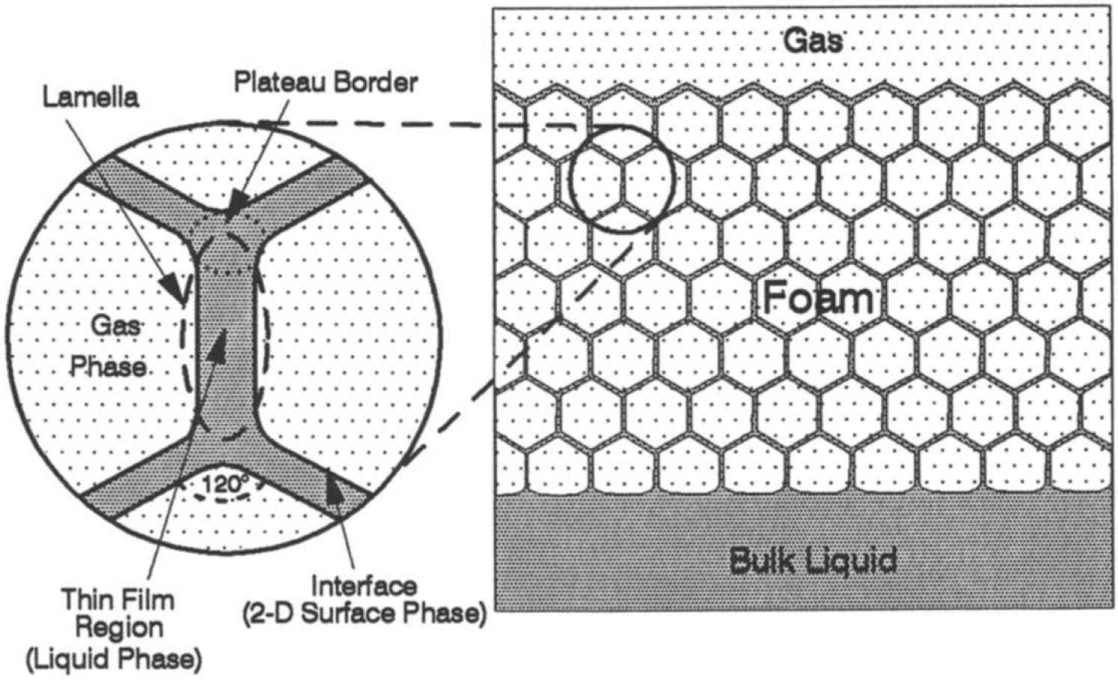

Figure 2.2: Bulk foam and lamella

Bulk foam is created by any gas passing through a liquid at a rate higher than the rate at which the liquid flows out of the lamellae. To this extent, foam can either be designated as wet or dry depending upon the shape of the bubbles which is ultimately related to the ratio of gas to liquid with the foam. A wet foam will have larger lamellae separating the individual bubbles which take a spherical shape. A dry foam will form polyhedral shapes due to the 120 degrees at which the lamellae meet. Often, a wet foam will turn into a dry foam as gravity and other effects discussed later drain the liquid outward causing the two sides of the lamella to collapse inward.

After the lamella is formed in a dry foam, there exists a difference in the radius of curvature between the center of the lamella and the plateau border. By the Young-Laplace equation, liquid is drawn from the lamella with a high radius of curvature to plateau borders with a lower curvature since curvature and surface tension dictate the pressure gradient within the liquid phase of the dispersion.

This process of films being drained due to the principles of the Young-Laplace equations is shown in Figure 2.3. The pressure of the internal, trapped gas phase, P_G, is higher than that of the liquid phase, but the bubble is held together by surface tension. Since the dry foam forms a polyhedral rather than a perfect sphere, two distinct curvatures exist. The lamella will have one curvature since its effective radius, R_{1A}, is much larger than the effective radius at the plateau border, R_{1B}. The differences in curvature lead to a higher pressure within the lamella, P_A, compared to the plateau border, P_B, and the thin film loses liquid as it moves away due to convection.

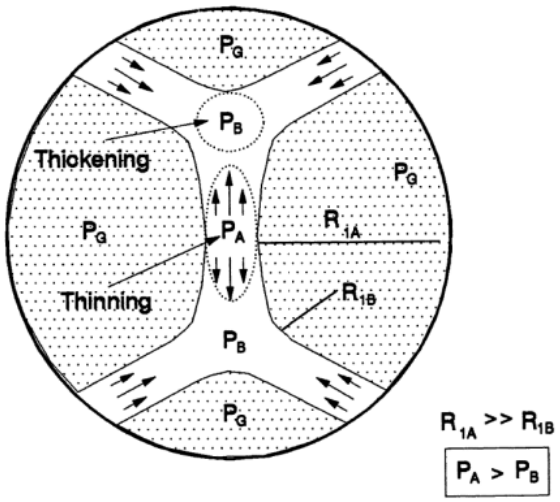

Figure 2.3: Lamellae drainage

In addition, Van Der Waals forces on either side of the lamella squeeze the film together. As liquid leaves the lamella by this capillary drainage, the film thins to a point where electrostatic forces from a surfactant are strong enough to resist further thinning. The convection of liquid out of the lamella carries surfactant out while dispersion carries the surfactant back in leading to "stable" foam. However, foam is inherently thermodynamically unstable and will eventually collapse with time.

Surfactants, or surface acting agents, can act to reduce the surface tension which can lower the pressure gradient within the lamellae. Surfactants are typically a compound

with one part having an affinity for polar compounds such as water and another part having an affinity for non-polar compounds. Whenever surfactants are present within a foam, they typically align on the gas-liquid interface creating a monolayer of surfactant. This monolayer establishes a repulsive force between the two sides of the lamella since parts of the molecules with the same partial charge are being forced together. This force serves to stabilize the foam and push against the thinning caused by liquid convection out of the film. Think of two magnets with the same polarity being forced together, they repel each other.

Bulk foam can be used to estimate and observe the strength of a surfactant and fluid combination for foam generation and stabilization. For the purposes of this project, foam potential will be defined as how much foam is generated under a fixed amount of shear for a fixed duration and how stabilized this foam is against capillary drainage and destruction over time. A high bulk foam potential is hoped to be transferred into a strong performance within a porous media.

2.4 FOAM IN POROUS MEDIA

2.4.1 Nature of Foam in a Porous Media

To understand foam within a porous media requires knowledge on how the lamella stabilize and coalesce as pore-network scale parameters such as capillary pressure and surfactant concentration play a large role on overall foam stability. For a dry foam outside of a porous media, the lamella stability principles are essentially the same as in a porous media. Capillary pressure will try to pull liquid away from the lamella while surfactants on the interface push and help stabilize the foam.

Foam within a porous media typically does not exist as what can easily be recognized as bulk foam. Instead, lamellae span the pore throats between solid grains. If enough lamellae exist in a channel of flowing liquid, the porous media foam acts as an inhibitor to flow meaning a higher pressure drop is needed to achieve the same flow rate

through the media. With foam present, Darcy's Law may be used to calculate an apparent viscosity for the foam since it acts almost as its own phase within the rock.

A certain amount of surface elasticity is associated with lamella which allows foam film to deform without breaking. This property is important within a porous media where lamellae need to expand and contract to fit across pore bodies and throats of different sizes. As a lamella is expanded, surface tension towards the middle of the lamella increases and the concentration of surfactant decreases since the effective area goes up as shown in Figure 2.4. As a result, liquid flows back into the site of high surface tension, and if excess surfactant is present within the film, it will move to the interface for the surfactant concentration to reach equilibrium. If there is no excess surfactant locally, dispersion will more slowly bring the concentration back to equilibrium. Surfactant must stabilize foam from the effects of capillary drainage while also allowing the lamella to deform without breaking.

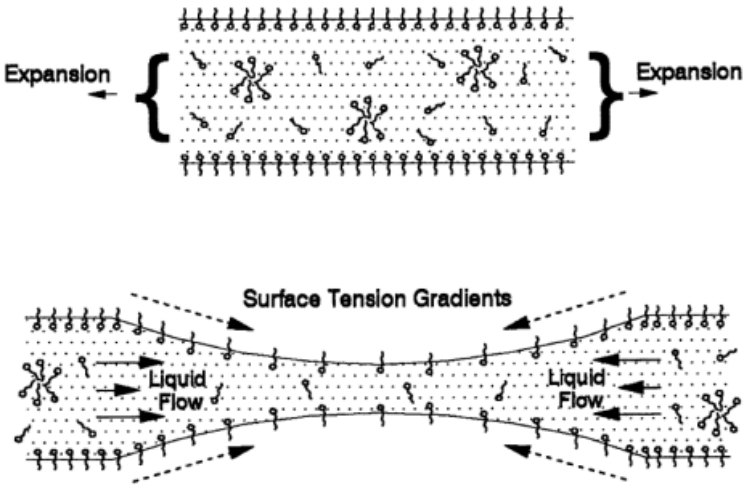

Figure 2.4: Surface elasticity

The sum of all the repulsive forces, electrostatic, steric, and dispersive, between the two sides of the lamella is called the disjoining pressure of a foam which shows strong dependence upon the surfactant properties, temperature, and pressure within a

porous media. Disjoining pressure pushes against the capillary pressure of the gas bubbles and the thinning of the lamella as was shown within foam.

However, disjoining pressure might not be sufficient enough to overcome destructive forces encountered within a porous media. As the lamellae are pushed through the pore throats and bodies, the effective cross section will become wider or smaller through the flow network. If the lamellae are mobilized too quickly over a large change in pore throat size, the surfactant will not have time to mobilize to the stretched film, and the lamella will burst. These mechanism for foam transport through a porous media are key in understanding its usage for EOR.

2.4.2 Foam for EOR

The idea behind using foam for EOR purposes ties back with the concept of sweep efficiency discussed early. It has been established that nitrogen is a poor fluid for EOR due to its moderate capillary number and high mobility ratio with reservoir fluids. Carbon dioxide, on the other hand, has a much lower MCM meaning that it is more readily miscible and lead to a better displacement efficiency by mobilizing more oil it contacts. Like nitrogen, CO_2 still suffers from poor sweep, but the introduction of foam into the system tries to solve this problem.

Having more lamella per unit length within the porous media is characteristic of a strong foam. The flow inhibition properties of the lamella are used to divert the injected gas away from high permeability zones and into zones that have previously been untouched. Typically, water with surfactant is alternated or coinjected with a gas to produce the foam where it then propagates into the reservoir for mobility control (Gupta 2003).

Chapter 3: Additive Screening

Y-grade is an industry term for the raw mixture of natural gas liquids produced in at the well head. These blends are then typically transported to centralized facilities and fractionalized into their discrete components to be sold on highly volatile markets. Profits are often slim depending upon the composition of the y-grade and the ease at which the products can be moved to sales points (Cooperman 2013).

The composition of y-grade used in our experiments was provided by the sponsoring company and inhibits easy testing of many additives since the y-grade needs to be under high pressure to exist primarily as a liquid. To make the screening process quicker, n-pentane was substituted for y-grade. Pentane is the lightest component of y-grade that is still a liquid under room conditions, so replacing y-grade with pentane and pure nitrogen with air provides several main advantages for the experiment. First, using a pentane-air system allows us to work at room temperature and pressure so that many more samples could be completed at one time. Secondly, the process to synthesize y-grade is time intensive so the day or more that it takes to create a new batch is saved. Finally, we have the option to use larger testing vessels with pentane and air compared to the small pressure cells for y-grade, which allows a greater range of additive concentrations to be tested. The pentane-air tests are simply a screening system to determine which additives might be successful with y-grade and pure nitrogen.

In addition to just pentane, two additional screening processes were tried. The first additional process was mainly pentane with a smaller fraction by volume of DI water. The main idea here was that water will naturally be occurring in reservoirs if a y-grade injection scheme is ever implemented, so it might be possible to take advantage of the fluid already in place to generate foam, thus, decreasing the amount of injected fluid necessary.

The second additional screening solvent was commercial grade diesel fuel. Diesel fuel is comprised of approximately 75% heavy paraffins and 25% aromatic hydrocarbons. The heavy paraffins are comprised of n-, iso-, and cyclo- varieties from mainly C10 to

C15. The combination of a variety of hydrocarbons found within diesel fuel and the fact that it can create foam without the use of any additive makes it a good candidate for a third round of screening after pentane and pentane with DI water. If an additive helps create a stable, fine foam within diesel fuel but fails with pure pentane, this is evidence that there is some chemical difference in the solvent allowing the additive to achieve better results.

3.1 MATERIALS

Over the course of the project, 38 different additives were tried to see what effect their presence would have on foam generation and stability. Additives were selected by finding similar cases with non-aqueous foam in literature and through recommendations from supplying companies. The numbering scheme for the additives was based mainly upon the order in which they arrived from suppliers. For simplicity, all additives will be referred to by this Testing Number.

Most of the additives tried are proprietary, so the exact chemical compositions of the samples were not able to be obtained. The information available for each additive such as active content within the sample provided and component information was obtained through provided Safety Data Sheets (SDS) or by speaking with company representatives directly. All available information pertaining to the additives that were tested is presented in Table 3.1.

Table 3.1: Additive names, manufacturers, types, and obtainable composition information

Testing Number	Trade Name	Type	Active Content	Primary Component	Secondary Components	Additional Details
1	XUR-PD-4 #1	Nonionic	0.99	Nonionic surfactant		Ethylene oxide, proplylene oxide, 1,4-dioxane
2	XUR-PD-4 #2	Nonionic	0.99	Nonionic surfactant		Ethylene oxide, proplylene oxide, 1,4-dioxane
3	XUR-PD-4 #3	Nonionic	0.99	Nonionic surfactant		Ethylene oxide, proplylene oxide, 1,4-dioxane
4	XUR-PD-4 #4	Nonionic	0.99	Nonionic surfactant		Ethylene oxide, proplylene oxide, 1,4-dioxane
5	XUR-PD-4 #5	Nonionic	0.99	Nonionic surfactant		Ethylene oxide, proplylene oxide, 1,4-dioxane
6	XUR-PD-4 #6	Nonionic	0.99	Nonionic surfactant		Ethylene oxide, proplylene oxide, 1,4-dioxane
7	SRA-451	Fluorosurfactant	0.25	Ethyl acetate	Fluorochemical acrylate copolymer	
8	Silsurf B608	Siloxane	1	Polydimethylsiloxane copolymer		High silicone content surfactant
9	Silsurf Di-2012	Siloxane		Silicone polyether		High EO content silicone surfactant
10	Silsurf J1015-O	Siloxane	1	Dimethylsiloxane and polyoxyalkane block copolymer		High EO and PO content silicone surfactant
11	Silube 316	Silicone Emulsifier		Silicone alkyl ether		Emulsifier
12	Silube J208-812	Silicone Emulsifier	1	Alkyl polyether polydimethylsiloxane		Emulsifier
13	-	Nanoparticle		PEG nanoparticles (5 nm)		
14	Sunsoft Q-12D	Fatty Acid Esters		Diglycerol esters of myristic acid and lauric acid		
15	Sunsoft 700P-2	Fatty Acid Esters	0.9	Gylcerol monocaprylin		
16	Sunsoft 750	Fatty Acid Esters	0.92	Glycerol monolaurin		
17	Sunsoft 760	Fatty Acid Esters	0.914	Glycerol monocaprin		
18	-	Nanoparticle		PEG nanoparticles (8 nm)		
19	EXP-17-AN6329-01	Nonionic		Aromatic branched ethoxylate	Nonionic surfactant, dinonylphenyl polyoxyethylene	Ethylene oxide, formaldehyde, 1,4-dioxane, acetaldehyde
20	EXP-17-AN6329-02	Nonionic		Ethylated nonionic surfactant	Nonionic surfactant 7, nonionic surfact 2	
21	EXP-17-AN6329-03	Nonionic		Aromatic branched ethoxylate	Nonionic surfactant 2	
22	EXP-17-AN6329-04	Nonionic		Aromatic branched ethoxylate	Nonionic surfactant 2	Ethylene oxide, formaldehyde, 1,4-dioxane, acetaldehyde
23	EXP-17-AN6329-05	Nonionic		Aromatic branched ethoxylate	Nonionic surfactant 2	Ethylene oxide, formaldehyde, 1,4-dioxane, acetaldehyde
24	EXP-17-AN6329-06	Nonionic		Nonionic surfactant 1		
25	EXP-17-AN6329-07	Nonionic		Nonionic surfactant 1	Nonionic surfactant 2, nonionic surfactant 3	Ethylene oxide, 1,4-dioxane, acetaldehyde, formaldehyde
26	EXP-17-AN6329-08	Nonionic		Aromatic branched ethoxylate	Nonionic surfactant 2	Ethylene oxide, formaldehyde, 1,4-dioxane, acetaldehyde, 2,6,8-trimethyl-4-nonanal
27	EXP-17-AN6329-09	Nonionic		Nonionic surfactant		
28	EXP-17-AN6329-10	Nonionic		Nonionic surfactant 1		Ethylene oxide, proplylene oxide, 1,4-dioxane
29	EXP-17-AN6329-11	Hydrocarbon		Sulfonated anionic surfactant	Solvent naptha, aromatics, xylene, cumene	Naphthalene
30	EXP-17-AN6329-12	Nonionic		Aromatic branched ethoxylate	Nonionic surfactant 2	Ethylene oxide, formaldehyde, 1,4-dioxane, acetaldehyde
31	EXP-17-AN6329-13	Nonionic		Aromatic branched ethoxylate	Nonionic surfactant 2, dinonylphenyl polyoxyethylene	Ethylene oxide, formaldehyde, 1,4-dioxane, acetaldehyde
32	EXP-17-AN6329-14	Siloxane		Aromatic hydrocarbon 1	Aromatic hydrocarbon 2, toluene, unknown components	Xylene, ethylbenzene
33	(Proprietary)	Fluorosurfactant	0.3	4-Methylpentan-2-one	Partially Fluorinated Acrylic Copolymer	
34	(Proprietary)	Fluorosurfactant	0.35	n-Butyl acetate	Partially Fluorinated Acrylic Copolymer	
35	Masurf FS-910	Fluorosurfactant	0.11	Hydrotreated heavy, nonaromatic naphtha	Fluoroacylate copolymer resin	Isoparaffinic hydrocarbon
36	Masurf FS-3020	Fluorosurfactant	0.2	Hydrotreated heavy, nonaromatic naphtha	Fluoroacylate copolymer resin	Isoparaffinic hydrocarbon
37	Monomuls 90-L 12	Glycerides		Dodecanoic acid, 2,3-dihydroxypropyl ester		
38	Myritol 331	Fatty Acid Esters		Glycerides, mixed coco, decanoyl, octanoyl		

Additives 1 through 6 were ethylene oxide based nonionic surfactants. The molecule length of these surfactants increased with testing number meaning Additive 6 had the largest ethylene oxide chain length while Additive 1 had the shortest chain length. This difference could be visualized within the samples as the higher numbers appeared solid and waxy while the lower numbers were liquid and clear. Additives 4, 5, and 6 were heated to around 60^{o} C in order to make the sample homogeneous and pourable. In addition, Additives 19 through 28, 30, and 31 were labelled as nonionic surfactants.

Silicone-based surfactants have been used within the oil and gas industry to create foam for hydrocarbon and aqueous mixtures in artificial lift (Koczo 2011) and are very common in other industries such as in polyurethane foams (Owen 1968). Additives 8 through 12 plus Additive 32 were all silicone-based surfactants or emulsifiers. Additives 8, 9, and 10 had a high silicone content, a high polyoxyethylene content, or both a high polyoxyethylene and polyoxyproylene content respectively. No more information about the exact compositions could be obtained from the manufacturers.

Nanoparticles have been shown to stabilize oil-based foams (Binks 2011), (Murakami 2010). Additives 13 and 18 were PEG coated nanoparticles of two different sizes. Additive 13 was the smaller at 5 nm while Additive 18 was larger at 8 nm. Both sizes of nanoparticles came in the form of a dry, white powder, but no additional information could be gained since the SDS were not available.

Through the review of literature, various types of fatty acid esters have proven to produce non-aqueous foam (Shresta 2011). Additives 14 through 17 as well as 37 and 38 were fatty acid esters. These additives were all solid, waxy substances with the exception of Additive 38 which was a viscous liquid that was still able to be extracted from the container with a pipette.

Finally, Additive 7 and 33 through 34 were fluorinated surfactants or “fluorosurfactants”. This type of surfactant has multiple carbons in a chain with attached

fluorine atoms and has been proved to be a very effective foaming agent as it reduces the surface tension of water and create a stable foam within dodecane (Bergeron 1997).

The three screening cases included pure n-pentane, pentane with a small fraction of DI water, and diesel fuel. The n-pentane utilized was supplied from Acros Organics™ with an assay minimum of 99.00%. The diesel fuel is of commercial grade purchased from a local Exxon gas station. Both the pentane and diesel fuel were untreated before use in the screening. The DI water was generated in house with a reverse-osmosis filter and tap water.

Preliminary screening tests were performed in 15 ml polypropylene test vials with screw on lids. The polypropylene tubes were soon replaced by Kimble™ glass, 40 ml vials with PTFE/silicone septas shown in Figure 3.1. The transition to larger glass vials came as a result of the polypropylene swelling in the presence of pentane and having a higher working volume allowed greater concentration ranges of additives to be more easily tested. It was important to use thin, tall vials to allow any foam generation to be measured easily over time. Short, wide vials would not see the same foam height decrease overtime since the foam would be spread over a larger area. Liquid additives were transferred to the screening vials using 4.5 ml plastic transfer pipettes with a narrow stem shown in Figure 3.2. The vials were labelled and sealed with standard electrical tape to prevent the tops from loosening.

Figure 3.1: Stock image of Kimble brand 40 ml glass vial for screening samples

Figure 3.2: Stock image of plastic transfer pipette with narrow stem used to move additives to testing vials

3.2 EXPERIMENTAL PROCEDURE

The first phase of the screening tests involved the additives being mixed with pure n-pentane. Each screening sample included 20 ml of pentane within a 40 ml vial. Since surfactants have been shown to increase foaming ability of traditional foam at concentrations even below 1.0%, a relatively low concentration of additive was applied to conserve samples. Since we were working with only 20 ml of pentane, the most prudent method to add the liquid additives was through counting drops from the transfer pipette.

An averaging of the mass from a single drop across several additives yielded an average drop mass of 0.03 g.

Either two drops of the liquid additive or 0.06 g of the solid additive were added to the pentane to yield a mass concentration of around 0.4-0.5% depending upon the exact mass of each drop which may slightly vary by additive and the density of the solvents involved in the screening. The samples were then shaken by hand rather vigorously for 30 seconds and observations recorded.

The second screening process involved 16 ml of pentane and 4 ml of DI water in the same vial to yield an 80% pentane and 20% DI water mixture. Without any additive, very defined interface between the two liquids was easily noticeable with the pentane on top of the DI water. As with the pure pentane screening, either two drops of the liquid additive or 0.06 g of the solid additive were added to the test vials. Since the DI water is more dense than the pentane that it replaced within the sample vial, the mass concentration of the additive relative to the entire liquid mass dropped by around 0.05%. All samples were shaken for 30 seconds in the same manner as the pure pentane test and observations were recorded.

Diesel fuel was chosen as a third screening process because its wide variety of components as well as its ability to readily form stable foam by itself without any supporting additive if shaken. If pentane and pentane with DI water were not able to generate foam with the additives tested, diesel fuel would be able to tell us if an additive had potential to support a completely non-aqueous foam, to inhibit the creation and stabilization of non-aqueous foam, or to have no effect on foaming ability. It was reasoned that if an additive could not generate and stabilize foam in pentane when shaken but could with diesel fuel, there must be some property of diesel fuel compared to pentane that caused this behavior. Again, 20 ml of diesel fuel was tested with two drops or 0.06 g of each additive. The resulting solute mass concentration for all samples was around 0.36% by mass. Samples were shaken for 30 seconds and observations were recorded.

Each of the 38 additives were tested for foam generation and stabilization ability in pentane, pentane with DI water, and diesel fuel leading to a total of 114 samples plus an addition 3 samples of just the solvents with no additive for visual comparisons. Once all samples were created, samples were again shaken by hand for 30 seconds each. The initial height of the produced foam as well as the decline in foam height in 10-minute intervals over an hour were recorded and plotted together by like solvent.

3.3 RESULTS

The results from these three screening tests indicated that none of our additives were able to generate any foam with pure pentane. By association, our hypothesis became that pure y-grade mixed with any of the additives would also be unable to generate any foam even under high-sheer situations. However, results from the pentane with DI water and diesel fuel screening tests indicated that some additives could generate very stable foam if the composition of the solvent was changed to be more foam friendly

3.3.1 Pentane

Pentane was wholly unable to generate any stable foam or even a single bubble that would last for more than half of a second. Below are the pictures immediately after the 30 seconds of vigorous shaking by hand. Some samples turn cloudy, but there was no pattern to translucency between additives of the same type. Most solids such as nanoparticles and fatty acid esters did not dissolve and sank to the bottom of the vial. It was observed that the fluorosurfactants and siloxane surfactant number 32 were all very soluble within the pentane. Toxic warning labels were used for some additives based upon the SDS provided. Refer back to Table 3.1 to match the number on the vial to the additive. Pictures of the pentane directly after being shaken with the additives appear as Figure 3.3. Observations are recorded in Table 3.2. As none of the pentane samples could generate foam, a graph displaying the foam's initial height and decline over an hour has not been included.

Figure 3.3: 20 ml pentane, approximately 0.48% solute by mass screening samples

Figure 3.3: Continued

Table 3.2: 20 ml pentane, approximately 0.48% solute by mass observations

Testing Number	Observation		Testing Number	Observation
1	Slightly cloudy		20	Nothing
2	Slightly cloudy		21	Nothing
3	Slightly cloudy		22	Nothing
4	Slightly cloudy		23	Nothing
5	Slightly cloudy		24	Nothing
6	Slightly cloudy		25	Nothing
7	Nothing		26	Nothing
8	Slight cloudy		27	Nothing
9	Nothing		28	Nothing
10	Slight cloudy		29	Nothing
11	Nothing		30	Cloudy
12	Nothing		31	Nothing
13	Additive sinks		32	Nothing
14	Nothing		33	Nothing
15	Nothing		34	Nothing
16	Additive sinks		35	Nothing
17	Additive sinks		36	Nothing
18	Additive sinks		37	Cloudy
19	Nothing		38	Additive sinks

3.3.2 Pentane and DI Water

The mixtures of 80% pentane with 20% DI water by volume showed a few interesting results. For Additives 1 through 6, the water portion of the mixture would turn turbid after a few shakes, but there was still a visible interface between the pentane and

water. As shaking continued, an emulsion formed such that there was no distinction between the pentane and the water, and this emulsion was able to create a fine, stable foam. Neither the stability of the foam nor the shaking time that it took for the sample to form a complete emulsion and foam seemed to show a pattern based upon the ethylene oxide chain length of the additive. As the foam degraded overtime, the emulsion did not separate into a pentane and water column but rather remained a single, turbid phase which was viscous enough to trap air bubbles from escaping. Since this foam was created from primarily pentane but also DI water as the continuous liquid external phase, it was dubbed "semi-aqueous foam". Similar results were also recorded for Additive 29, a sulfonated anionic surfactant.

The results from the other additives could be classified as having a slight emulsion form at the pentane-water interface, forming a large emulsion column with clear pentane on top, or completely forming an emulsion that was unable to stabilize foam. Other nonionic surfactants similar to Additives 1 through 6 were able to turn the water column turbid, or form a gel-like emulsion after shaking, but no others were able to create foam or trap more than a few tiny bubbles.

Figure 3.4 below shows the results of the screening immediately after 30 seconds of vigorous shaking. Table 3.3 shows the visual observations for each of the samples. Finally, Figure 3.5 shows the decline of any foam observed at ten-minute intervals for the first thirty minutes and then height after a full hour.

Several interesting observations were gathered from looking at the decline graph of the foam height. First, the initial heights of Additives 1 through 6 start at the same level, but additives 4 and 6 broke the trend found with the other similar additives. Secondly, Additives 3 and 4 increase in height over the first ten minutes. This increase is due to the foam taking a while to settle within the vial causing differences in the measurement early on. Finally, Additives 29 and 30, the only two surfactants able to create an emulsion-based foam other than 1 through 6, show very different decline profiles that drop off significantly overtime or have a lower initial height respectively.

Figure 3.4: 16 ml pentane and 4 ml DI water, approximately 0.43% solute by mass screening samples

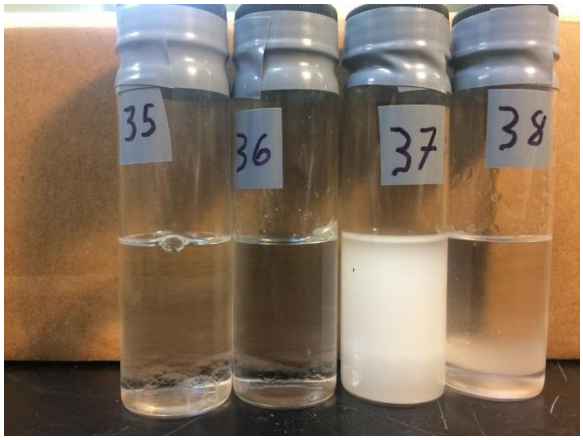

Figure 3.4: Continued

Table 3.3: 16 ml pentane and 4 ml DI water, approximately 0.43% solute by mass observations

Testing Number	Observation		Testing Number	Observation
1	Emulsion-based foam		20	Slick gel, no trapped bubbles
2	Emulsion-based foam		21	Small emulsion column
3	Emulsion-based foam		22	Small emulsion column
4	Emulsion-based foam		23	Slick gel, no trapped bubbles
5	Emulsion-based foam		24	Slick gel, no trapped bubbles
6	Emulsion-based foam		25	Slick gel, no trapped bubbles
7	Surfactant at interface		26	Small emulsion column
8	Slight cloudy		27	Small emulsion column
9	Cloudy water		28	Small emulsion column
10	Cloudy water		29	Emulsion-based foam
11	Large emulsion column		30	Some trapped bubbles
12	Cloudy water		31	Slick gel, no trapped bubbles
13	Additive sinks		32	Very small emulsion interface
14	Cloudy		33	Slick gel
15	Cloudy		34	Emulsion at bottom
16	Additive sinks		35	Emulsion at bottom
17	Additive sinks		36	Emulsion at bottom
18	Emulsion		37	Cloudy
19	Slick gel, no trapped bubbles		38	Cloudy water

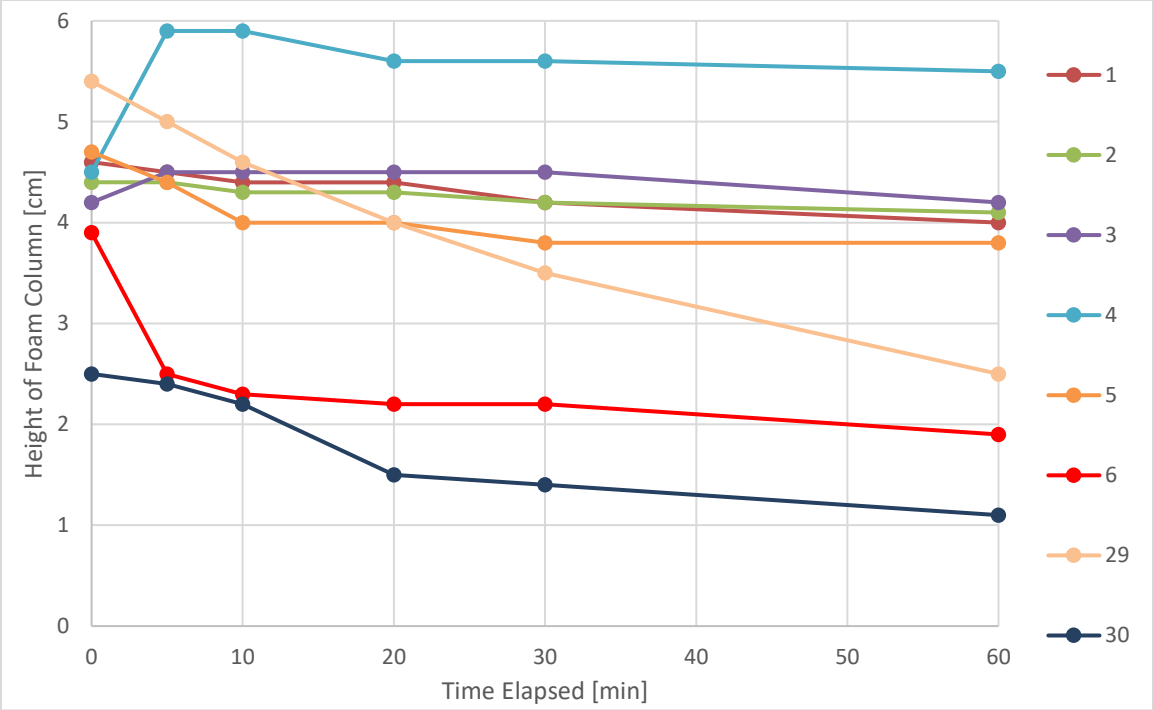

Figure 3.5: Pentane and DI water foam initial height and decline over an hour

3.3.3 Diesel fuel

The necessity of performing a diesel fuel screening became apparent after the pentane screening failed to produce any foam. Even though pentane with some DI water showed potential for creating an emulsion based foam, our research goals were for a foam without water or a “non-aqueous foam”.

The diesel fuel screening showed several interesting results which guide future efforts. First, nonionic surfactants were not able to increase the foaming potential of the diesel fuel compared with a base case not containing any additive. Siloxane-based additives either had an enhancing effect such as with Additive 11 and 32, a defoamer effect such as with additives 8 and 10, or no effect such as with additive 9. Both nanoparticle additives had good results creating very fine, stable foam. Between the two particle sizes, it was the smaller 5 nm particles that performed better than the larger 8 nm particles. Fatty acid esters showed similar results to the siloxane-based surfactants in that

they could slightly enhance, destroy, or have no effect upon the diesel fuel foam. One type of additive did show very promising results though. All to the fluorosurfactants tried showed a strong ability to increase the initial foam height and the stability of the foam throughout time.

Figure 3.6 below shows the results of the diesel fuel screening immediately after 30 seconds of vigorous shaking. Note that the first, unlabeled vial in the first picture is the base without any additive, and vials with Additives 33 and 34 are shown in both of the last two pictures. Table 3.4 shows the observations for each of the samples. Finally, Figure 3.7 shows the decline of any foam observed at ten-minute intervals for the first thirty minutes and then height after a full hour.

Since diesel fuel can generate foam without any enhancing additive, a lot more samples showed foam decline than the pentane with water screening experiment. The additives that were excluded from the decline graph were those that acted as defoamers or did not show the presence of foam after since they tended to all overlap and make the graph less readable.

Figure 3.6: 20 ml diesel fuel, approximately 0.36% solute by mass observations

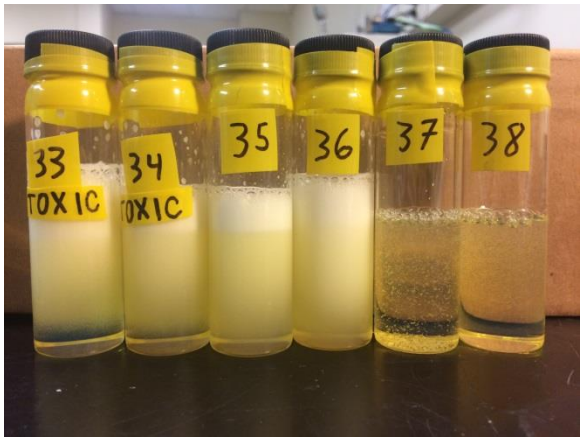

Figure 3.6: Continued

Table 3.4: 20 ml diesel fuel, approximately 0.36% solute by mass observations

Testing Number	Observation		Testing Number	Observation
1	No improvement		20	No or very slight improvement
2	No improvement		21	No or very slight improvement
3	No improvement		22	No or very slight improvement
4	No improvement		23	No or very slight improvement
5	No improvement		24	No or very slight improvement
6	No improvement		25	No or very slight improvement
7	Much improvement, long lasting		26	No or very slight improvement
8	Defoamer		27	No or very slight improvement
9	No improvement		28	Slight improvement
10	Defoamer		29	No or very slight improvement
11	Much improvement		30	No or very slight improvement
12	Slight improvement		31	None or very slight improvement
13	Much improvement, powder not seen, long lasting		32	Much improvement
14	Slight improvement		33	Much improvement, long lasting
15	Defoamer		34	Much improvement, long lasting
16	No improvement, particles sink		35	Much improvement, long lasting
17	No improvement, particles sink		36	Much improvement, long lasting
18	Slight improvement, powder not seen		37	No improvement
19	No or very slight improvement		38	No improvement

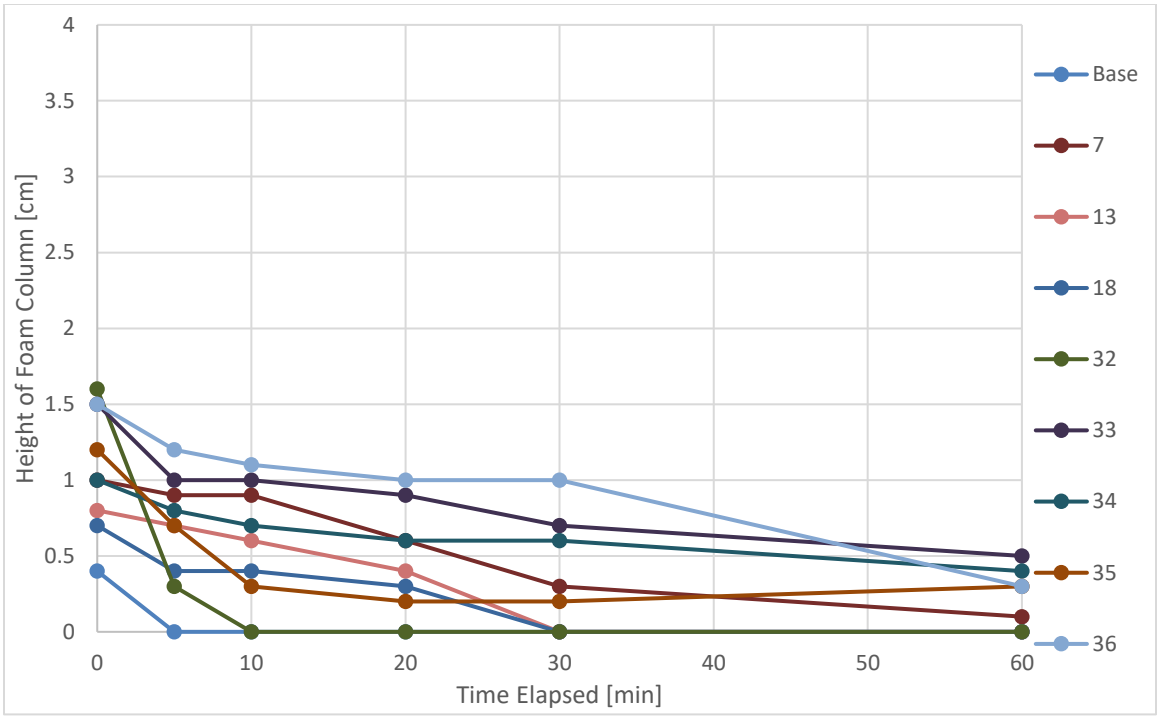

Figure 3.7: Diesel fuel foam initial height and decline over one hour

3.4 CONCLUSIONS

Several conclusions can be reached based upon the outcomes of the three screening processes. First, it seems highly unlikely that pentane can generate stable foam with any of the additives tried. By extension, y-grade by itself will probably not be able to be foamed with any of the available additives. Secondly, an emulsion-based, semi-aqueous foam is able to be created by a select few of the nonionic surfactants. Finally, some additives such as fluorosurfactants, nanoparticles, and a few siloxane-based surfactants were able to enhance the diesel fuel foam while not producing any results with just pentane. Thus, there must be something chemically different between the pentane and the diesel fuel that is allowing the additives to increase the foaming potential.

The conclusions of the additive screening now present two separate lines of research to create a y-grade dominant foam system. The first is semi-aqueous foam with

y-grade as the primary component, DI water as a secondary component, and Additives 1 through 6 and 29. The second is completely non-aqueous foam with y-grade, again, as the primary component, some hydrocarbon-based secondary component, and the most successful additives from the diesel fuel screening.

Chapter 4: Non-Aqueous Secondary Component Screening

Previous screening tests concluded that it was not possible to create stable foam with pentane as the only solvent. However, several additives were able to increase the foaming potential of diesel fuel, so if the pentane could be mixed with whatever in the diesel fuel was allowing for a strong foam, it might be possible to create a stable, non-aqueous foam with y-grade as the primary component by volume and an additional secondary component.

4.1 MATERIALS

The materials used for these experiments were originally components of diesel fuel to evaluate which were the best at increasing a hydrocarbon mixture's foaming potential. As the experiments progressed, a greater variety compounds were tried in an attempt to isolate if a certain chemical property was the reason for a strong foam to be formed.

The diesel fuel screening provided several additives that stood out as enhancing the foaming ability of a hydrocarbon blend. These select additives included PEG coated nanoparticles, a siloxane based surfactant, and five fluorosurfactants that increased both the initial foam height of diesel fuel and the stability of the foam. To keep the research focused on one area of interest, the solid nanoparticles were not further explored in these experiments. Thus, six surfactants, Additives 7, 32, 33, 34, 35, and 36, were chosen to evaluate the foaming behavior of possible secondary components to pentane.

Even though pentane by itself was unable to foam, the high percentage of linear alkanes within diesel fuel supported the hypothesis that a heavier linear alkane would be able to foam more readily than pentane. N-octane, n-decane, and a light mineral oil blend were chosen to evaluate the impact of heavier linear alkanes on foaming potential. Both the octane and decane were manufactured by Acros Organics part of Thermo Fisher Scientific™ and had an assay of 99.0%. The light mineral oil was manufactured by Fisher Chemical™ another part of Thermo Fisher Scientific. The exact composition of

the light mineral oil was not available, but it is almost entirely midrange, linear and cyclo-alkanes. The dipole moment of both the octane and decane was 0.07 D. The decane had a dynamic viscosity of 0.876 cP, and the octane had a dynamic viscosity of 0.524 cP at room temperature. The light mineral oil had a density of around 0.83 g/ml and viscosity around 15 cP based upon the available certificate of analysis. The exact dipole moment of the light mineral oil was not available, but was averaged around 0.1 D based on available literature.

In addition to heavier linear alkanes, diesel fuel contains a significant number of aromatic compounds. Toluene, a benzene ring with an added methyl group, was used to observe the foaming potential of an aromatic compound and the six surfactants. The toluene used for the experiment was provided by Fisher Chemical with an assay of >99.5%. The dipole moment of the toluene was 0.36 D and the dynamic viscosity was 0.552 cP.

While diesel fuel does not contain many, if any, alcohols, 1-butanol was tested as a possible secondary component. The basis for testing the butanol was to see how the select surfactants would react to having a more polar secondary component. In addition to a large shift in polarity for the secondary component, butanol is also more viscous than both lighter linear alkanes and toluene. The butanol was manufactured by Fisher Chemical and had an assay of 99.9%. The dipole moment of the butanol was 1.660 D and the dynamic viscosity was 2.593 cP.

Triglycerides are typically derived from three fatty acids combined with glycerol and having alkoxy groups replacing the hydroxyl groups. The result is a largely non-polar molecule that is significantly more viscous than pentane. Food grade olive oil purchased from a local food store was chosen as our triglyceride source to see how the select surfactants would interact with the more complex triglycerides compared to just heavier linear alkanes. If the viscosity of the pentane-secondary component mixture was indeed the defining factor as to whether a stable foam could be created, olive oil would be a

good starting point. The dipole moment of the olive oil was estimated to be around 0.15 D, and the dynamic viscosity was 52.0 cP.

In addition to the select six surfactants, olive oil was also tested by itself in a similar procedure to that found in a paper by Shrestha et al. in 2010. In this research paper, a surfactant, diglycerol monomyristate, was shown to have a very high foaming potential with olive oil. The company that had supplied the surfactant used in the paper, Taiyo Kagaku Company, was reached out to, but no longer manufactured the diglycerol monomyristate. As a substitute, they provided samples of diglycerol esters of myristic acid and lauric acid, glycerol monocaprylin, glycerol monolaurin and glycerol monocaprin. These different fatty acid esters were labelled as Additives 14 through 17. While the diglycerol monomyristate used in referenced paper was a fine powder, Additives 14, 15, and 17 were all waxy solids while Additive 16 was a rather coarse powder.

In addition to linear alkanes, diesel fuel also contains a significant number of heavier cycloalkanes. While cyclooctane has the same chemical formula as linear octane, having a ring structure leads to a higher viscosity. Cyclooctane was tested to see if the structure of the alkane had a significant impact upon its foaming potential. The cyclooctane used was manufactured by Alfa Aesar^{TM} and had an assay of 99.0%. The exact dipole moment of the cyclooctane could not be found in literature, but is estimated to be very low around 0.0 D, and the dynamic viscosity was around 2.133 cP.

4.2 EXPERIMENTAL PROCEDURE

Most of the secondary components at the beginning of the experiment were tested with 4 drops of each of the six select additives, 7, 32, 33, 34, 35, and 36. Four drops were used instead of two as in the screening tests so that there would be no doubt that it was not due to a low concentration of additive that lead to no foam being seen. Octane, decane, light mineral oil, toluene, butanol, and olive oil were tested with all six of the select additives.

As the experiment progressed, results from the full tests of all six surfactants indicated that Additives 34 and 36 showed the highest foaming potential under different conditions. Due to this observation, the glycols and the acetates were only tested with Additives 34 and 36. Cyclooctane was only tested with 36 and compared to linear octane with the same additive. For each sample, 20 ml of the prospective secondary component was added to 40 ml vials with 4 drops of additive. As with the screening tests, all samples were shaken for 30 seconds and the initial height and decline of the foam column was measured over time.

As mentioned previously, the olive oil had an expanded procedure in addition to testing the six select additives. The procedure used to test Additives 14 through 17 matched closely to that of Shrestha et al. Each additive was weighed and combined with 10 ml of olive oil to yield a 3% by weight sample. This concentration showed the best foaming results for the diglycerol monomyristate tests. The samples were then heated in an 80^{o} C oven for 30 minutes to melt the additives into the olive oil. After a half hour, the samples were removed from the oven and shaken for 30 seconds, and observations were recorded.

4.3 RESULTS

4.3.1 Octane

N-octane is a linear alkane like pentane, but has a longer chain length leading to a higher viscosity and very slightly higher polarity. After 30 seconds of shaking, vials with additives 7, 34, 35, and 36 could generate foam while 32 and 33 could not. The height of foam for Additives 35 and 36 always performed better than the others, but the better of the two was not always consistent. After 30 seconds of shaking, sometimes 35 would be slightly higher and sometimes 36 was slightly higher. A picture of the initial foam is shown in Figure 4.1, and the declines in the foam height over time is shown in Figure 4.2.

Additive 35 showed the highest foaming potential both initially and overtime with Additives 36 and 34 close behind. Additive 7 showed foam at the beginning, but it soon collapsed before five minutes. Additives 32 and 33 showed no foam.

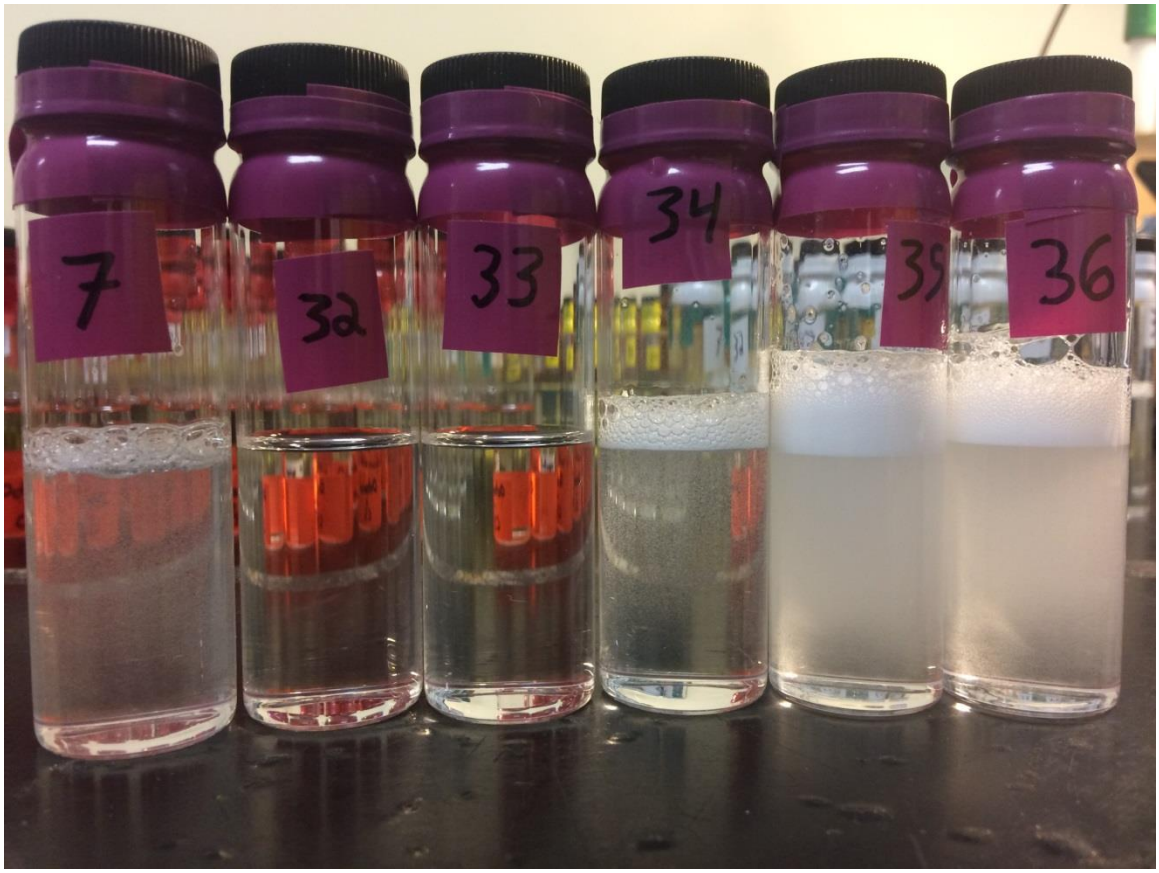

Figure 4.1: 20 ml of n-octane with 4 drops of additives after 30 seconds of shaking, approximately 0.85% solute by mass

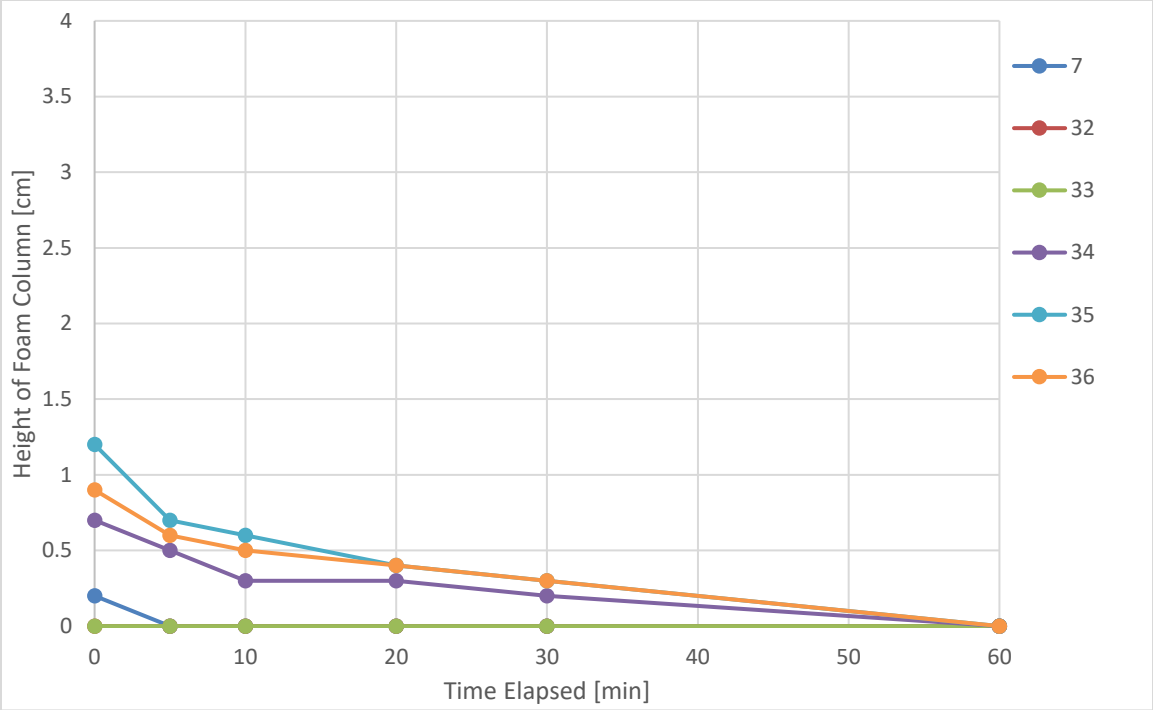

Figure 4.2: 20 ml of n-octane with 4 drops of additives foam initial height and decline

4.3.2 Decane

Decane continues the trend of increasing the length of linear alkanes further. It has a slightly higher viscosity and polarity. Additives 35 and 36 again showed high foaming potential, but Additive 34 also had very good results. Additives 32 and 33 were able to be foamed, and additive 7 performed about the same as with octane. A picture of the initial foam is shown in Figure 4.3, and the declines in the foam height over time is shown in Figure 4.4.

For at least the first 20 minutes, Additive 36 performed the best in creating a stable foam. However, at 30 minutes elapsed time, Additives 34 and 35 had a higher height of foam, which was still seen after a whole hour. Additive 33 had foam lasting for less than 20 minutes, and additives 7 and 32 lasted less than 5 minutes.

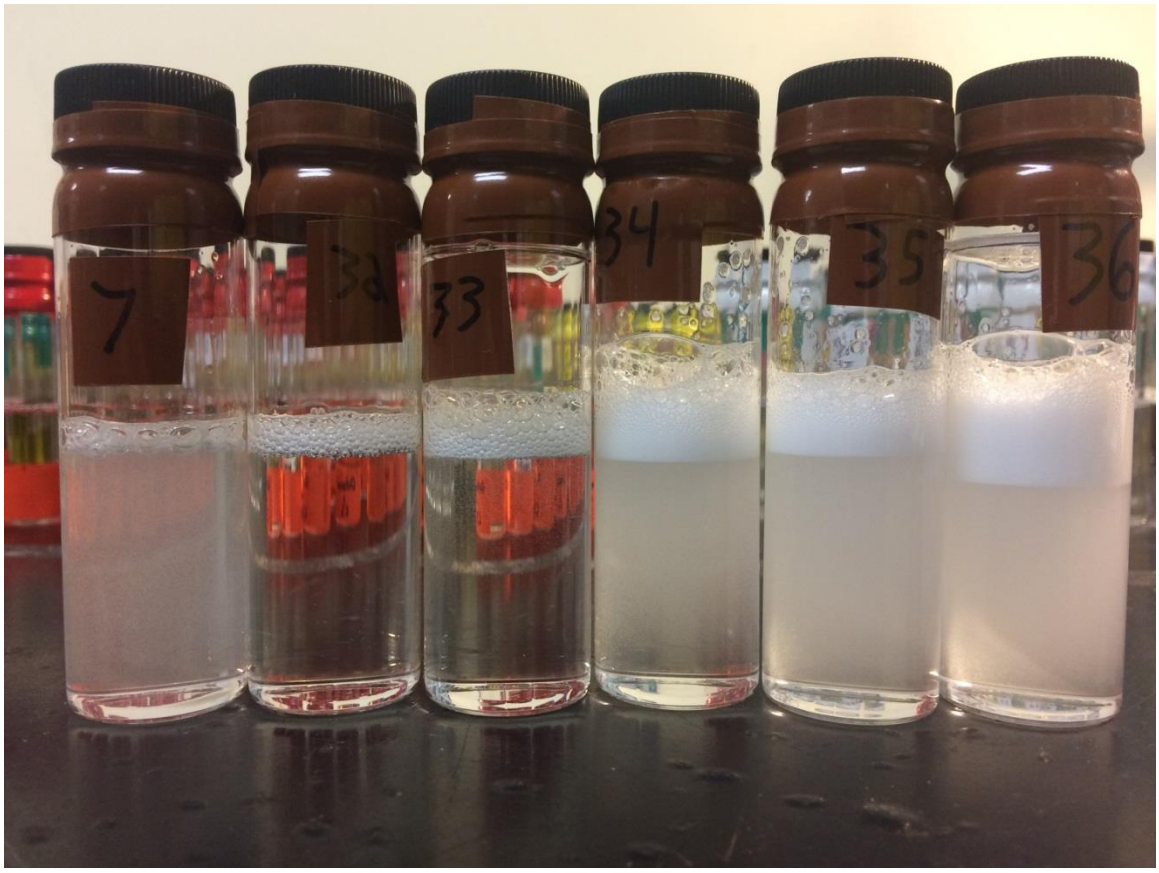

Figure 4.3: 20 ml of n-decane with 4 drops of additives after 30 seconds of shaking, approximately 0.82% solute by mass

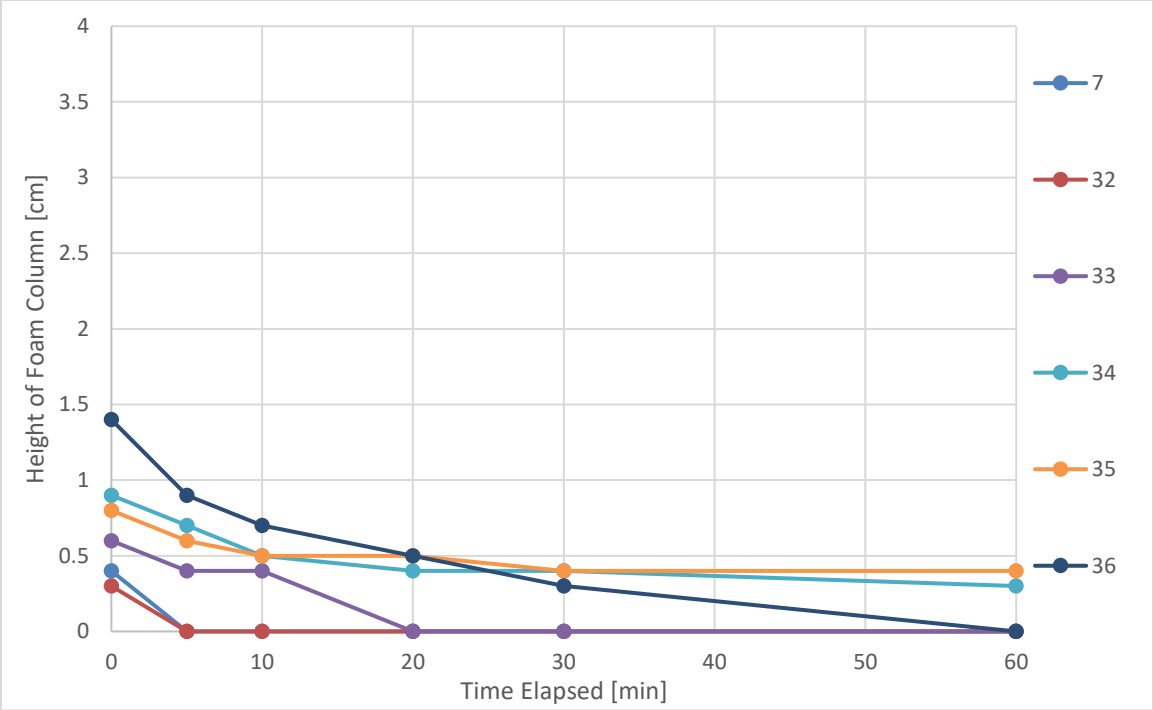

Figure 4.4: 20 ml of n-decane with 4 drops of additives foam initial height and decline

4.3.3 Light Mineral Oil

Light mineral oil is comprised primarily of linear alkanes larger than decane meaning it has a much higher viscosity. So far with linear alkanes, it was observed that as the viscosity increased, so did the foaming ability of the secondary component. However, this trend was broken with light mineral oil as very little foam could be generated. Additives 36 and 32 could only generate a foam column less than 0.5 cm high which lasted less than 10 minutes. The other of the select six additives were unable to create any foam. If the viscosity of the secondary component was the critical physical property to create a high, stable foam, it is evident that there is an ideal region for foam generation and stabilization. A picture of the initial foam is shown in Figure 4.5, and the declines in the foam height over time is shown in Figure 4.6. Only Additives 32 and 36 could generate any foam. Both lasted for over 5 minutes but less than 10.

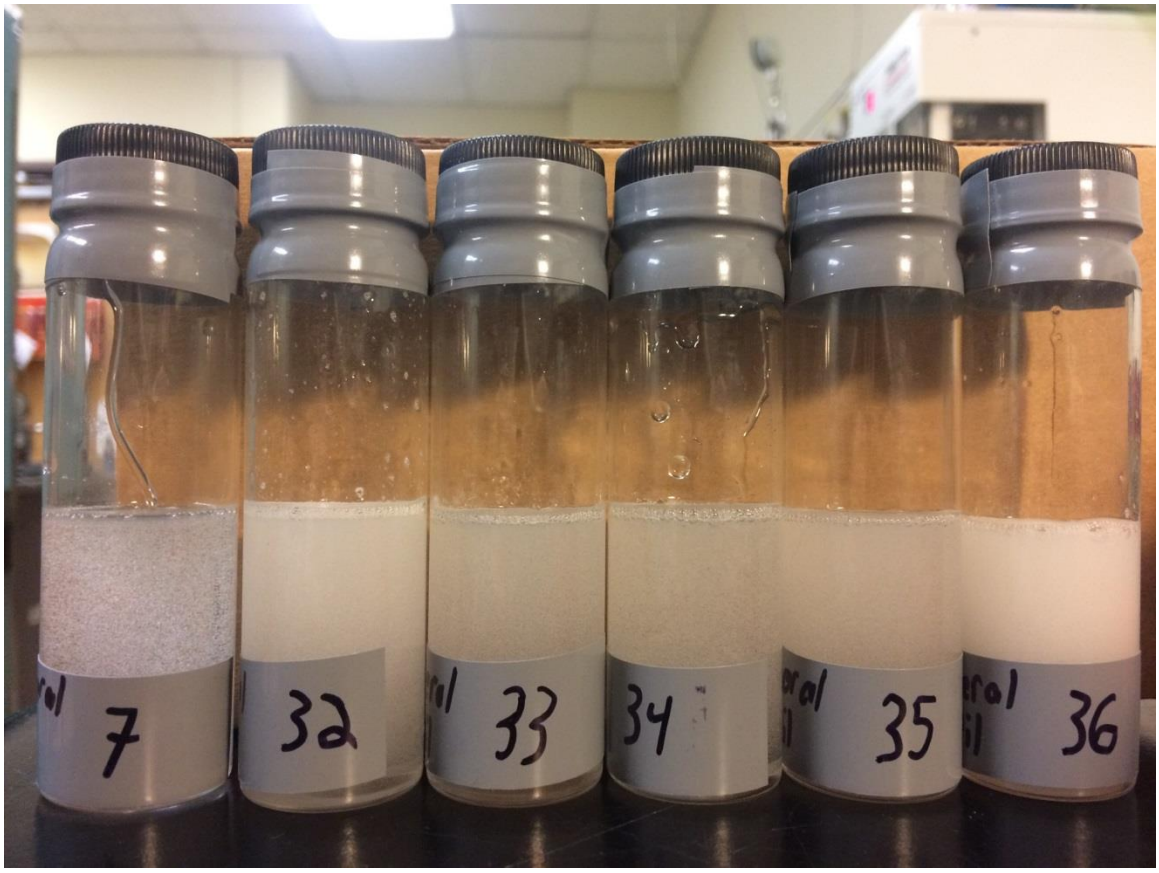

Figure 4.5: 20 ml of light mineral oil with 4 drops of additives after 30 seconds of shaking, approximately 0.72% solute by mass

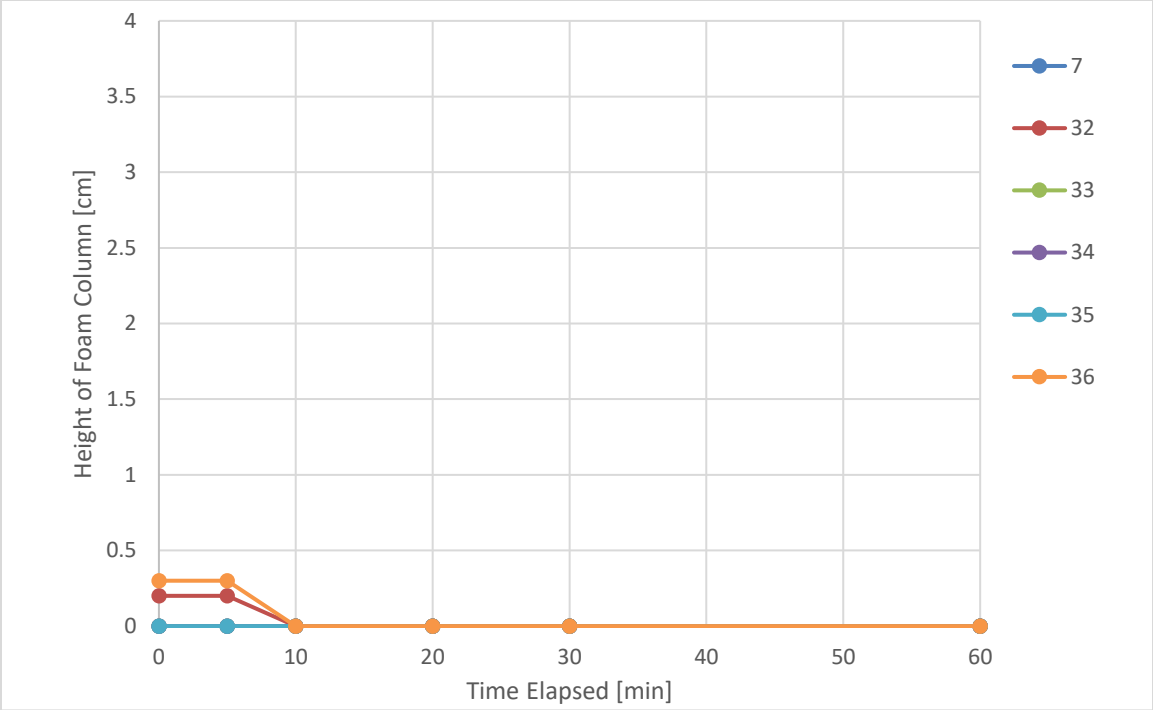

Figure 4.6: 20 ml of light mineral oil with 4 drops of additives foam initial height and decline

4.3.4 Toluene

Getting away from linear alkanes, toluene is an aromatic compound and showed very good foaming potential for all six of the select additives. Additive 34 was very dominate at after shaking, Additives 36 and 35 showed similar potential with additive 7 slightly lower. Additives 32 and 33 again performed the worst. All of the samples displayed very fine foam with a small bubble size indicating a high level of energy to create the foam and suggesting high stability. Toluene's viscosity is only slightly higher than that of linear octane and lower than that of decane suggesting that the structure and not just viscosity of the secondary component is important to foam generation and stabilization. A picture of the initial foam is shown in Figure 4.7, and the declines in the foam height over time is shown in Figure 4.8.

Additive 34 performed the best for the first 20 minutes but had a significant drop in foam height overtime. Additives 7 and 36 started at around the same height but 7

declined sharply and disappeared before 30 minutes while the foam created from 36 was much more stable. Additive 35 also sharply declined but was able to last longer past 30 minutes. Additives 32 and 33 initially looked promising, but the foam was unable to last past 10 and 5 minutes respectively.

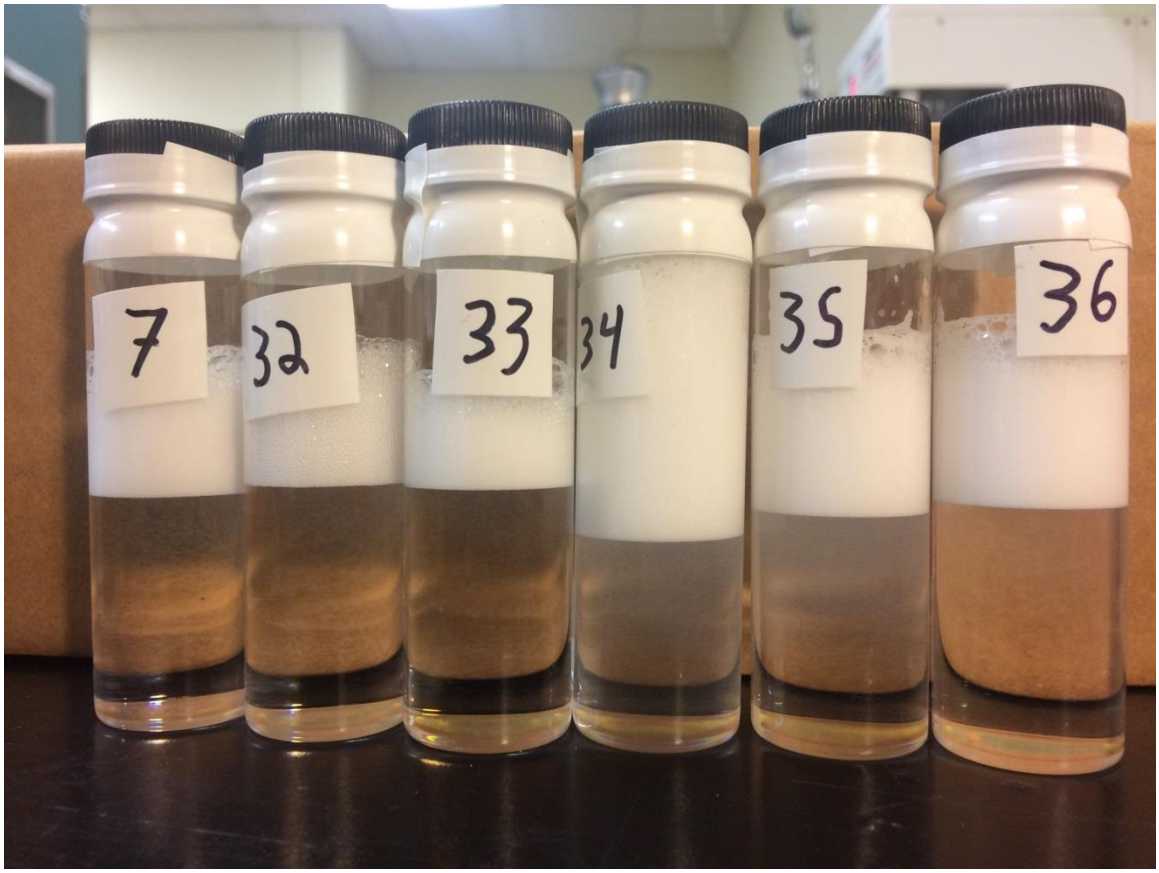

Figure 4.7: 20 ml of toluene with 4 drops of additives after 30 seconds of shaking, approximately 0.69% solute by mass

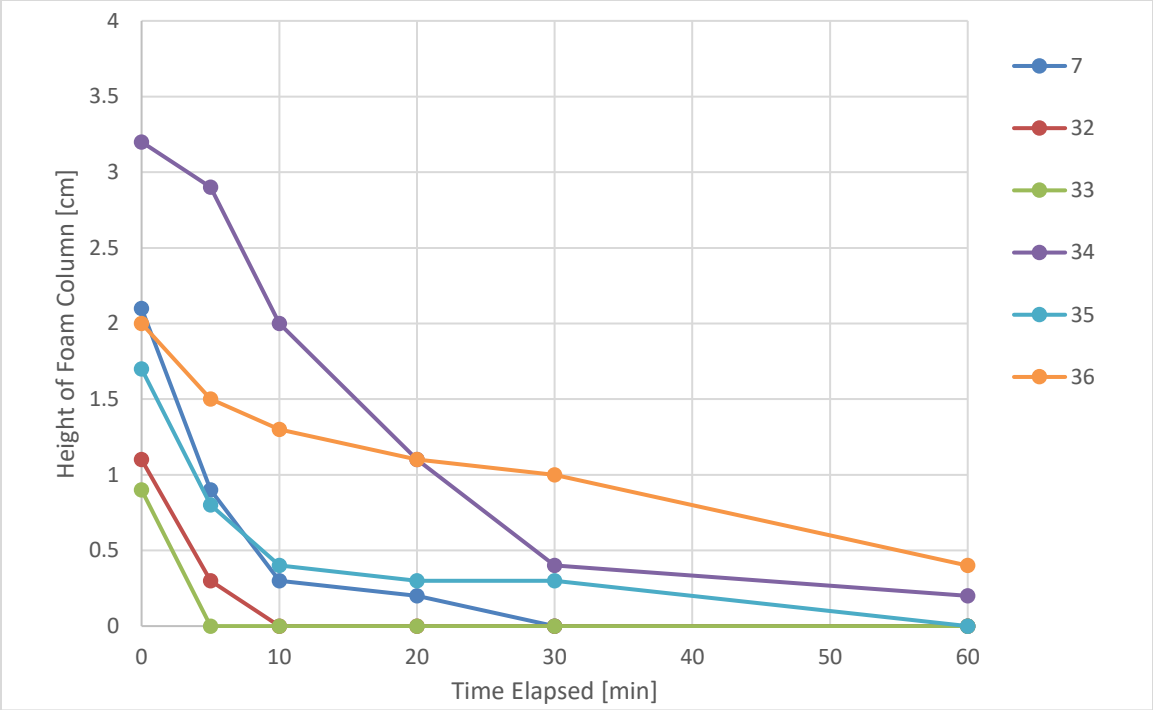

Figure 4.8: 20 ml of toluene with 4 drops of additives foam initial height and decline

4.3.5 Butanol

Toluene is slightly more polar than the linear alkanes suggesting that maybe it is the polarity of the secondary component that is working well with the additives to create stable foam. Butanol tests this hypothesis further since it is much more polar than toluene. Conversely to what was observed previously with non-polar linear alkanes, Additives 32, 33, and 34 performed the best. In addition, additives 7, 35, and 36 all precipitated out of solution and formed very small white specks. These cases were not able to generate any foam, and the additive sank to the bottom of the vial. This drastic change in performance for the additives was strong evidence that the additives were sensitive to the polarity of the solvent and that there was no best additive. The performance would depend strongly on the secondary component. A picture of the initial foam is shown in Figure 4.9, and the declines in the foam height over time is shown in Figure 4.10.

Both Additives 34 and 32 started at the same initial height, but 34 showed a higher stability overtime. Additive 33 lasted less than 10 minutes.

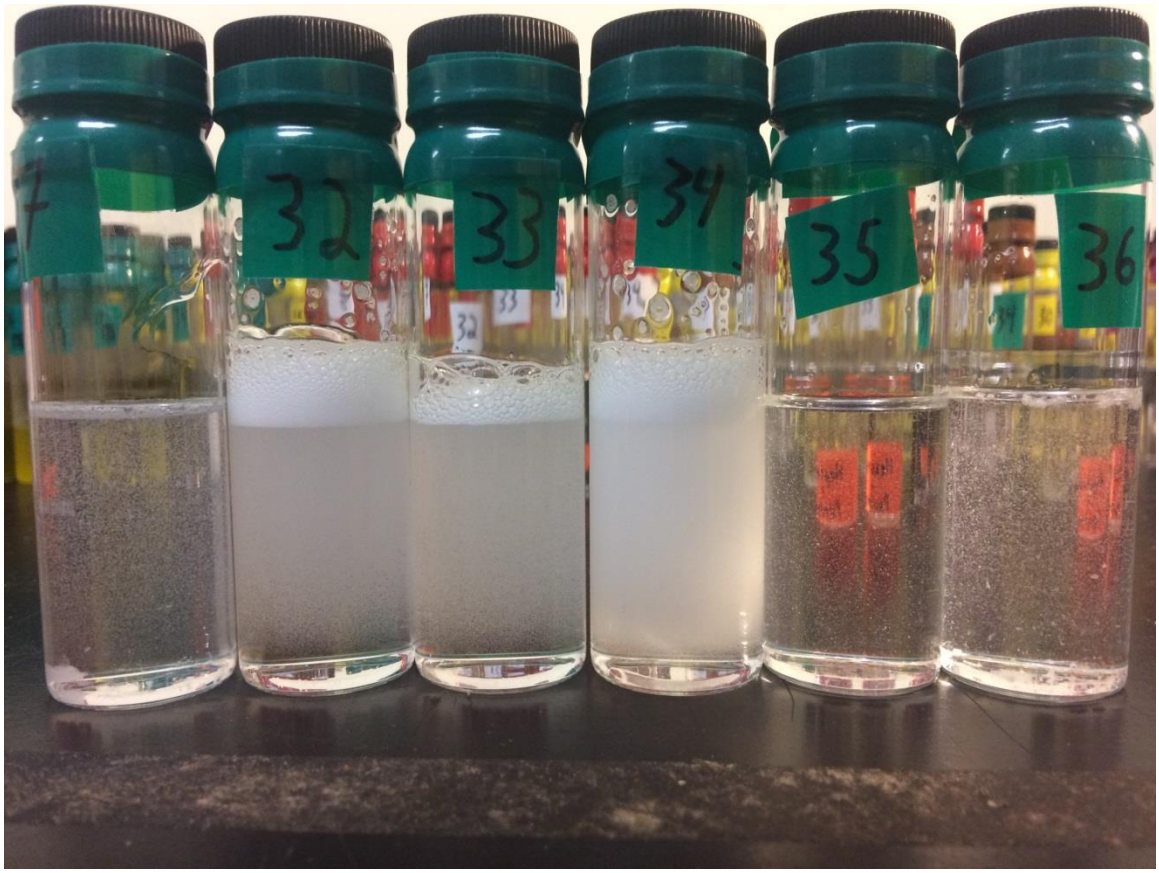

Figure 4.9: 20 ml of butanol with 4 drops of additives after 30 seconds of shaking, approximately 0.75% solute by mass

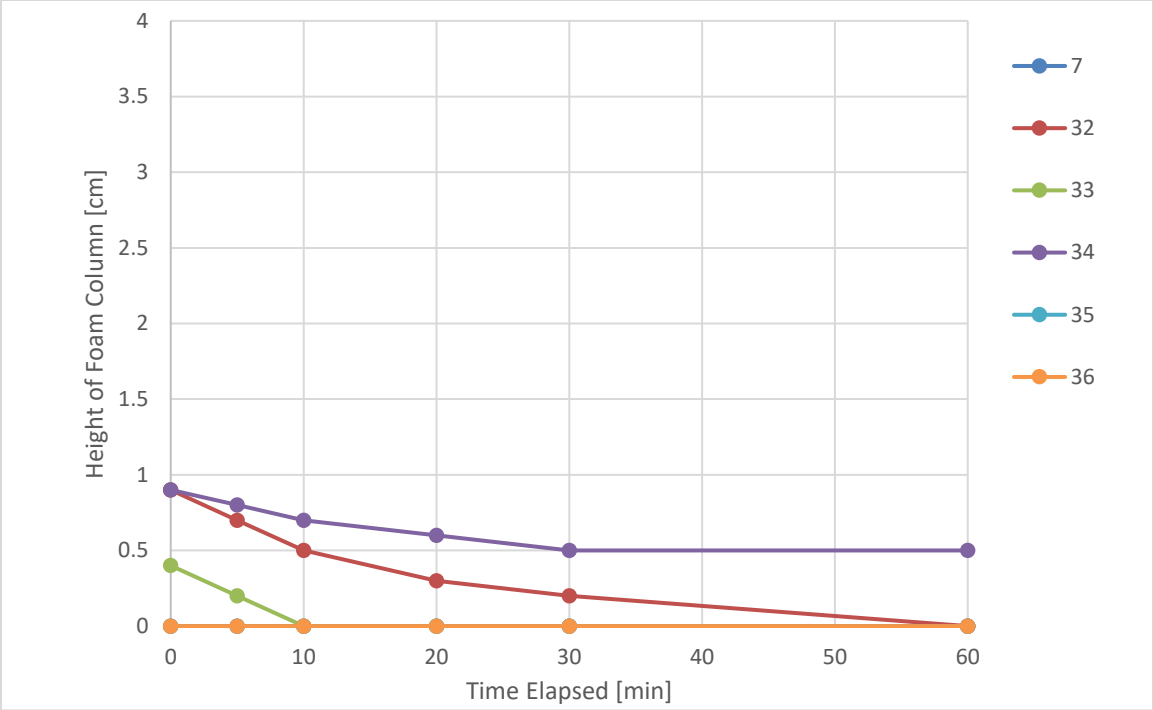

Figure 4.10: 20 ml of butanol with 4 drops of additives foam initial height and decline

4.3.6 Olive Oil

Olive oil has a low dipole moment but a viscosity higher than light mineral oil. After experimenting with the light mineral oil, it was expected that the olive oil would have similar results and not produce stable foam since the viscosity was too high. After 30 seconds of shaking, tiny bubbles were noticed within the olive oil that slowly rose to the oil-air boundary, but only a single layer of bubbles around the edges of the vials was noticed for Additives 32, 33, 35, and 36. By the time the height of the bubbles were measured, only Additive 32 still had enough to quantify. A picture of the initial foam immediately after shaking is shown in Figure 4.11, and the declines in the foam height over time is shown in Figure 4.12.

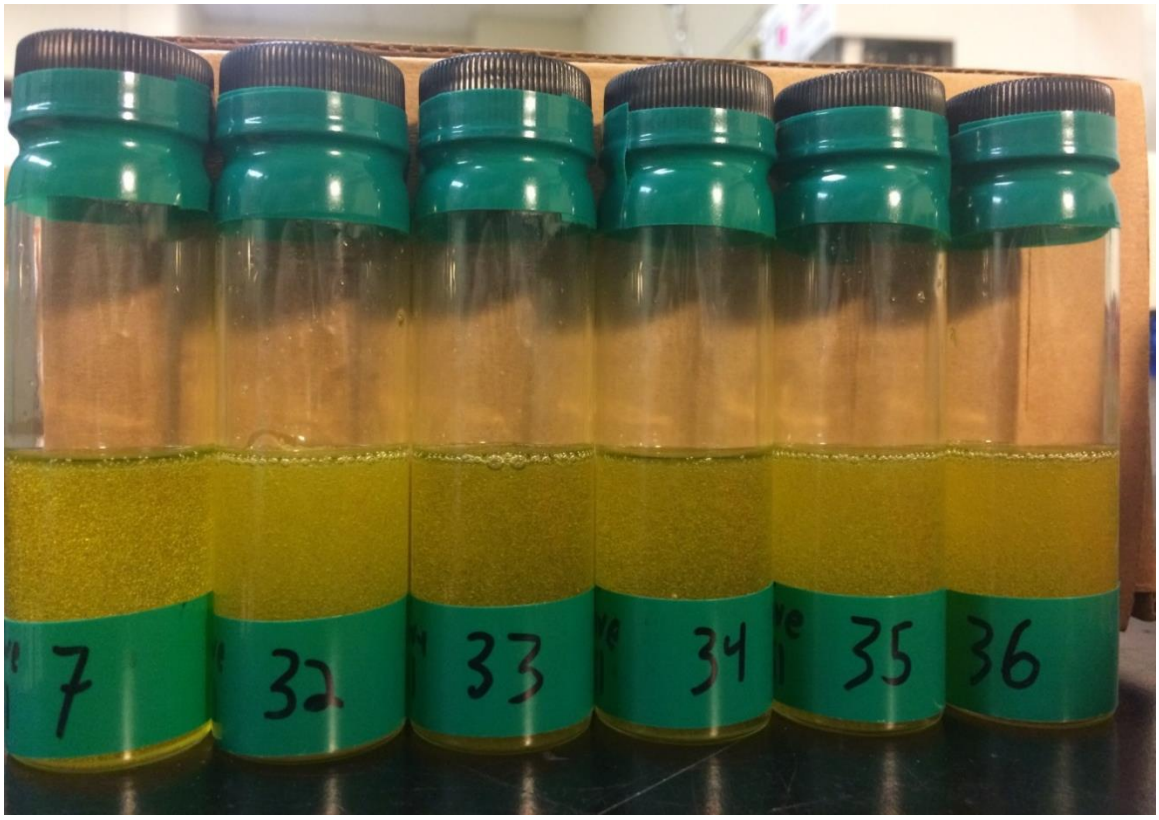

Figure 4.11: 20 ml of olive oil with 4 drops of additives after 30 seconds of shaking, approximately 0.67% solute by mass

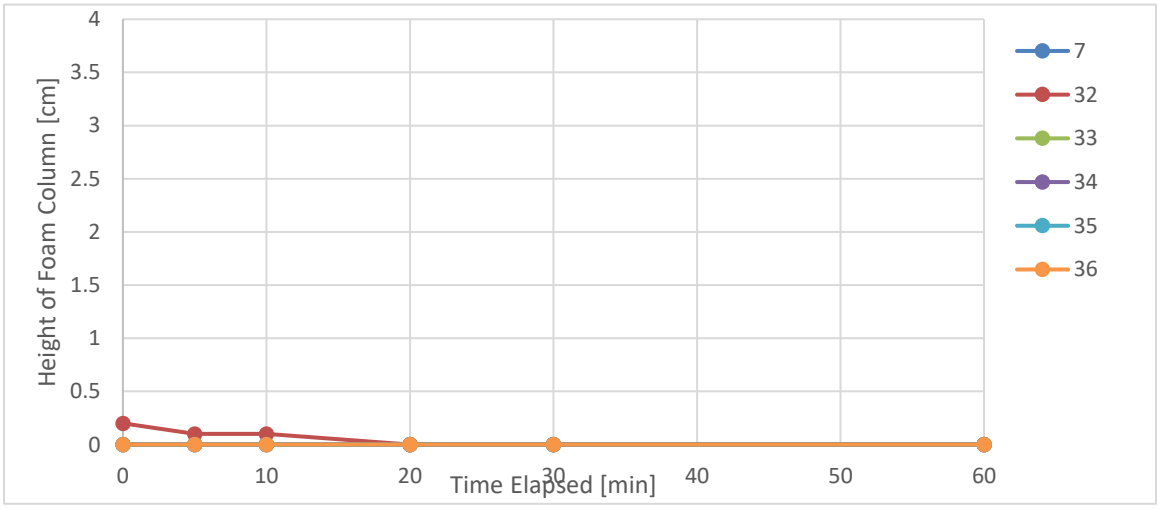

Figure 4.12: 20 ml of olive with 4 drops of additives foam initial height and decline

The results from the expanded procedure for olive oil were surprising given the ease that diglycerol monomyristate could, reportedly, create a high column of very stable foam. Samples with Additives 14 and 15 turned cloudy and showed only a small ring of bubbles around the edge of the vial. Additives 16 and 17 did dissolve into the olive oil, but did not enhance the foaming ability at all. The results of each additive after shaking is shown in Figure 4.13.

There may be two reasons that the foaming results from the monomyristate tests were not seen here. First, it is possible that the chemical properties of monomyristate were different enough from those of the four fatty acid esters experimented with here. Secondly, the monomyristate was a finer powder which maybe the reason for its high foaming potential. Further refining Additive 16 into a powder with a smaller particle size may increase its foaming ability.

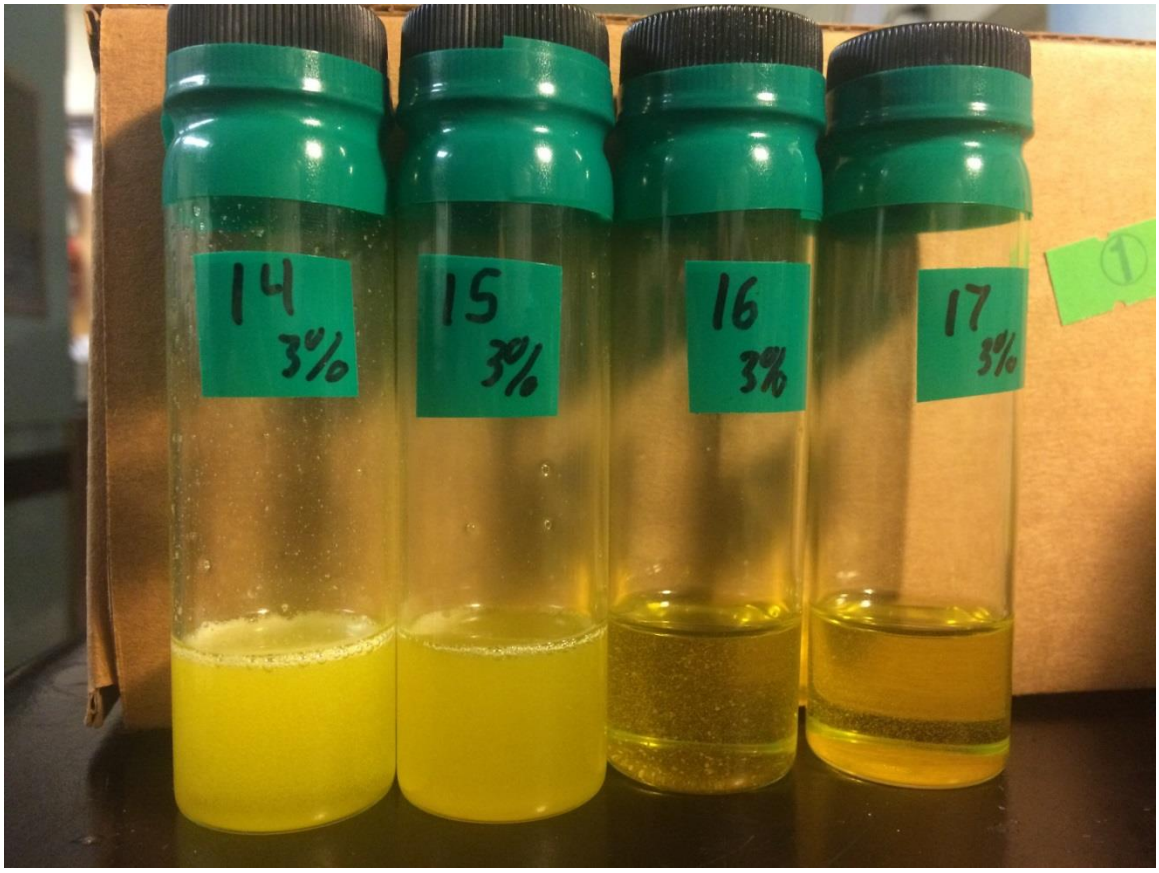

Figure 4.13: 10 ml of olive oil with 3% solute by mass after 30 seconds of shaking, heated to 80º C

4.3.7 Cyclooctane

Cyclooctane was only tested with Additive 36 since it showed a strong foaming ability with non-polar secondary components previously such as octane and decane. The results with cyclooctane were rather surprising since it had the same molecular weight and polarity as the linear octane, but a higher viscosity. A lot of fine bubbles were generated at it took a few seconds for them all to float up to the foam column on top. The good performance of the cyclooctane suggests that either molecular structure or the increased viscosity associated with the structure has a strong influence on foaming potential and qualities such as polarity and molecular weight have little to no effect when

the same additive is present in both secondary components. In Figure 4.14, n-octane is compared to the cyclooctane after shaking, and the declines are shown in Figure 4.15.

Overtime, both linear octane and cyclooctane appear to have the same slopes, but cyclooctane simply started out much better. Cyclooctane had a decent foam height at 30 minutes, but both do not make it to one full hour.

Figure 4.14: 20 ml of n-octane and cyclooctane with 4 drops of Additive 36 after 30 seconds of shaking, approximately 0.85% and 0.72% solute by mass

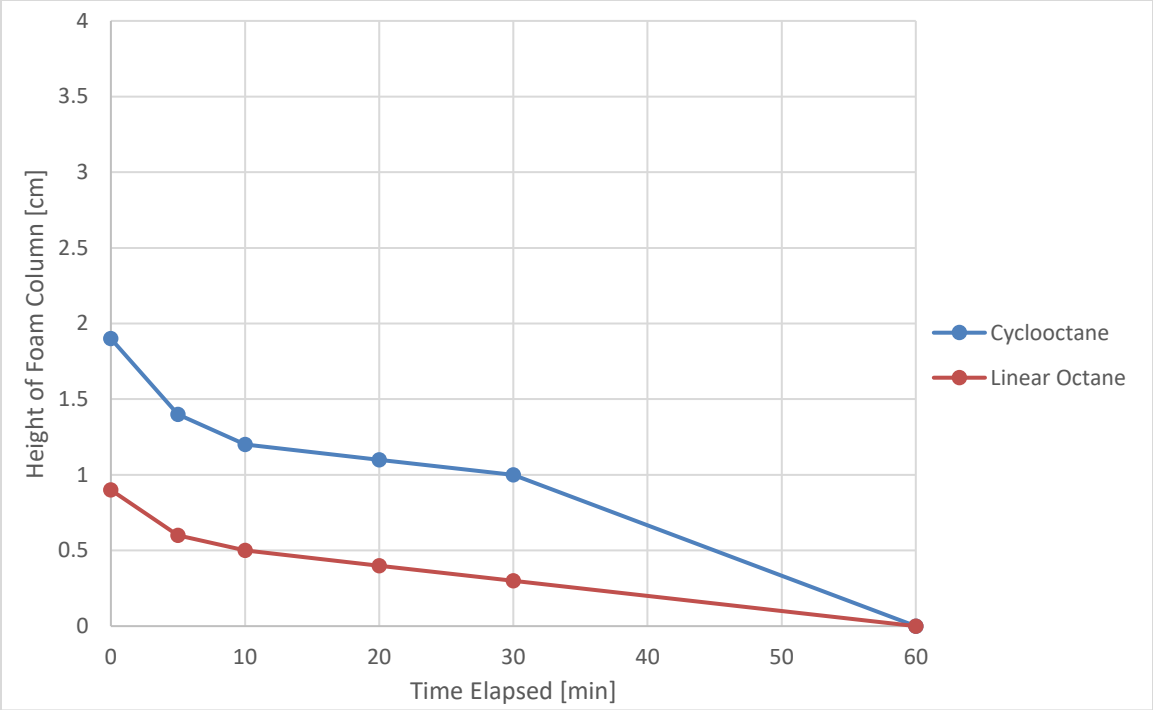

Figure 4.15: 20 ml of cyclooctane and linear octane with 4 drops of additives foam initial height and decline

4.4 CONCLUSIONS

Based on the results from the non-aqueous secondary component screening, several conclusions can be reached. First, there exists a sweet spot in the range of viscosity for a compound to create a stable foam. Comparing the foaming potential of pentane, octane, decane, and light mineral oil, the biggest change between these four compounds is the viscosity change due to an increase in hydrocarbon chain length. Decane showed the best response while light mineral oil could not produce very much foam. In addition, cyclooctane had very good foaming potential with a viscosity between that of decane and light mineral oil suggesting somewhere between 2.133 cP and 15 cP is the ideal viscosity to generate foam.

Secondly, the high potential that toluene showed as a secondary component indicated that viscosity was not the only factor. The viscosity of toluene is lower than that of decane, but the aromatic structure likely leads to the large amount of stable foam. In

addition, the difference in performance between n-octane and cyclooctane suggests that either the viscosity or structural differences play a large role.

Finally, the butanol test showed that the performance of individual additives is highly dependent upon the polarity of the solvent. Some additives that performed very well with non-polar solvents precipitated out in polar solvents and produced no foam. Thus, three criteria, viscosity, structure, and polarity, for secondary components matter in terms of generating and stabilizing foams with the select six additives. Table 4.1 includes the dipole moment and dynamic viscosity at room temperature of all the tested secondary components in this experiment and in later experiments for reference.

Table 4.1: Dipole moment and dynamic viscosity comparison of secondary components

Component	Dipole Moment [D]	Dynamic Visc. [cP]
Glycerol	2.560	1412.000
Propylene Glycol	2.550	42.000
Ethylene Glycol	2.360	16.200
Ethyl Acetate	1.880	0.450
DI Water	1.855	0.937
n-Butyl Acetate	1.840	0.658
1-Octanol	1.760	7.590
2-Heptanol	1.710	5.970
1-Pentanol	1.700	3.470
Ethanol	1.690	1.070
1-Butanol	1.660	2.593
2-Propanol	1.660	2.040
1-Hexanol	1.650	4.590
Toluene	0.360	0.552
Olive Oil	0.150	52.000
H. Mineral Oil	0.150	35.000
L. Mineral Oil	0.100	15.000
Decane	0.070	0.876
n-Octane	0.070	0.524
n-Pentane	0.007	0.222
Cyclooctane	~0.000	2.133
Nitrogen	0.000	0.018

https://www.nist.gov/
https://en.wikipedia.org

Chapter 5: Non-Aqueous Secondary Component Testing with Pentane

Once the properties were established that could lead to strong non-aqueous foam, the secondary components were tested with either or both Additive 34 and/or Additive 36 and some fraction of pentane to again stand in for y-grade. Ultimately, the goal of this experiment was to reduce the amount of secondary component needed to still allow for foam that would last at least 10 minutes. This time was chosen because it was believed to be of a stable enough condition to propagate within a porous media. Additives 34 and 36 were chosen because they showed the strongest results for polar and nonpolar secondary components respectively. The results from this experiment would be the basis for tertiary corefloods and apparent viscosity measurements with the foam later.

5.1 MATERIALS

For this experiment, some secondary components from non-aqueous secondary component screening were again used, and some new secondary components were added that skipped the screening entirely due to trends seen previously. Due to their positive results in the non-aqueous secondary component screening, only Additives 34 and 36 were evaluated further. Primarily, Additive 34 would be used with more polar compounds with a dipole moment greater than that of toluene, and Additive 36 would be used with non-polar compounds with a dipole moment less than that of toluene. Toluene showed strong foam for both additives so it's dipole moment was considered as a midway point between the two conditions.

Light mineral oil, seen previously, was tested since it was believed that adding pentane would decrease the solution's viscosity down into the ideal range for non-aqueous foam generation. In addition, a heavy mineral oil with a viscosity of 35 cP and density of 0.83 g/ml was obtained from Fisher Chemical. If creating the ideal viscosity from a blend of pentane and mineral oil was the answer to non-aqueous foam, having a higher viscosity mineral oil to start would allow for a lower volume fraction of mineral oil to produce the same resulting viscosity. Light mineral oil was tested with only

Additive 36 since it is almost entirely nonpolar, but heavy mineral oil was tested with both Additive 34 and 36.

Aromatics and less refined petroleum products were also tested. Based upon its strong performance to generate stable foam on its own, toluene was investigated further with pentane and Additive 34. Diesel fuel, used previously in the screening tests, was also tested to see if it could stabilize pentane-based foam with both Additives 34 and 36. Finally, a medium-weight crude oil sample was evaluated. Evidence exists that natural surfactants and asphaltenes within crude oil can act as indigenous foam stabilizers (Zaki 2002), (Callaghan 1985).

Testing crude oil as a secondary component has two benefits. First, if oil is already naturally present within the reservoir, it would not need to be injected with the y-grade and surfactant. It would mix naturally and potentially act to stabilize the foam. Secondly, knowing the amount of crude oil needed to stabilize y-grade foam could help to optimize an injection strategy later.

Butanol showed a decent performance with Additive 34, so a wider array of alcohols was tested to see if there was a trend in foam stability. Alcohols tested included 2-propanol, 1-butanol, 1-pentanol, 1-hexanol, 2-heptanol, and 1-octanol. All alcohols were tested with Additive 34 due to their polar nature. The assay and supplying company for the alcohols are listed in Table 5.1.

Table 5.1: Assay and supplier for various alcohols tested

Compound	Min. Assay	Supplier
2-Propanol	99.60%	Thermo Scientific
1-Butanol	99.90%	Fisher Chemical
1-Pentanol	99.00%	Acros Organics
1-Hexanol	99.00%	Alfa Aesar
2-Heptanol	99.00%	Acros Organics
1-Octanol	99.00%	Sigma Aldrich

To take the testing of polar compounds one step further, ethylene glycol, propylene glycol, and glycerol were tested as secondary components since chemically they contain saturated carbon chains ending in hydroxyl groups like alcohol, but have an even higher polarity and viscosity due to a higher number of the groups. Alcohols contain one hydroxyl group, the glycols contain two, and glycerol contains three. The polarity of the ethylene glycol, propylene glycol, and glycerol were 2.36, 2.55 and 2.56 D respectively, and the dynamic viscosities were 16.2, 42.0, and a very high 1412.0 cP respectively. The ethylene glycol, propylene glycol, and glycerol were manufactured by Fisher Chemical. Both glycols and glycerol had assays of >99.5%.

Ethyl acetate and n-butyl acetate are esters similar to triglycerides, but has a much higher polarity and lower viscosity. The main reason that these two acetates were investigated was that additives 7 and 34 were dissolved within ethyl acetate and n-butyl acetate respectively. As the listed concentration for these two surfactants were only 25% and 35% by weight, each drop of untreated surfactant was primarily acetate, and the effect that the solvent had on foaming potential was unknown. The two acetates tested were manufactured by Acros Organics. The assay of the ethyl acetate was 99.5% and the n-butyl acetate was 99.0%.

Myritol is a blend of fatty acid esters that was originally provided to be tested as an additive to y-grade. Thus, it is listed as Additive 38. However, the liquid displayed a viscosity similar to that of light mineral oil, so it was further investigated as a potential secondary component with pentane without being screened on its own. Since the product was listed as being mainly nonpolar glycerides, myritol was tested with Additive 36. The product is listed as being comprised of mainly caprylic and capric triglycerides with a viscosity of 27 to 33 cP.

Finally, cyclooctane was once again examined based upon its past performance. The cycloalkane was tested with both Additive 34 and 36 to verify that the hypothesis that 34 works better with polar secondary components and 36 works better with nonpolar secondary components.

5.2 EXPERIMENTAL PROCEDURE

A form of wet chemical analysis was used primarily for this experiment to evaluate the foaming potential at different volume fractions of pentane and secondary component. Samples were created from 50% pentane and 50% secondary component by volume to 95% pentane and 5% secondary component by volume at 5% intervals. This method helped determine the minimum volumetric fraction of secondary component needed to still allow foam to be seen at 10 minutes, the goal time. The total liquid volume in the 40 ml vials was always 20 ml with 4 drops of additive.

All vials were labelled with the primary and secondary component present, the number of the additive used, and the volume of the secondary component over the volume of pentane in milliliters. Samples were shaken for 30 seconds before a picture of the initial foam height was taken and the decline in the foam height in at select intervals out to 1 hour. All legend labels on the right side of the graphs are volume percentages of the pentane within the sample. Thus, we expect the 50% samples to perform better than the 95% samples. Some new secondary components failed to create any foam with pentane and additive in the 50/50 percent vial, thus the analysis for that component did not continue.

5.3 RESULTS

5.3.1 Light Mineral Oil and Pentane

A volume fraction analysis was performed on light mineral oil, and it was observed that the mineral oil can be taken down to approximately 25% by volume and still produce 10-minute foam. The initial height of the foam is shown in Figure 5.1. Mineral oil as a secondary component is very exciting since it is widely available, chemically simple, and works well to support pentane-based foam. The decline in the foam heights overtime is shown in Figure 5.2.

The results of 50% to 70% by volume of pentane with the light mineral oil are close in performance. A definite trend is seen where the initial height of the foam column increases as the volume fraction of light mineral oil also increases. While a 75% by

volume pentane mixture did make it past ten minutes, there is significant improvement in performance for the 70% by volume mixture indicating that this might be the ideal fraction for a foam injection strategy.

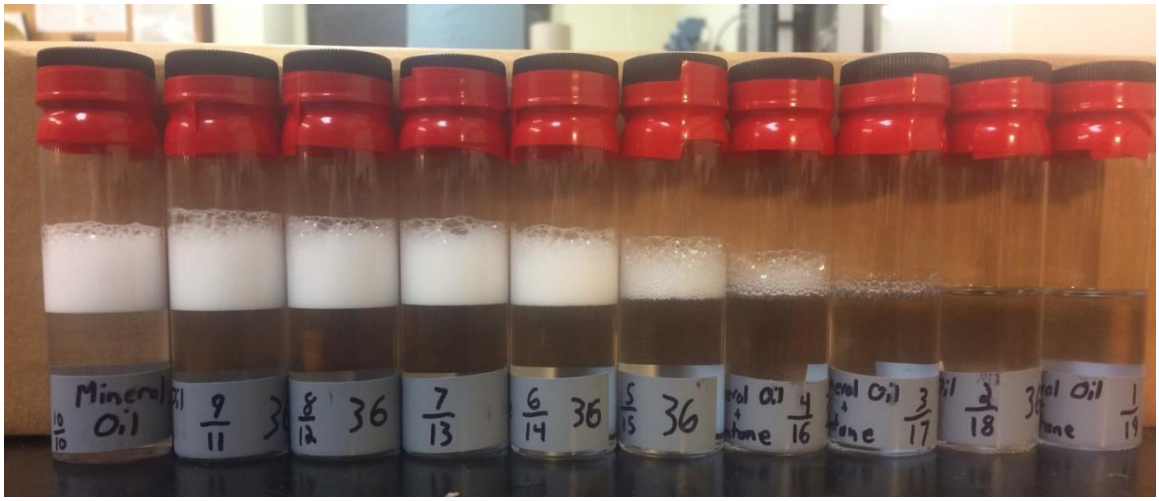

Figure 5.1: Analysis of light mineral oil and pentane from 50% to 95% pentane by liquid volume, 4 drops of additive per vial

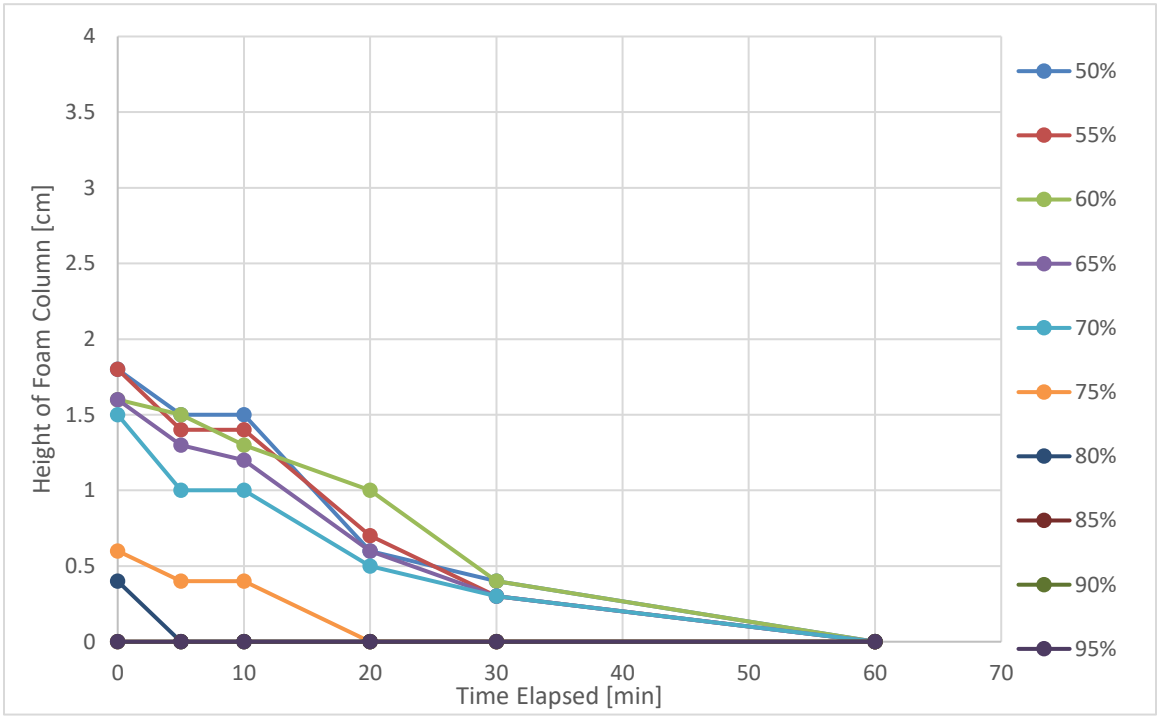

Figure 5.2: Analysis of light mineral oil and pentane from 50% to 95% pentane by liquid volume, 4 drops of additive per vial

5.3.2 Heavy Mineral Oil and Pentane

As mentioned previously, a hypothesis was presented that the volume fraction of heavy mineral oil to produce a ten-minute foam would be lower than that of light mineral oil since not as much heavy mineral oil would be needed to hit the ideal liquid viscosity range. Some evidence exists to support this hypothesis if the cases with the same additive are compared, but there is no definitive proof that the higher viscosity of the heavy mineral oil was highly beneficial. The first test heavy mineral oil and pentane was done with Additive 34 and is shown in Figure 5.3 and Figure 5.4. The second test of with Additive 36 is shown in Figure 5.5 and Figure 5.6.

Although some of the initial recorded heights of the heavy mineral oil with Additive 34 were higher compared to light mineral oil with Additive 36, all samples saw a sharp decline in foam height at the five-minute mark. In addition, no foam was able to last longer than thirty minutes. This evidence supports the assessment that Additive 34 does not work with nonpolar secondary components as well as Additive 36.

Heavy mineral oil with Additive 36 showed very similar trends to light mineral oil. One slight difference between the two is that the best heavy mineral oil results were actually for the 55% by volume of pentane compared to the 50% by volume being the best for light mineral oil. This fact could suggest that 55% by volume of pentane with heavy mineral oil is at the ideal viscosity for this surfactant. However, the results for heavy mineral oil show that the is no improvement for which lowest volume fraction can hit the ten-minute foam mark, which disproves the original hypothesis.

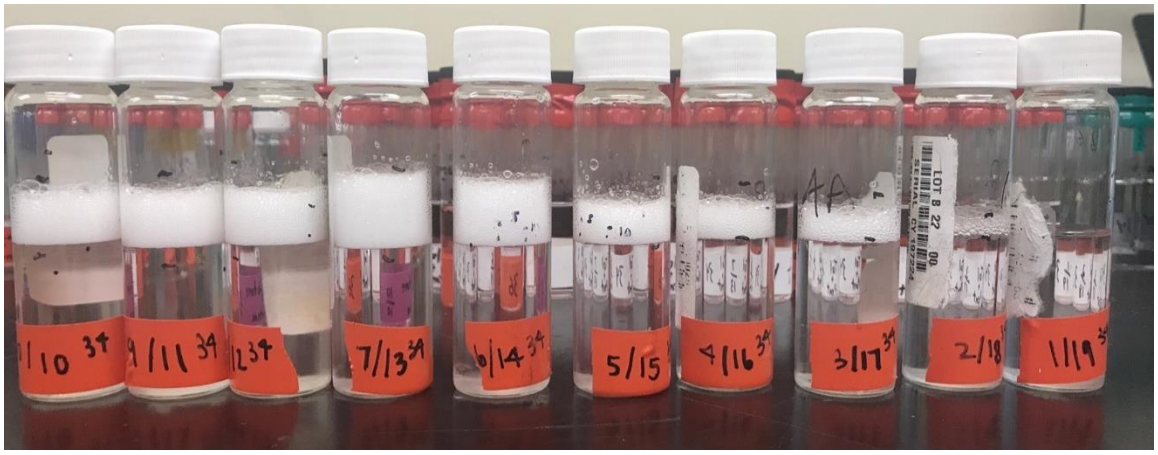

Figure 5.3: Analysis of heavy mineral oil and pentane from 50% to 95% pentane by liquid volume, 4 drops of Additive 34 per vial

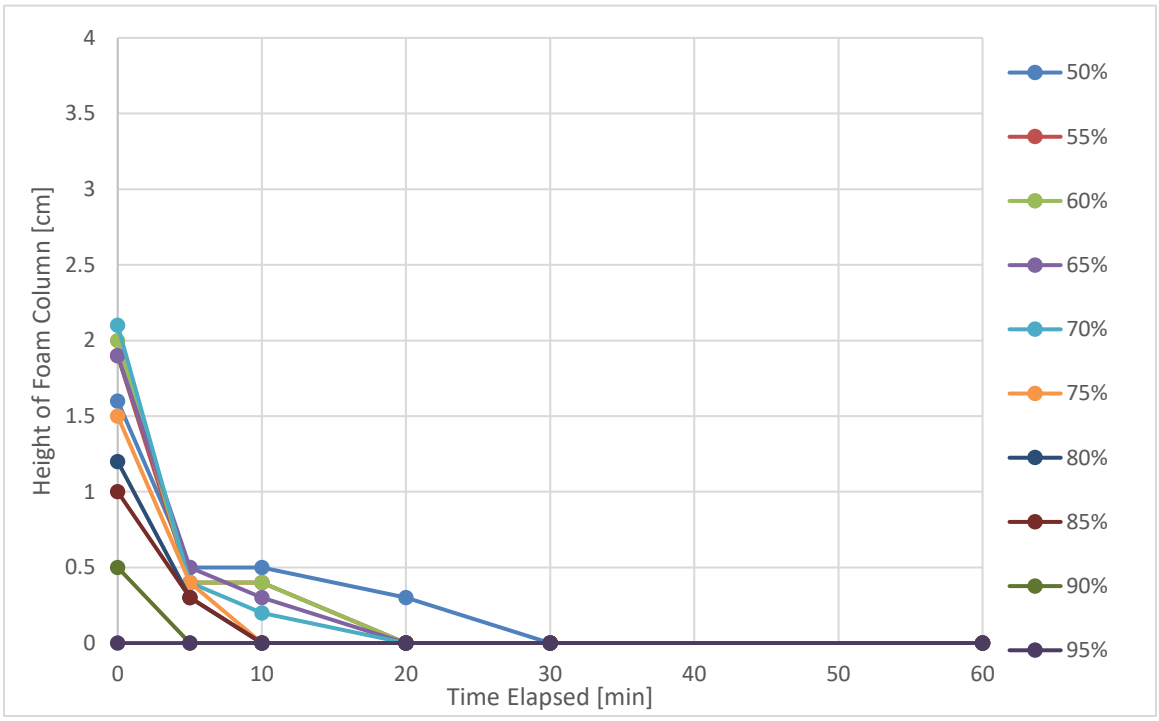

Figure 5.4: Analysis of heavy mineral oil and pentane decline profiles, Additive 34

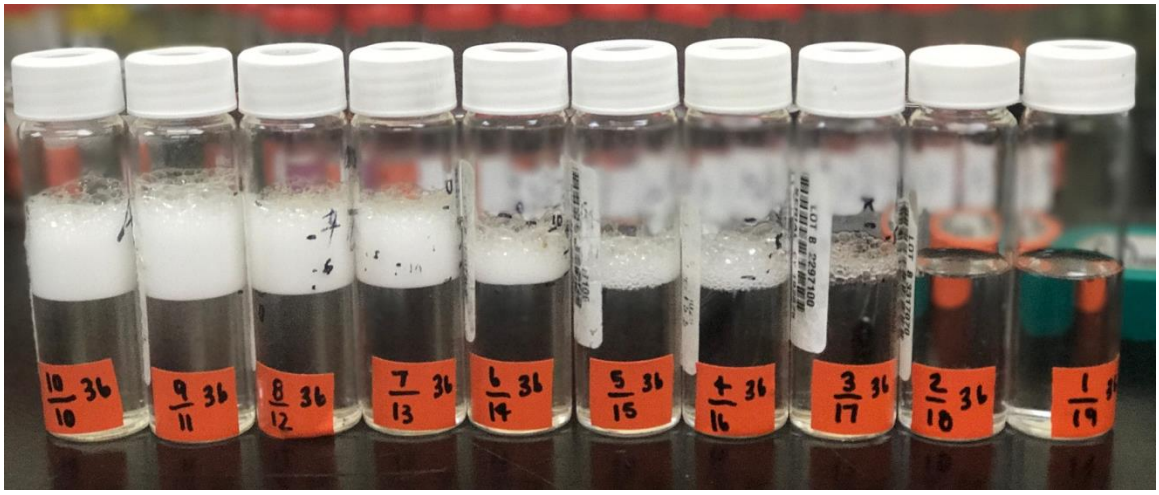

Figure 5.5: Analysis of heavy mineral oil and pentane from 50% to 95% pentane by liquid volume, 4 drops of Additive 36 per vial

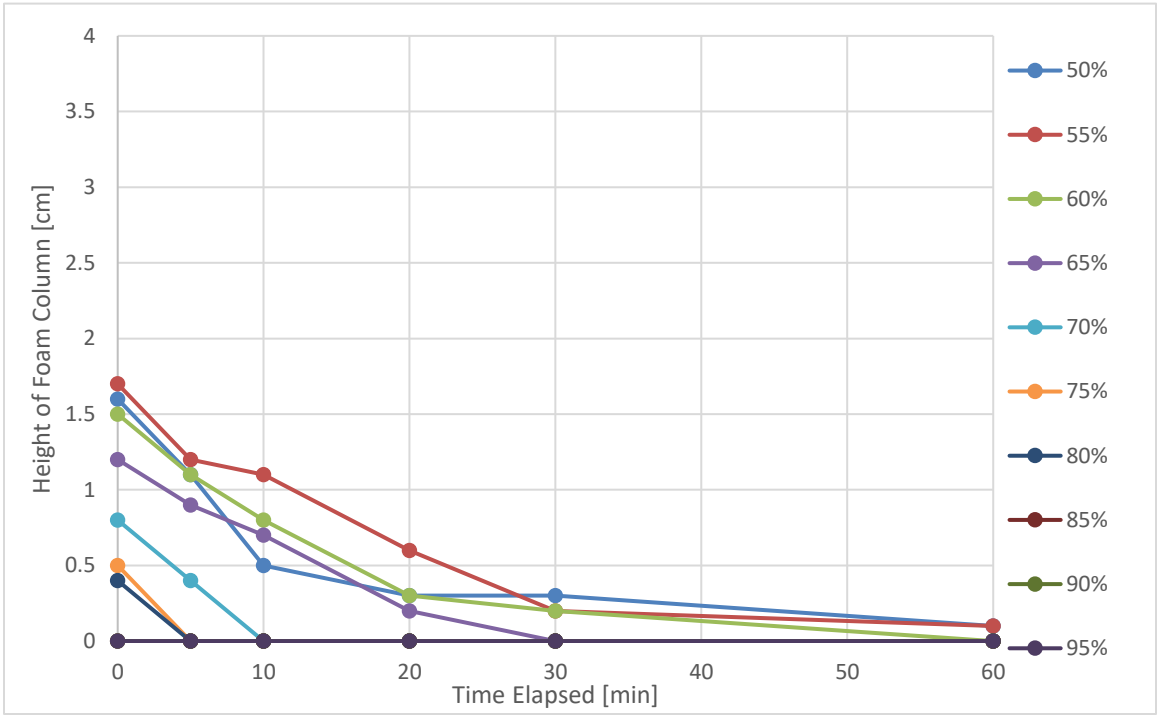

Figure 5.6: Analysis of heavy mineral oil and pentane decline profiles, Additive 36

5.3.3 Toluene and Pentane

Toluene mixed with the pentane performed well at higher fractions of toluene, but did not show very strong results as the fraction of toluene was decreased. The assumption here is that the foaming potential benefit of the aromatic compound was not enough to overcome negative effects of the mixture not being viscous enough to stabilize foam.

The sample with the highest amount of toluene showed the best result in foam initial height and stability overtime. As more pentane is added, both initial foam height and height overtime fall in a uniform fashion. Results showed that 35% toluene and 65% pentane by volume could support 10-minute foam while samples under 80% toluene by volume did not generate any foam that lasted longer than a few seconds.

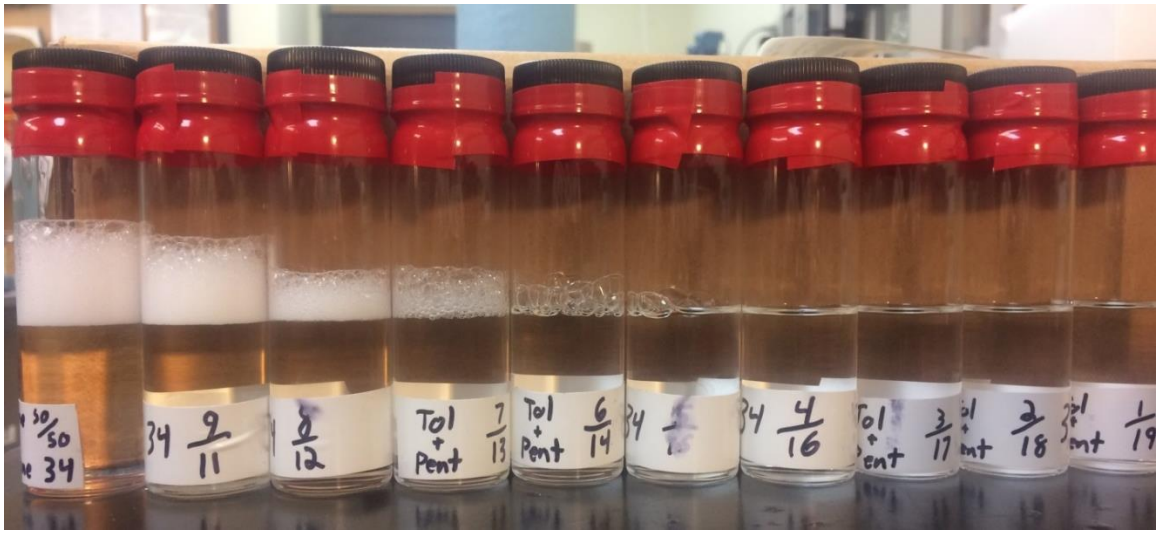

Figure 5.7: Analysis of toluene and pentane from 50% to 95% pentane by liquid volume, 4 drops of Additive 34 per vial

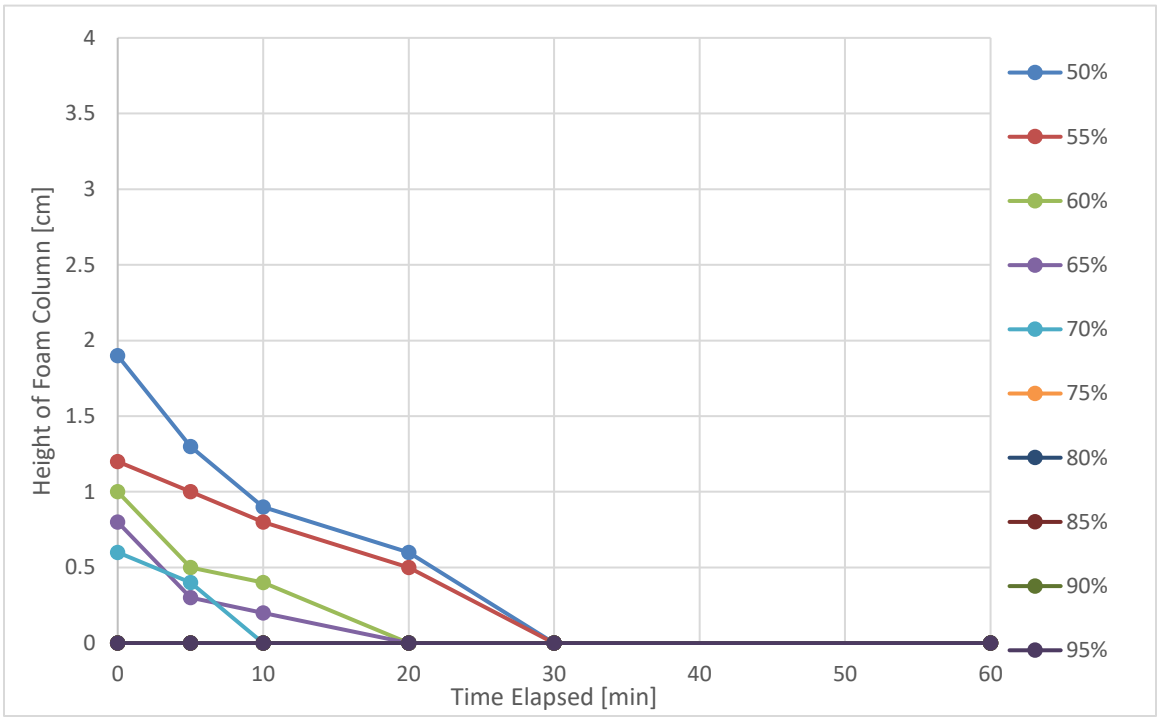

Figure 5.8: Analysis of toluene and pentane decline profiles, Additive 34

5.3.4 Diesel Fuel and Pentane

Samples with a diesel fuel fraction of 50% to 5% and Additive 34 were clustered initially, but showed different declines overtime. All samples show a very sharp decline similar to that of heavy mineral oil with Additive 34 suggesting that this additive is capable of initially generating a considerable amount of foam, but is unable to then support the foam overtime for nonpolar secondary components and pentane. The 65% diesel fuel and 35% pentane sample with Additive 34 was to stabilize foam for longer than ten minutes. Initial foam heights and the foam declines through time with Additive 34 are shown in Figures 5.9 and 5.10.

Diesel fuel and pentane with Additive 36 showed better results since this additive has been identified as being tailored to nonpolar solvents. The three samples with the highest fractions of diesel fuel were grouped together to begin, and declined at roughly the same rate. The sample with 75% pentane and 25% diesel fuel with Additive 36 was identified as being the lowest fraction to still maintain 10-minute foam. Initial foam heights and the foam declines through time with Additive 34 are shown in Figures 5.11 and 5.12.

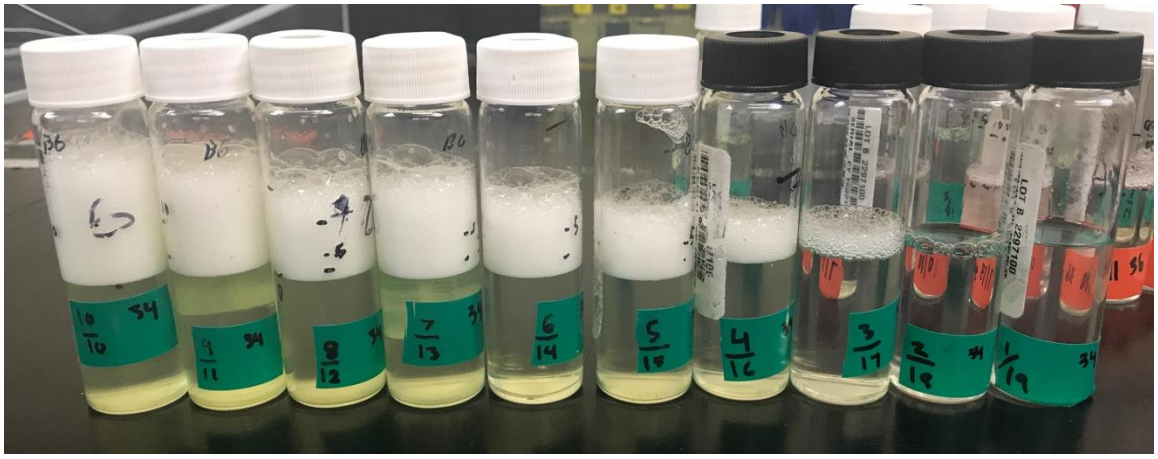

Figure 5.9: Analysis of diesel fuel and pentane from 50% to 95% pentane by liquid volume, 4 drops of Additive 34 per vial

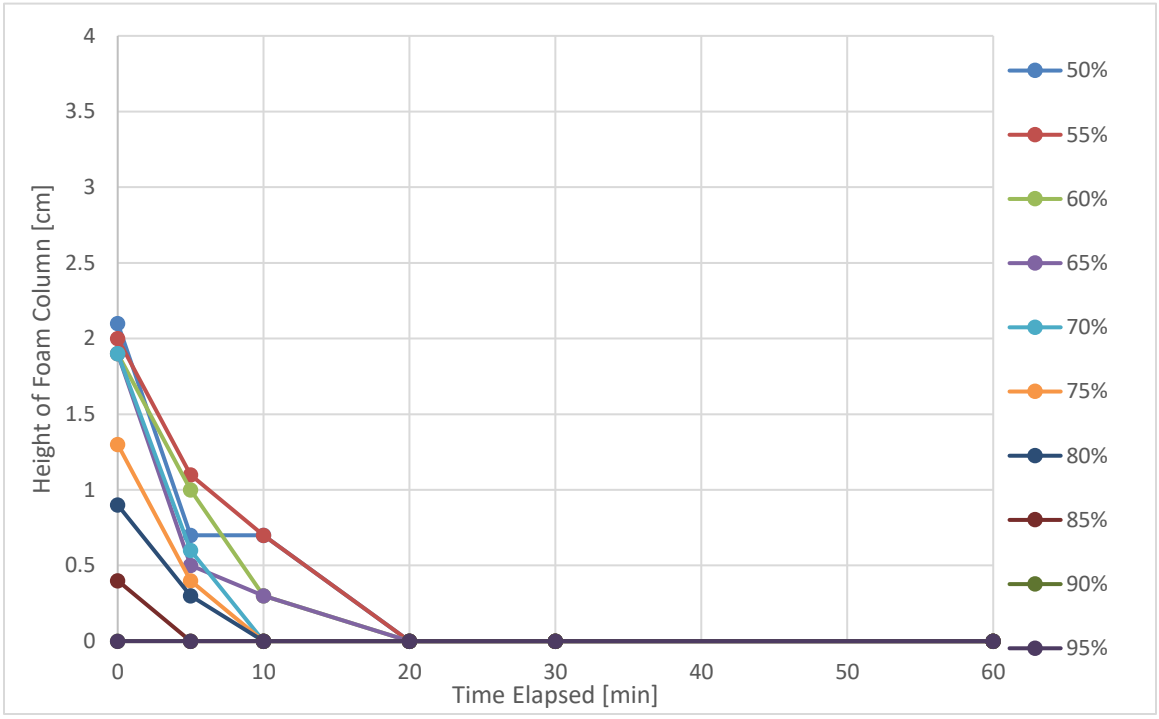

Figure 5.10: Analysis of diesel fuel and pentane decline profiles, Additive 34

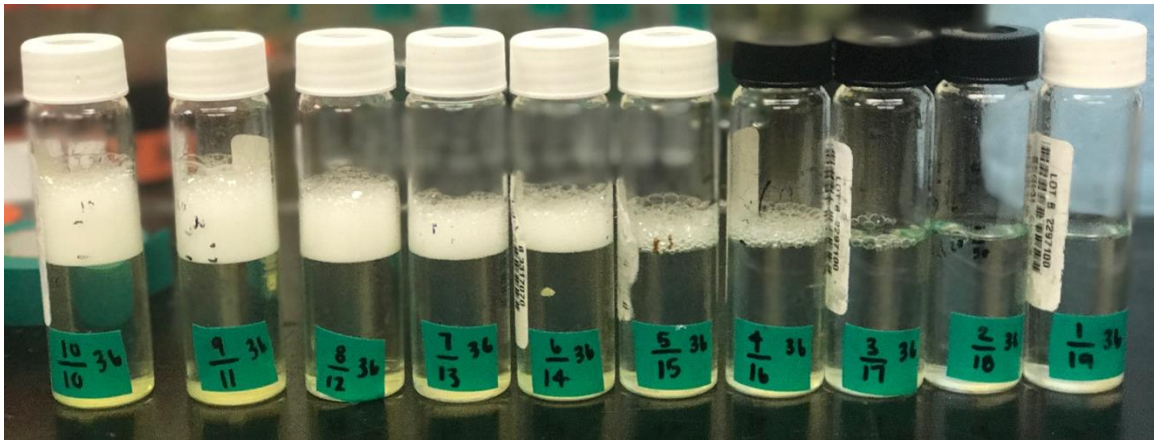

Figure 5.11: Analysis of diesel fuel and pentane from 50% to 95% pentane by liquid volume, 4 drops of Additive 36 per vial

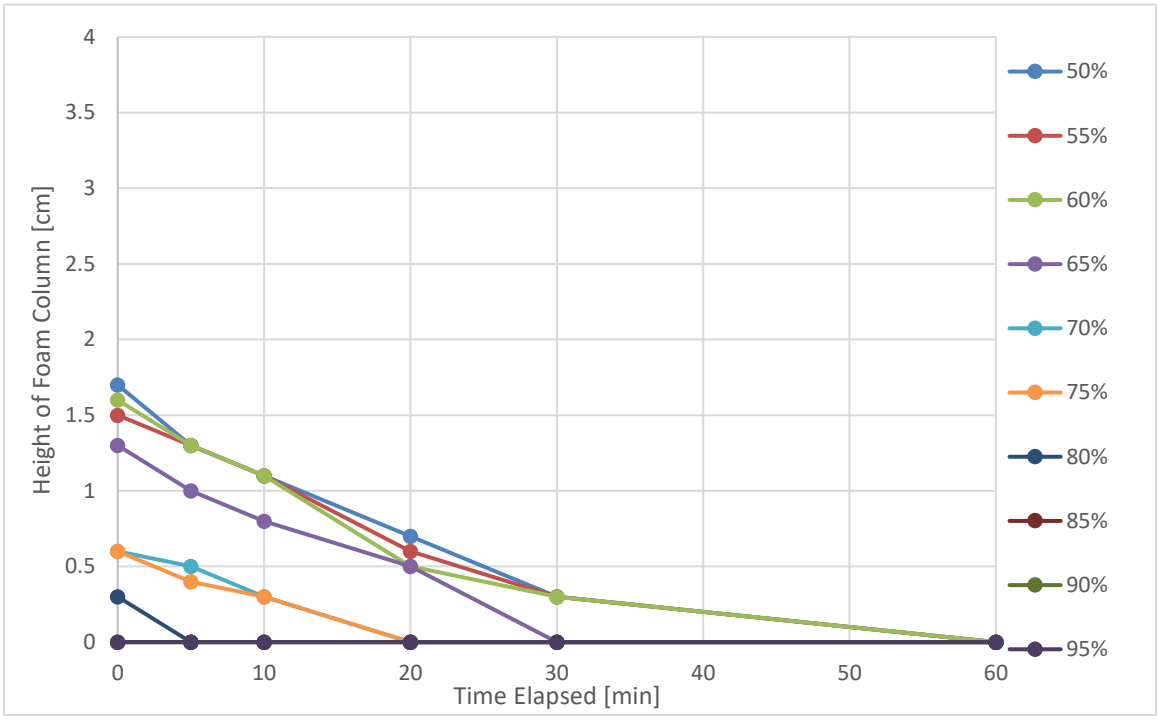

Figure 5.12: Analysis of diesel fuel and pentane decline profiles, Additive 36

5.3.5 Crude Oil and Pentane

The crude oil sample worked well with Additive 36 to stabilize resulting foam. The initial height of the foam generated was comparable to that of other secondary components with the same additive, but crude oil proved to be an effective stabilizer as considerable foam columns were observed at low fractions of crude oil even out to 30 minutes. The high levels of heavy aromatic compounds and presence of asphaltene within the crude oil are thought to be the main factors for this performance. A 10-minute foam was able to be produced with only 25% crude oil by volume. Initial foam heights and the foam declines through time with Additive 36 are shown in Figures 5.13 and 5.14.

Figure 5.13: Analysis of crude oil and pentane from 50% to 95% pentane by liquid volume, 4 drops of Additive 36 per vial

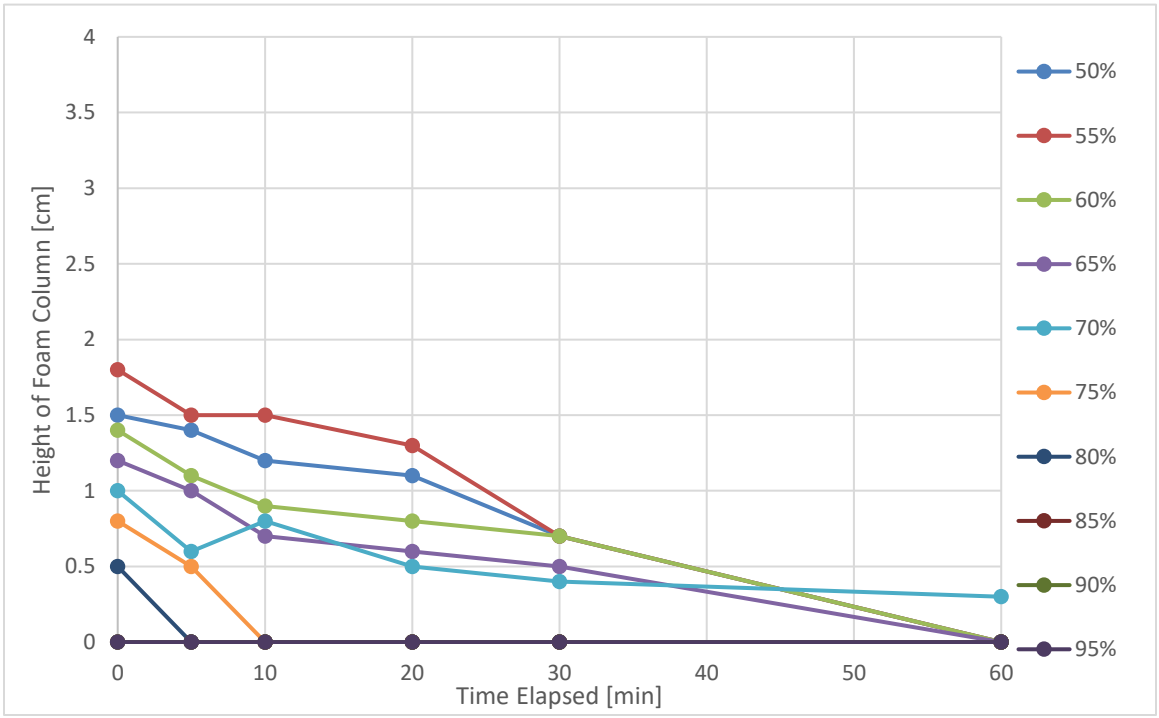

Figure 5.14: Analysis of crude oil and pentane decline profiles, Additive 36

5.3.6 Alcohols and Pentane

Alcohols from 2-propanol up to 1-octanol were tested at the same fraction to pentane and with the same amount of Additive 34. It was observed that heavier alcohols were better at generating and sustaining foam while the lightest alchol, propanol, could not generate a foam that would last longer than a few seconds. It is believe that the higher viscosities of the heavier alcohols contributed to the stability. Intestingly, hexanol seemed to perform better than heptanol at foam stabiliization even though heptanol is heavier. Since octanol showed the best initial height and stability through time, it was selected to undergo further analysis to see how low the octanol fraction could be taken. Initial foam heights and the foam declines for the various alcohols through time with Additive 34 are shown in Figures 5.15 and 5.16.

The octanol performed very well with the sample containing 30% octanol and 70% pentane showing foam for over 10 minutes. Higher concentrations of octanol were able to support foam for over an hour. This success suggests that Additive 34 can compete with 36 given the correct, polar secondary component. Initial foam heights and the foam declines through time for octanol and pentane with Additive 34 are shown in Figures 5.17 and 5.18.

Figure 5.15: Comparison of various alcohols and pentane and toluene with pentane, 4 drops of Additive 34 per vial

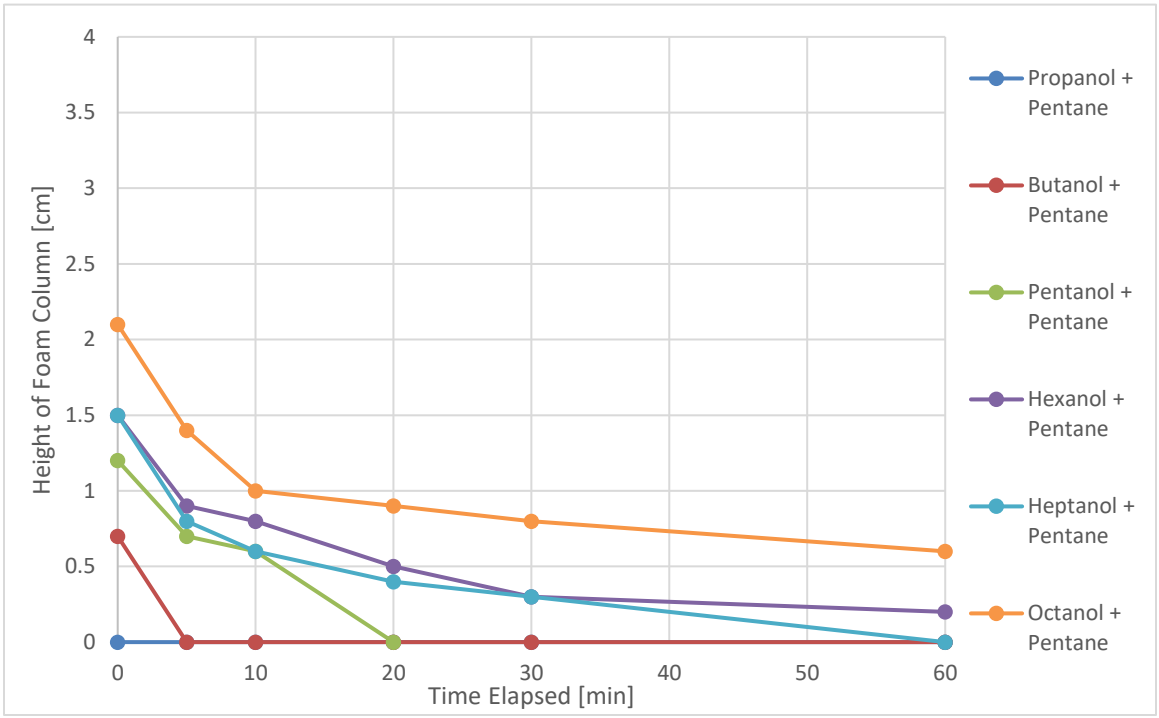

Figure 5.16: Various alcohol with pentane decline profiles, Additive 34

Figure 5.17: Analysis of octanol and pentane from 50% to 95% pentane by liquid volume, 4 drops of Additive 34 per vial

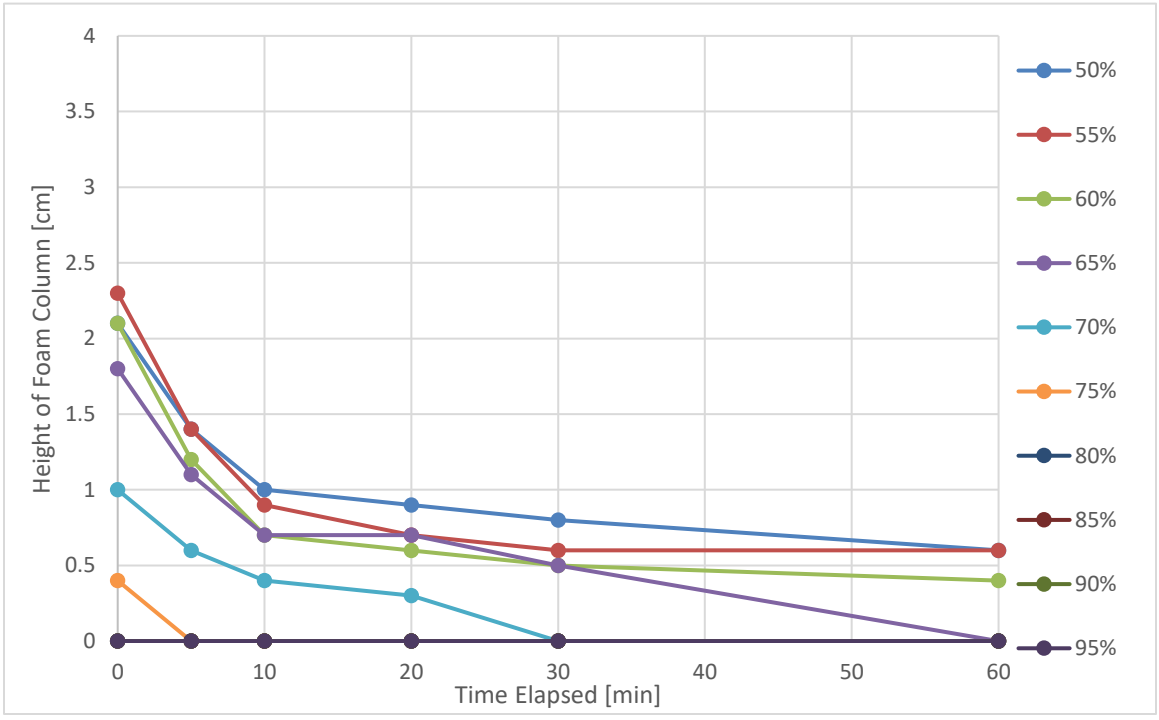

Figure 5.18: Analysis of octanol and pentane decline profiles, Additive 34

5.3.7 Glycols

Ethylene and propylene glycol are both very polar even compared with the alcohols tested previously. However, when they were combined with pentane and Additive 34, no foam was able to be generated at 50% glycol and 50% pentane by volume. Instead, the mixture turned cloudy. Overtime, there was a noticeable separation of the phases where the bottom phase remained cloudy and small globules were noticed at the interface of the two phases. It appears that the glycol is either too polar to work with Additive 34 or there is something else at play preventing foam generation. The two glycols with pentane samples are shown in Figure 5.19.

Figure 5.19: 10 ml of ethylene glycol and propylene glycol with 10 ml of pentane and 4 drops of Additive 34 after 30 seconds of shaking, approximately 0.54% and 0.58% solute by mass respectively

5.3.8 Glycerol

One step further from glycol is glycerol which is both very polar and very viscous. Similar results to glycol were seen where the glycerol beaded and no foam was stabilized. In addition, the seal at the top of the testing vial began to push outward signifying a pressure build up in the vial. A leak in the vial's top eventually occurred and the pentane evaporated off before a picture was taken the next day.

5.3.9 Acetates

Both acetate tests could not support foam for more than a few seconds. While the acetate is polar and Additive 34 works well with polar secondary components, the viscosity of the acetates is not much higher than that of pentane which would support viscosity as a major parameter for foam potential. It can be concluded that the miniscule amount of acetate that comes with the surfactant has no effect on foam stability, so all stabilizing effects come directly from the surfactant themselves. The two acetate samples with pentane are shown in Figure 5.20.

Figure 5.20: 10 ml of ethyl acetate and n-butyl acetate with 10 ml of pentane and 4 drops of Additive 34 after 30 seconds of shaking, approximately 0.67% and 0.68% solute by mass

5.3.10 Myritol and Pentane

Based upon the tests with olive oil, expectations for myritol with pentane were low. However, this secondary component was able to produce a high initial foam height and stable foam across a wide range of volume fractions. The 40% and 35% volume fractions of myritol performed better than the higher fractions at initial height which was surprising since the myritol is not that viscous of a material. In addition, most samples showed a rather uniform decline overtime shifted by initial foam height. A 10-minute foam was observed by the sample with 25% myritol and 75% pentane, a good showing of foam stability. Initial foam heights and the foam declines through time for myritol and pentane with Additive 36 are shown in Figures 5.21 and 5.22.

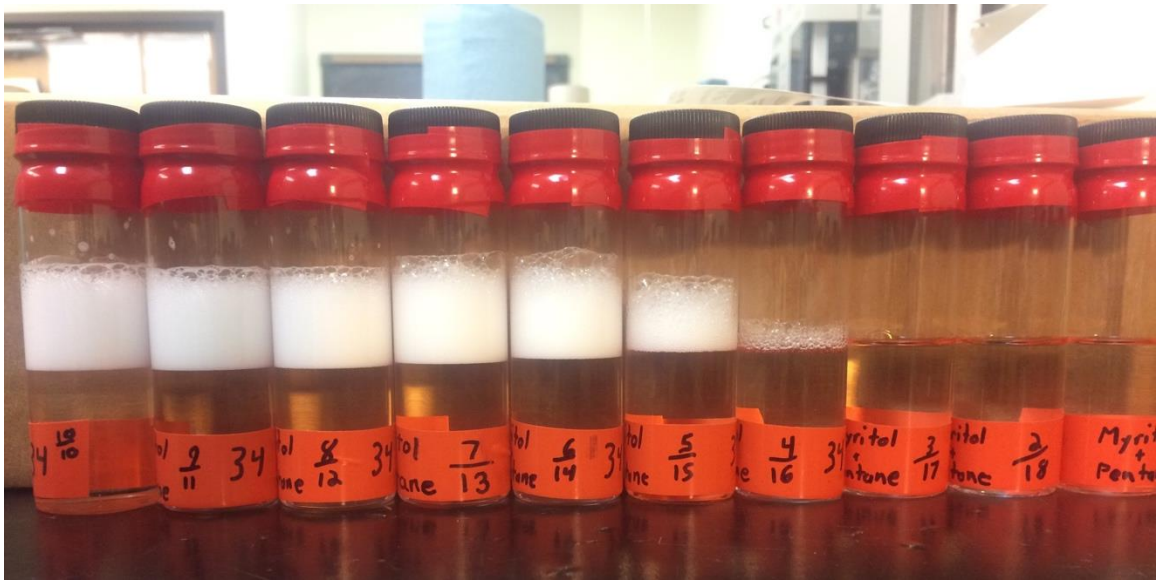

Figure 5.21: Analysis of myritol and pentane from 50% to 95% pentane by liquid volume, 4 drops of Additive 34 per vial

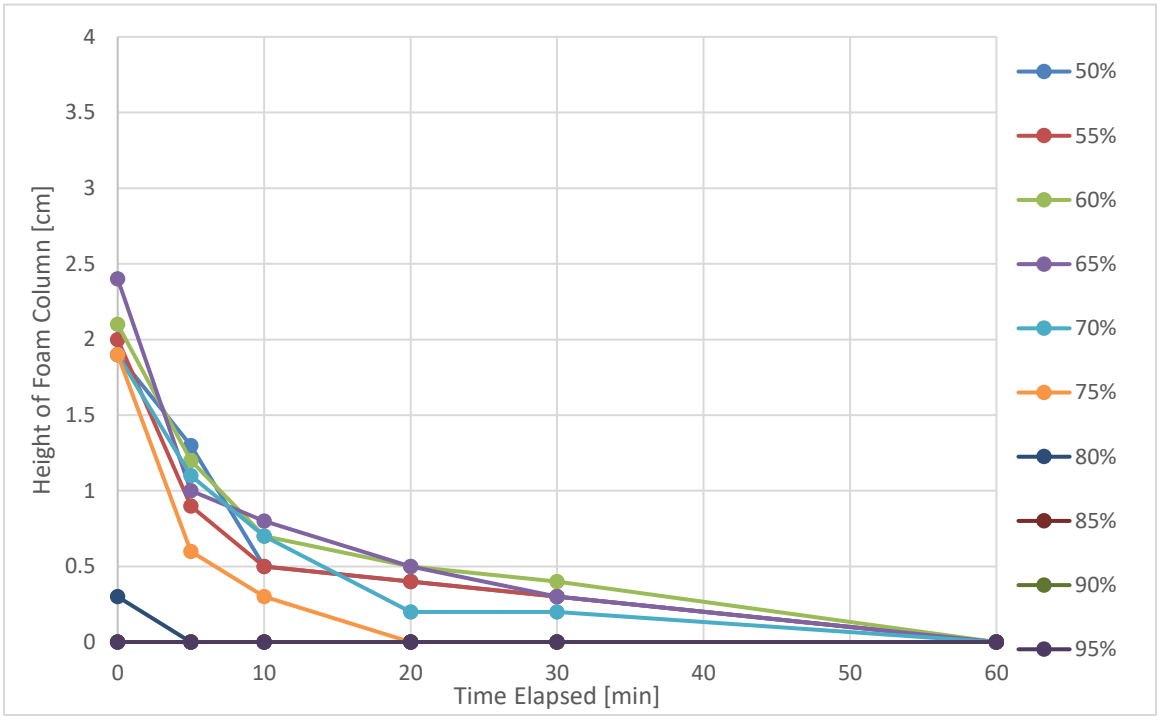

Figure 5.22: Analysis of myritol and pentane decline profiles, Additive 34

5.3.11 Cyclooctane and Pentane

Cyclooctane and pentane was tried with both Additive 34 and 36, and once again we see a similar trend. The samples with Additive 34 show a good initial foam height but sharply drop through time. Additive 36, on the other hand, showed good results at higher amounts of cyclooctane to pentane, but not so much towards the lower fractions of the secondary component. The sample with 70% pentane and 30% cyclooctane was the lowest cut of cyclooctane to generate 10-minute foam. Initial foam heights and the foam declines through time for cyclooctane and pentane with Additive 34 are shown in Figures 5.23 and 5.24 while the same results are presented for Additive 36 in Figures 5.25 and 5.26.

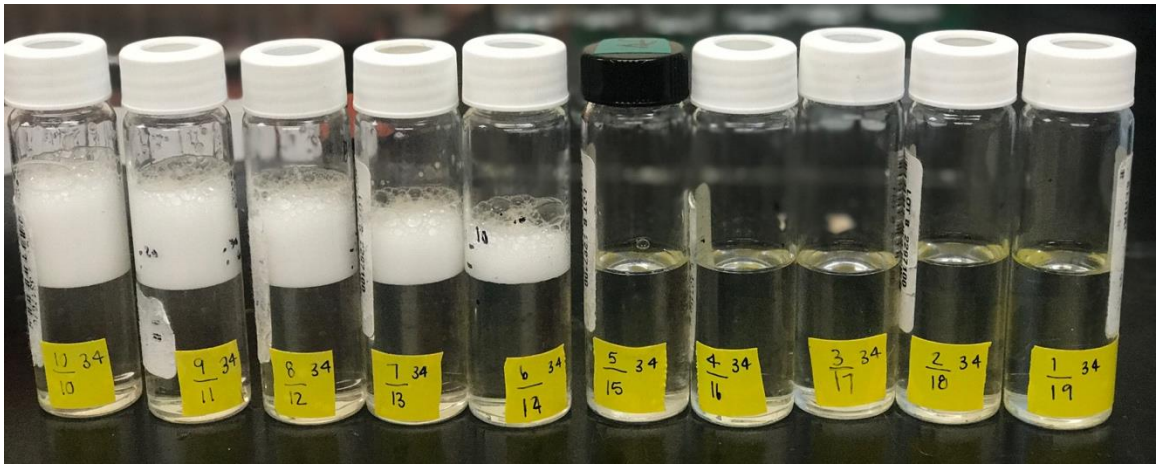

Figure 5.23: Analysis of cyclooctane and pentane from 50% to 95% pentane by liquid volume, 4 drops of Additive 34 per vial

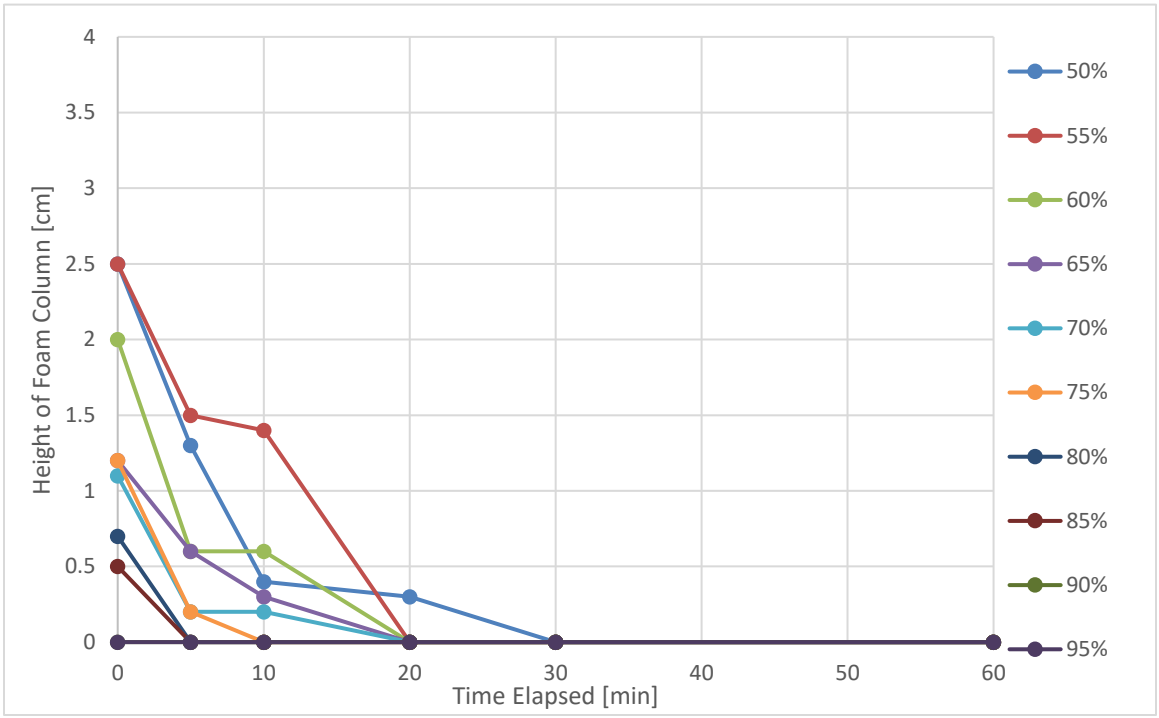

Figure 5.24: Analysis of cyclooctane and pentane decline profiles, Additive 34

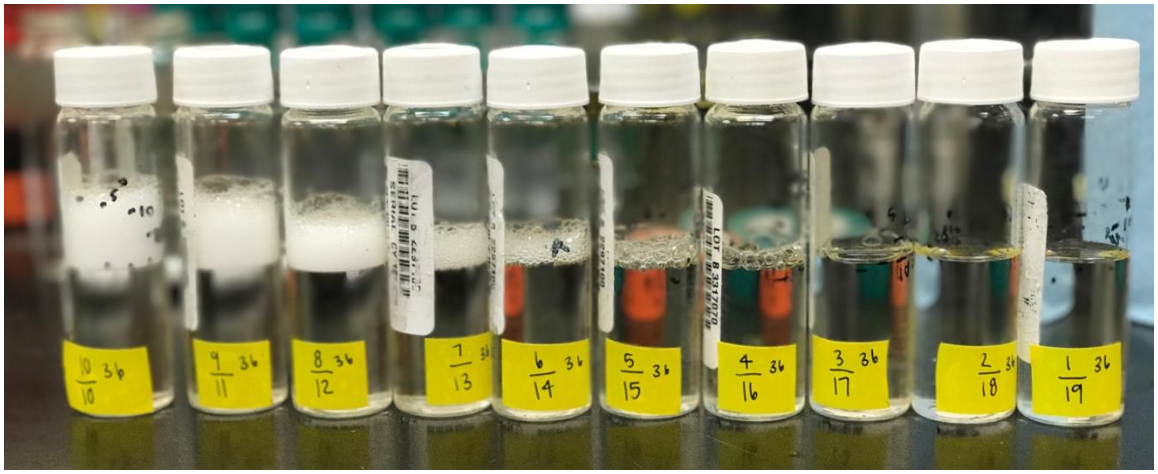

Figure 5.25: Analysis of cyclooctane and pentane from 50% to 95% pentane by liquid volume, 4 drops of Additive 36 per vial

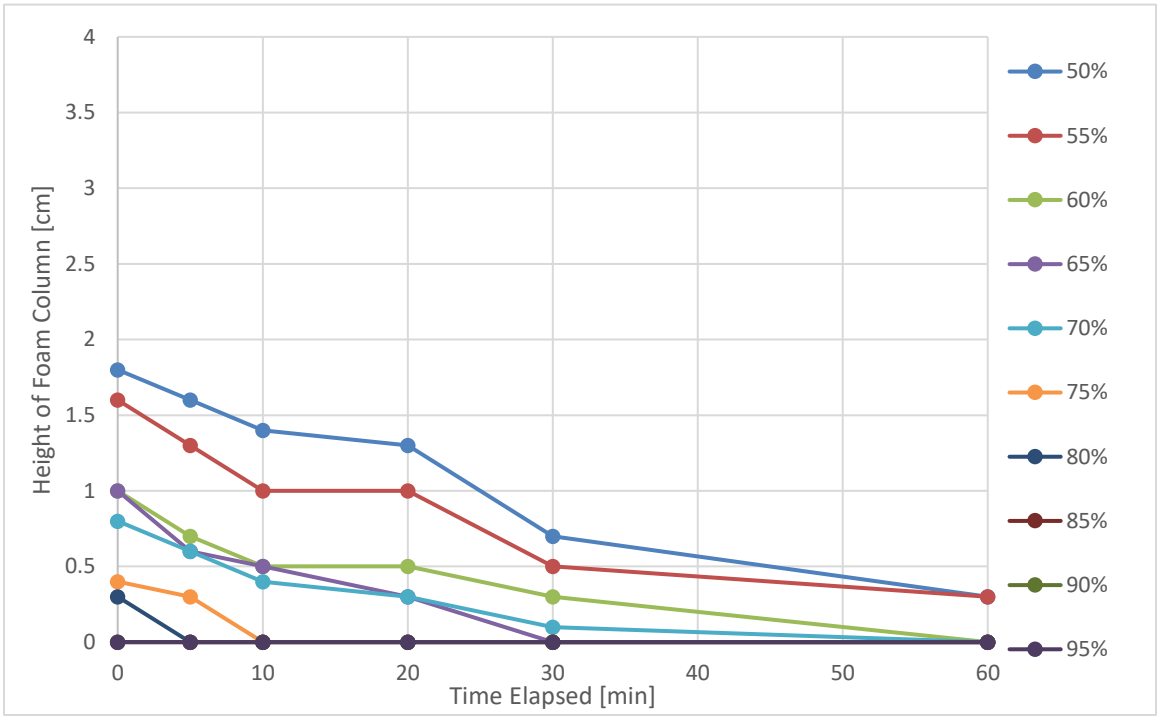

Figure 5.26: Analysis of cyclooctane and pentane decline profiles, Additive 36

5.4 CONCLUSIONS

Most secondary components were able to stabilize a 10-minute foam with a volumetric fraction of 25 to 30%. Two directions could be taken to obtain this desired foam duration. First, a nonpolar component such as mineral oil or crude oil could be used in conjunction with Additive 36. Secondly, a polar component such as octanol or myritol could be used with Additive 34. Both routes provide roughly the same amount of foaming potential at the same volumetric fractions.

Several of the secondary components tried did not work. Ethylene glycol, propylene glycol, and glyceride simple beaded at the interface of with pentane and were not able to generate any foam. Ethyl acetate and n-butyl acetate also proven to be insufficient in generating any foam.

Moving forward, the availability of the secondary components was taken into account when deciding which to continue investigating. Some samples such as cyclooctane and myritol had a limited supply on hand while others such as mineral oil and diesel fuel were readily available. Since the duality between Additive 34 and 36 seemed interesting to explore further, one polar and one nonpolar secondary component was selected as the candidate to be used in further experiments. Octanol was selected as the polar secondary component candidate and light mineral oil was chosen as the nonpolar candidate because of their strong performances and the amount potentially needed of each was easy to obtain.

A final major conclusion from this experiment was the ability of crude oil to form a strong foam. Since the oil is naturally present already within the reservoir, it may be possible to use it to our advantage as an in-situ secondary component. The y-grade injected with a surfactant would mix with the crude oil, bringing it down to a viscosity that could be foamed, and nitrogen gas could then be injected to create the foam in situ and push the injected fluids further into the reservoir. This method would eliminate the need for a stabilizing secondary component to be co-injected.

Figure 5.27 details the current methods tried to create a y-grade/pentane based foam. The first branch is semi-aqueous foam seen in Chapter 3 which will be discussed in further detail in Chapter 6. The second branch is for all secondary components with a dipole moment greater than or equal to that of toluene. These secondary components work best with Additive 34 if they can foam at all. Finally, the third branch is for all secondary components with a dipole moment less than to that of toluene. These all work best with Additive 36 even though Additive 34 provides some results.

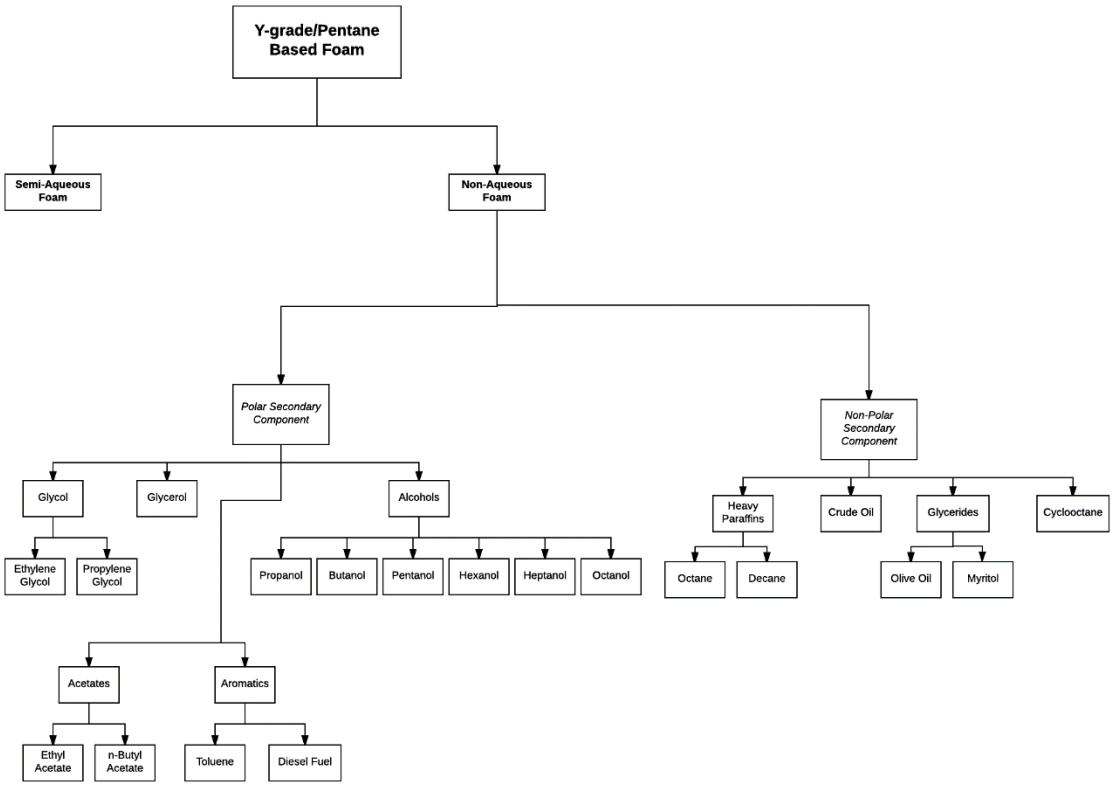

Figure 5.27: Hierarchy of y-grade/pentane based foam with secondary components and applicable additives

Chapter 6: Aqueous Secondary Component Analysis

As seen in the additive screening in Chapter 3, pentane based foam is able to be created through the addition of DI water and nonionic surfactant Additives 1 through 6 and a sulfonated anionic surfactant Additive 29. Additive 1 through 6 are all very similar with the only difference being the chain length of the ethylene oxide groups within the surfactant. Similar to the wet chemical analysis done with the non-aqueous secondary components shown previously, the water amount relative to the pentane amount was decreased to determine the lowest fraction of water necessary to yield stable foam. However, unlike the previous analysis, the concentration of the additive within the water phase was also varied to see how low that could be taken while still yielding positive results.

In addition, the salinity of the water was increased to see if it had a detrimental effect on the foam generation. Some surfactants are sensitive to salinity, and this test was just to confirm that Additive 1 would work in a saline environment. Also, a cloud point test was performed on Additive 1 with a variety of concentrations and salinities in water to determine the ideal temperature for foam generation.

6.1 Water and Surfactant Concentration Limits

Additive 1, a nonionic surfactant, was selected to investigate how low the surfactant concentration and water concentration can be taken with pentane to still yield an emulsion-based gel that can trap air bubbles. To begin, six water stocks of 2.0% KCl by weight were created from DI water. The surfactant was then added by a plastic pipette dropper to each of the stocks to yield a surfactant concentration ranging from 0.5% to 3.0% mass concentration in half percentage intervals. Finally, each aqueous stock was combined with pentane in Kimble 40 ml vials from 6.25% water to 37.50% water by volume in 6.25% intervals. Both pentane and the aqueous solution was transferred to the testing vial by pipette dropper.

All vials were only half filled to allow a 50/50 gas to liquid ratio in the vials. All samples were shaken for 30 seconds. Observations and heights of the foam and water columns were taken at the beginning and at standard intervals used in this project. Figures 6.1 to 6.12 were compiled to show how the foam column would decrease overtime for different water percentages at different surfactant concentrations. The samples are aligned from lowest water fraction to highest water fraction for each additive concentration tested.

Figure 6.1: 0.5% surfactant concentration in the aqueous phase

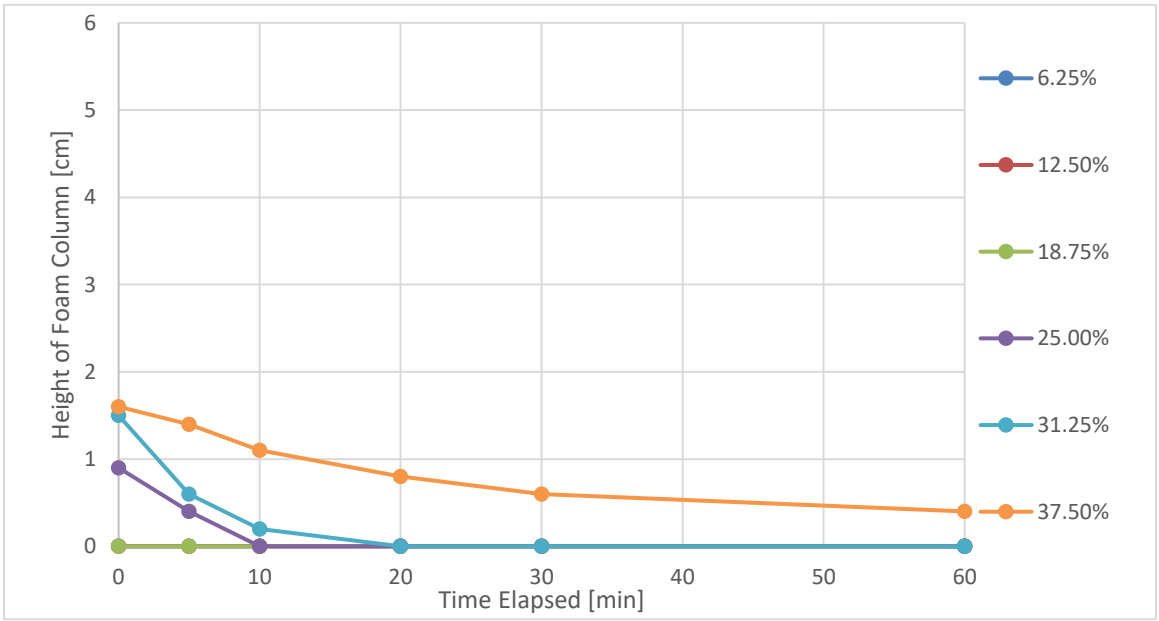

Figure 6.2: 0.5% surfactant concentration in the aqueous phase decline

Figure 6.3: 1.0% surfactant concentration in the aqueous phase

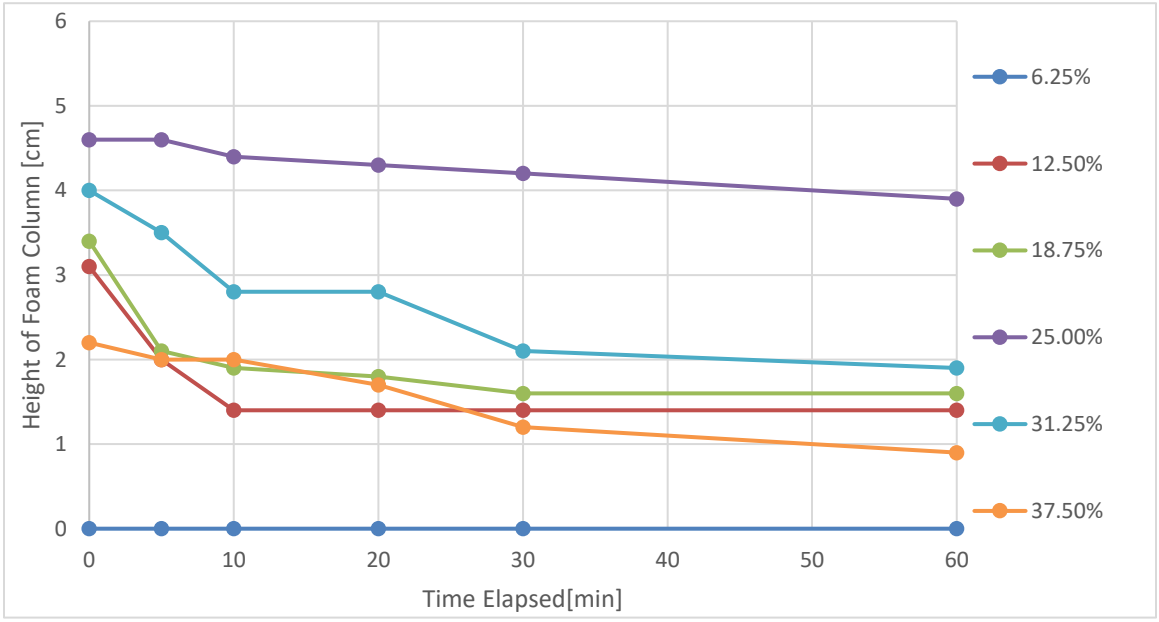

Figure 6.4: 1.0% surfactant concentration in the aqueous phase decline

Figure 6.5: 1.5% surfactant concentration in the aqueous phase

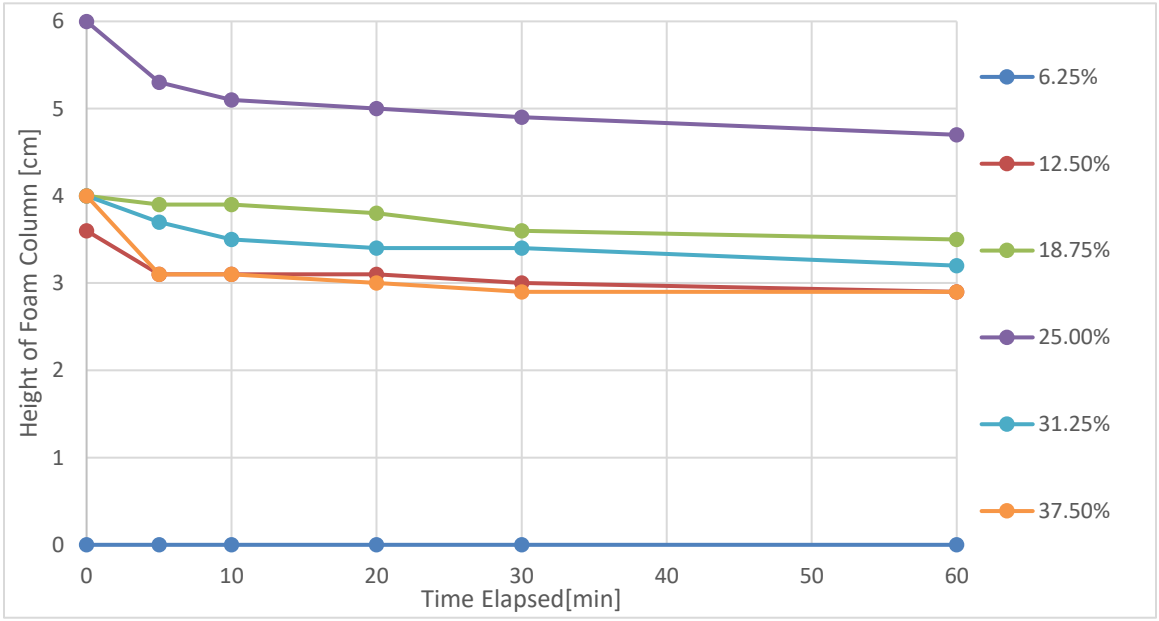

Figure 6.6: 1.5% surfactant concentration in the aqueous phase decline

Figure 6.7: 2.0% surfactant concentration in the aqueous phase

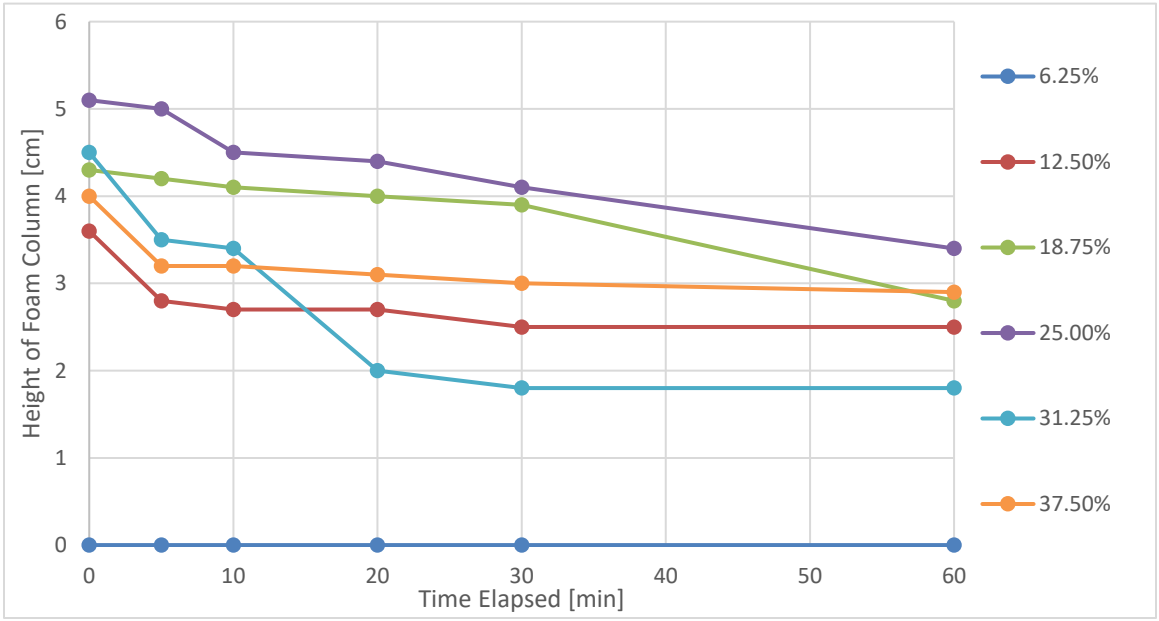

Figure 6.8: 2.0% surfactant concentration in the aqueous phase decline

Figure 6.9: 2.5% surfactant concentration in the aqueous phase

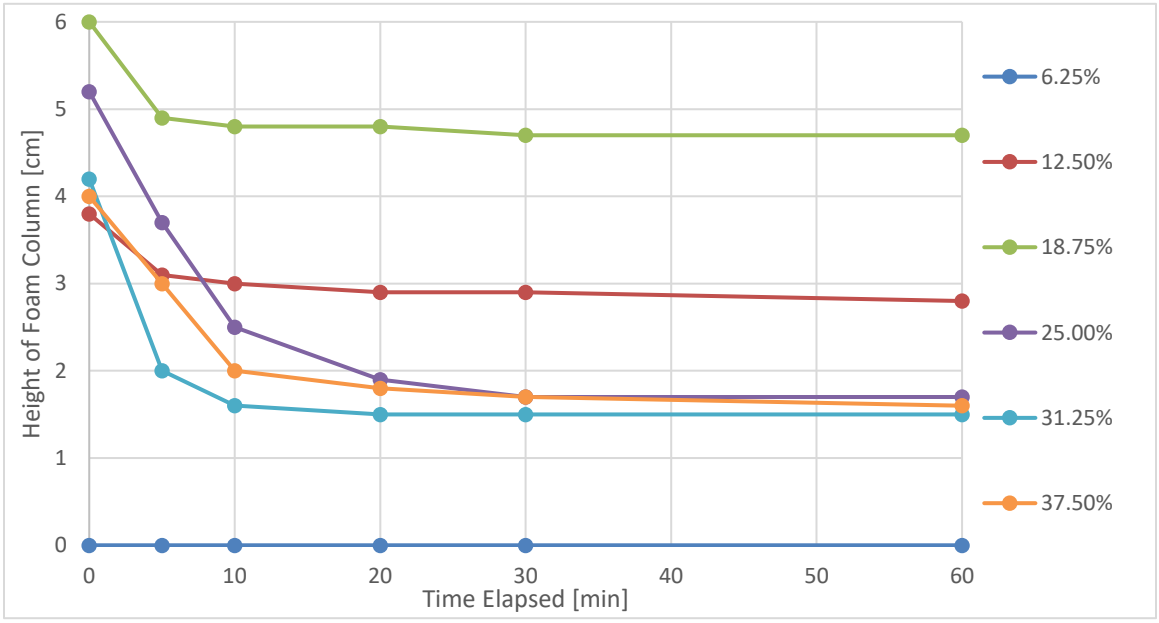

Figure 6.10: 2.5% surfactant concentration in the aqueous phase decline

Figure 6.11: 3.0% surfactant concentration in the aqueous phase

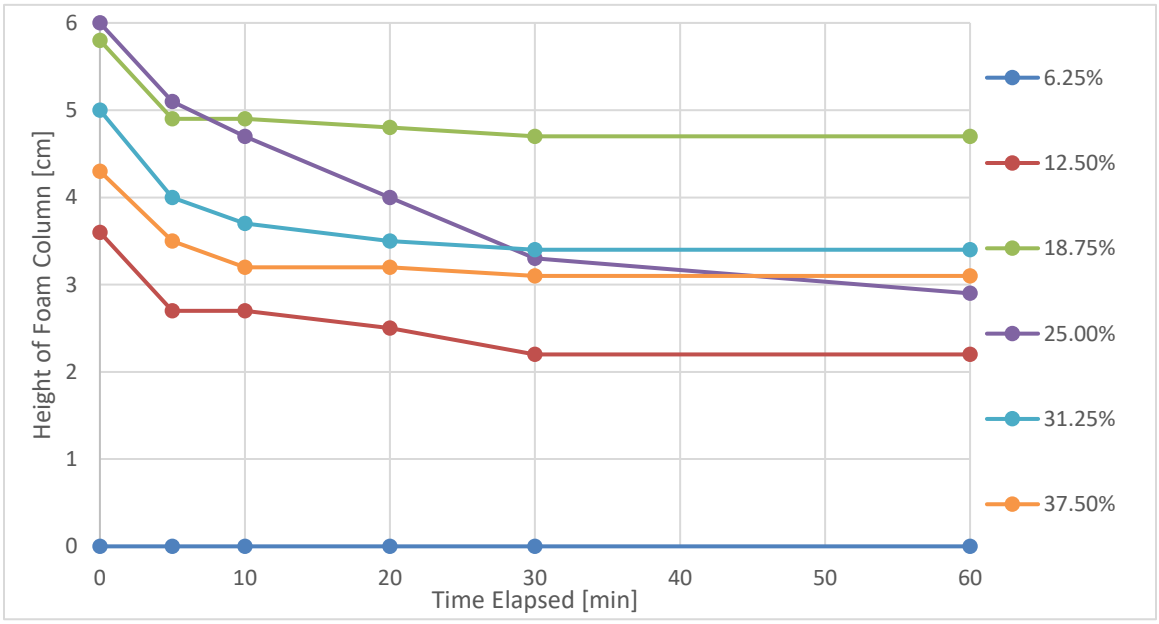

Figure 6.12: 3.0% surfactant concentration in the aqueous phase decline

At 6.25% water, the sample sometimes was able to create a thick emulsion with 30 seconds of shaking while other times, only a slight emulsion was seen in the aqueous phase with a large column of pentane still present. At 12.5 %, a viscous gel was formed that was able to trap air bubbles. As the water and surfactant concentrations increased, a strong, white, conventional looking foam was more easily formed. However, at most water concentrations of 25% and above, a water column of no foam on the bottom was observed leading to the belief that there is excess water in the system that is not contributing to the foam stability.

For application later, a surfactant concentration of around 1.0% by mass to the water phase and a water percentage of around 12.50% by volume would be optimal for an emulsion that can trap gas for a long period of time. For a more conventional foam, a surfactant concentration of 1.5% and water percentage of 18.75% is recommended, but this is all potentially dependent upon salinity and shear rate within the system.

6.2 EFFECTS OF SALINITY

The second test carried out on semi-aqueous foam, varies the salinity of the water within the system with foam. In this experiment, 4 ml of saline water was added to 16 ml of pentane. However, instead of the KCl used in the previous test, sodium chloride was added to the water in increasing mass percentage relative to the water present. Salinity varied from 0.1% to a high 5.0% to cover the whole range that might be seen in an average reservoir.

Samples were shaken for 30 seconds each and formed a gel after only a few seconds. Higher salinities led to lower height of the foam even though the texture was still rather fine as shown in Figure 6.13. In addition, the drainage of the water out of the foam appears to be less for a higher salinity mixture as evident in the 5.0% sample. In some aqueous foams, a high salinity can be detrimental to foam production, but thankfully, the presence of salt did not inhibit the foaming abilities of the additive in this particular case.

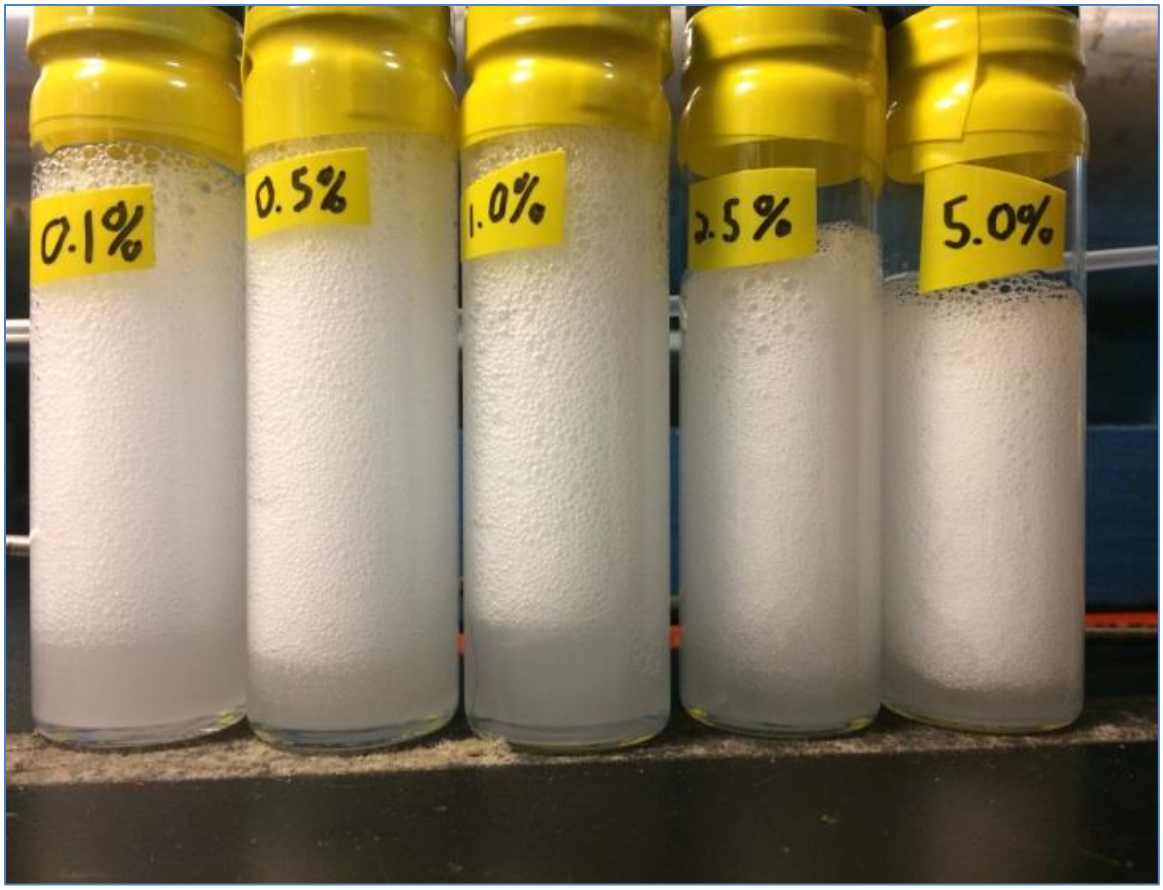

Figure 6.13: Pentane, water, and additive #1 with increasing salinity after 30 minutes

6.3 CLOUD POINT TEST

The cloud point is the temperature above which an aqueous solution of a water-soluble surfactant becomes turbid. For nonionic surfactants, such Additives 1 through 6, optimal results for foaming generally occur near or slightly below the cloud point while operating above the temperature might result in phase separation and instability. In addition, the presence of salt within the system may decrease the cloud point (Nasr-El-Din 1996).

Knowing the cloud point will allow us to find an optimal temperature and salinity for our surfactant. Therefore, a test was performed where the temperature, surfactant

concentration, and salinity will be varied to determine how the cloud point varies with these three parameters.

This test was carried out with nonionic surfactant Additive 1. Sample stocks of the appropriate surfactant mass concentration were created using a scale to measure out the proper mass of surfactant into 100 ml of water to yield surfactant concentrations from 0.5% to 2.0% by mass. Sodium chloride was then measured by mass and added to the sample stocks to yield a salinity of 0.0% to 4.0% for each of the four surfactant concentrations.

The samples were stirred until homogenous, transferred to pipettes, sealed with a blow torch, and labelled. Each pipette contained 15 ml of the solution. The pipettes were then placed in an oven, and the temperature was increased by 5^{o} C starting from 30^{o} C every hour while observing if the water became turbid.

Higher salinity samples with lower surfactant concentrations were seen to turn cloudy first as shown in Figure 6.14. The samples with 4.0% salinity all turned turbid at the same temperature, but the fact that the samples with a lower surfactant concentration always turned cloudy first indicates that cloud point is inverse to surfactant concentration at this range.

This experiment shows that the foaming potential of Additive 1 is likely best at higher temperatures slightly below cloud point that one may see at reservoir conditions. In addition, salinity and surfactant concentration, to a less extent, influenced the cloud point.

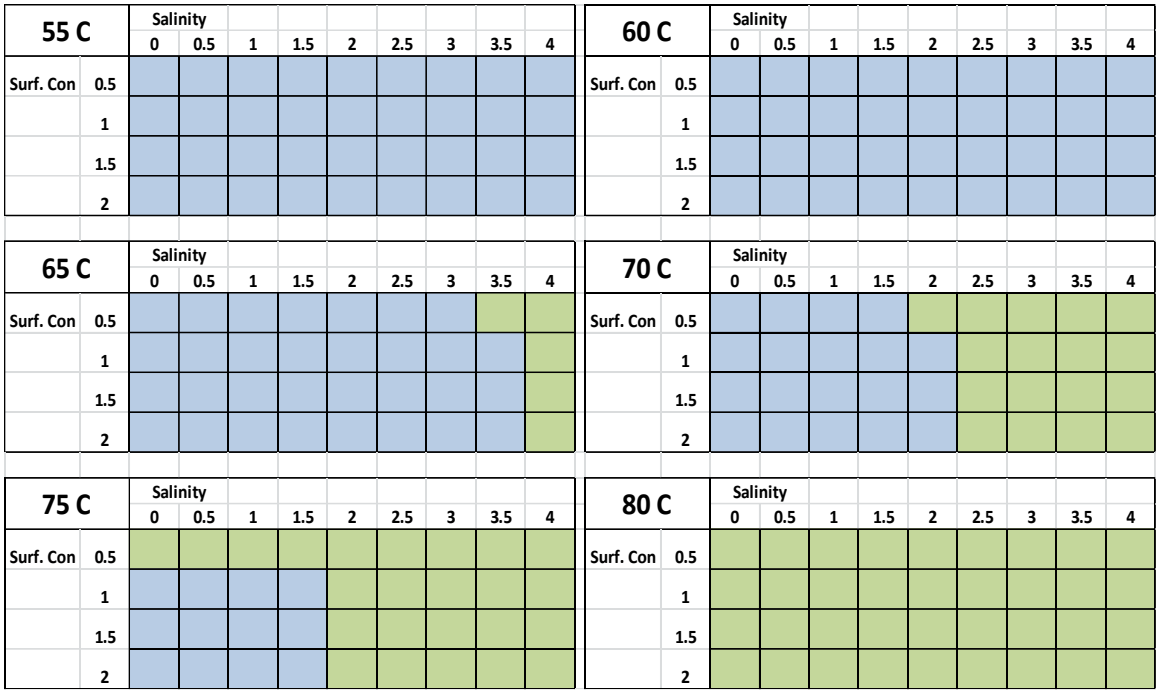

Figure 6.14: Whether a sample is turbid (green) or still clear (blue) at a certain salinity, surfactant concentration, and temperature

Chapter 7: Y-Grade Synthesis

In order to prove the results obtained from testing additives in liquids at room pressure would be concordant with y-grade at higher pressures, synthesized y-grade was required for further testing. A sample blend of y-grade was provided by the sponsoring company for research purposes, and the possibility of purchasing a pre-made batch of this y-grade from a third-party dealer was explored.

However, several challenges arose that made it clear that producing our own y-grade blend in-house would be the more pragmatic choice for this project. First, purchasing a pre-made batch of y-grade and having it delivered had a long lead time of two to three weeks that would have delayed testing if high quantities of usage were not anticipated in advance. Secondly, the y-grade would need to be delivered and stored in a piston or bladder type accumulator to ensure a constant pressure and composition when using the y-grade. Finally, having a system in-house gave us the freedom to modify the composition of the produced y-grade at will if various compositions needed to be tested. These factors provided enough reason to develop our own system of creating y-grade.

In order for the synthesis of y-grade to be successful, a four-step plan was developed. First, thermodynamic phase behavior analysis was conducted on the proposed y-grade blend and on the individual components. This analysis gave indication to the conditions that would be needed for an accurate synthesis and the quantities of each component needed. Second, a set up to hold each of the components and then mix then together at the proper molar fractions was designed. Third, the set up was constructed over the period of a month as several custom parts and design changes were necessary. Finally, a procedure was adopted that would allow the synthesis to be efficient, accurate, and easily repeatable by anyone working on the project.

7.1 Phase Behavior Analysis

In order to synthesize our own y-grade, the phase behavior of both the y-grade and its components needed to be characterized to develop a plan of combining the

components under ideal mixing conditions. To do so, commercially available software was used to plot phase behavior diagrams in addition to obtaining other pertinent information such as densities and compressibility factors.

A sample blend of y-grade was provided for use in the project to match potential y-grade compositions in the field. This original composition contained all alkanes from ethane to octane on the increasing carbon number scale. Butane, pentane, and hexane were further broken down into both “iso” and “normal” isomers of the alkane, and heavier components heptane and octane were grouped together without an exact chemical structure identified.

The composition of the sample y-grade was simplified by combining the molar percentages of the “i-“ and the “n-“ isomers together into just the normal alkane, and heptane and octane were reduced from an unspecified blend of isomers into just normal alkanes as well. The combining of the two specified isomers was done to both reduce the number of unique components needed to blend together and to decrease time spent switching between components in the eventual blending process. Heptane and octane are represented by just the normal alkane for the same reasons.

Phase behavior analysis for both the original and simplified compositions was performed to test our assumptions that simplifying the mixture would have only a trivial effect upon its phase behavior. CMG WinProp^{TM} version 2015, commercially available software created by Computer Modelling Group Ltd., was used for the analysis. The program used the Peng-Robinson 1978 equation of state to develop a complete two-phase envelope of components selected from a built in chemical library and molar percentages of the components entered by the user.

For the original composition y-grade simulation, each of the ten components was chosen from the chemical library with the exception of i-hexane. I-hexane did not exist within the WinProp library, but the library did contain an entry that was an average of all hexane isomers as to represent a general hexane sample. The average hexane, heptane, and octane were used to represent i-hexane, heptanes, and octanes respectively. For the

simplified composition y-grade, the normal isomers of all the alkanes were available within the programs library.

The phase envelope was constructed over the full range of pressures and temperatures allowed by the program and quality lines of 25%, 50% and 100% constant volume fraction in the vapor phase were added. The differences in simulated phase behavior between the original and simplified compositions of y-grade were deemed small enough as to have little to no effect. The original composition has a slightly higher cricondentherm and cricondenbar due to the difference between the i- and n-isomers. Phase diagrams for both the original and simplified compositions are shown in Figure 7.1 and Figure 7.2 respectively.

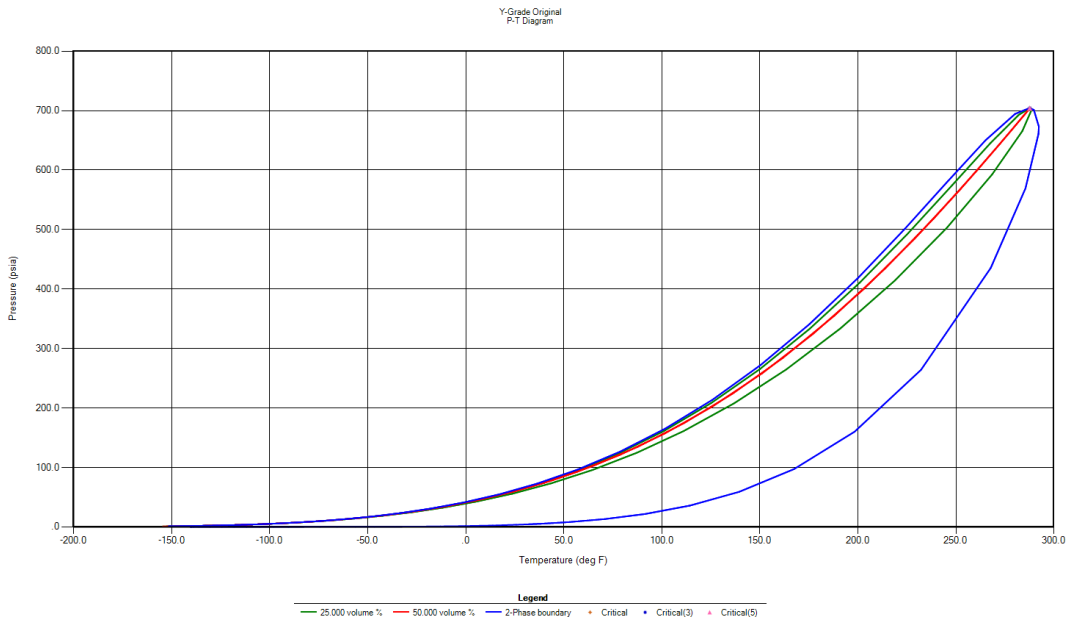

Figure 7.1: Phase behavior envelope for the original composition of y-grade

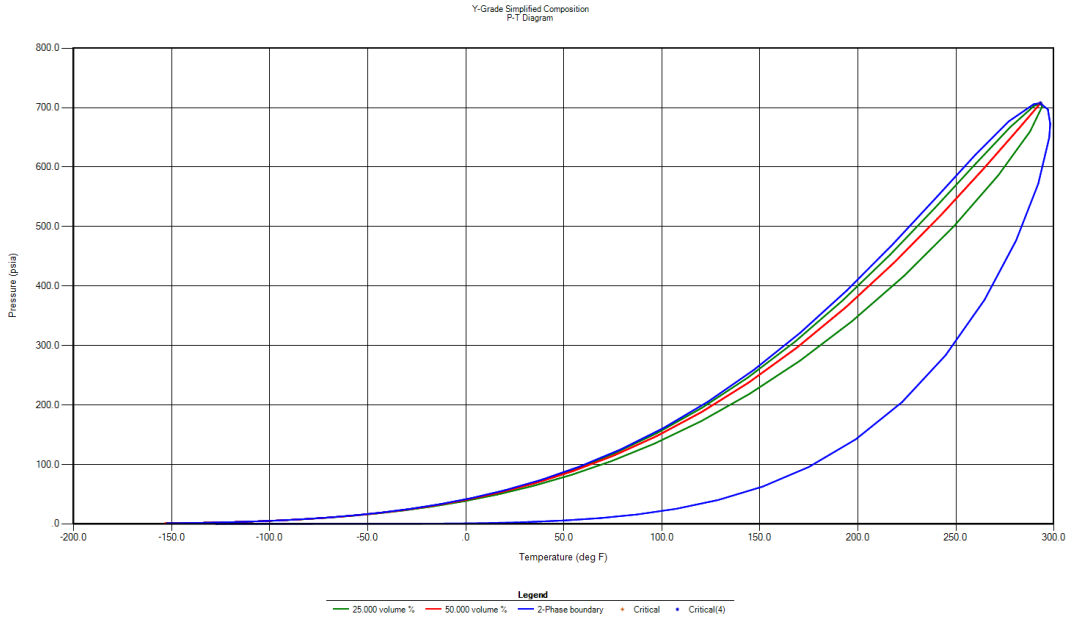

Figure 7.2: Phase behavior envelope for the simplified composition of y-grade

In addition to the phase envelopes for the y-grade blend, phase diagrams for the seven components of the simplified compositions were created. The data obtained from looking at the components by themselves was useful later when a procedure was created to blend the different alkanes. Phase diagrams of the seven components are seen in Figure 7.3.

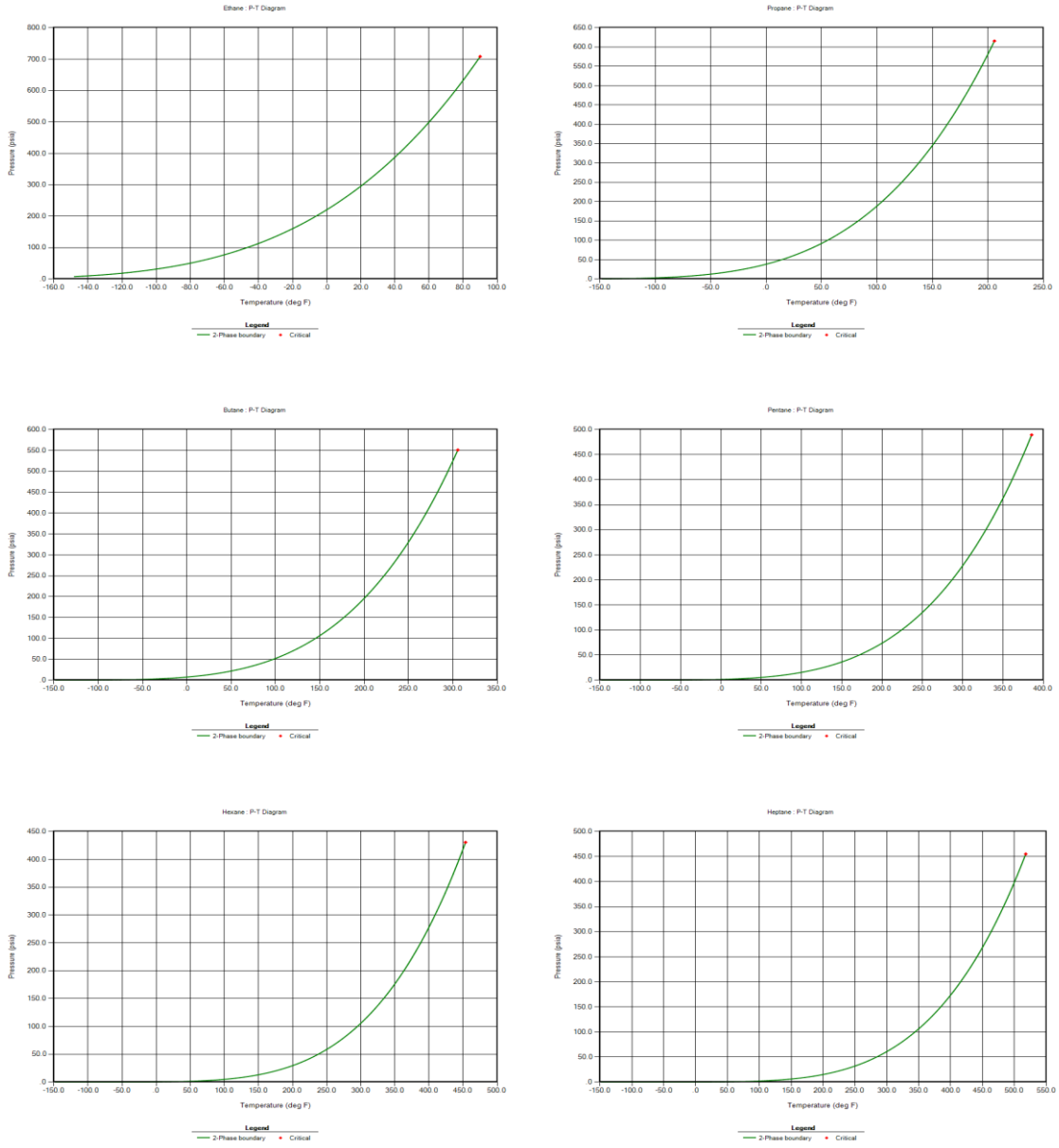

Figure 7.3: Phase behavior diagrams for components ethane through octane

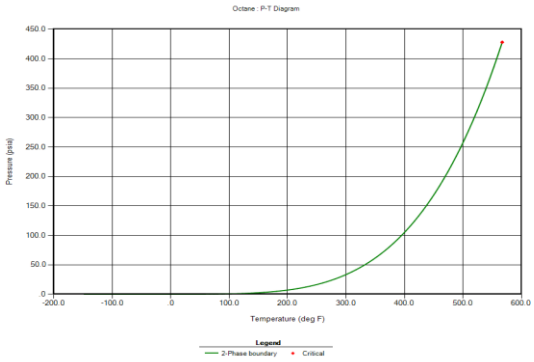

Figure 7.3: Continued

7.2 Y-Grade Synthesis Assembly Design

Once the phase behavior of the y-grade blend and individual components was better understood, a design was put together for a setup, dubbed the Synthesis Assembly, that would allow the components to be mixed together at a correct molar ratio. Several challenges were faced when designing the set up leading to several iterations of the design.

The first challenge was that under room temperature and pressure, ethane, propane, and butane exist as gases. In addition, the other components are volatile and would quickly evaporate out of any open container which would affect our accuracy. The components needed to be blended together in a closed system to prevent loses to the surrounding environment. Thus, each alkane would first be transferred to an individual component accumulator from its source tank if gas or storage bottle if liquid. This way, the exact amount of alkane present would be known based upon calculations utilizing outputs such as density and compressibility from the phase behavior analysis.

The second challenge was that even in sealed, separate component accumulators, it would be difficult to displace the correct amount of each alkane into a vessel where

they would then be blended together. This issue was especially true for ethane, propane, and butane since the compressibility of the gas would make it hard to displace accurately. To solve this problem, each component accumulator was attached to a water inlet where DI water could be pumped into each accumulator to increase the pressure enough to render all components in the liquid phase. Since water is more dense and immiscible with the hydrocarbons, it acts as a piston to decrease volume and increase the pressure in the sealed component accumulator.

The final challenge was how to combine these now pressurized components together into the same vessel with accurate results. The solution was to use a large accumulator with an internal piston divider and a second water pump to provide back pressure while each component was added in sequence. If all the components were set initially at the same pressure by injecting water into the component accumulators, a channel could be opened connecting the pressurized component accumulator to the Mixture Piston Accumulator (MPA). The first pump would drive the alkane out of the component accumulator at a constant rate into one half of the MPA. The other half of the MPA would initially be entirely filled with DI water and the second water pump would be set to maintain a constant pressure. If the injection rate was slow enough, the volume of water injected to drive the alkane would also be ejected out of the other side of the MPA. Thus, each component could be sent to the MPA under constant pressure.

The final design of the Synthesis Assembly revolves around the assumptions that the compressibility of liquids is negligible at high pressures and a water-hydrocarbon system is completely immiscible. Our final design for the Synthesis Assembly is shown in Figure 7.4.

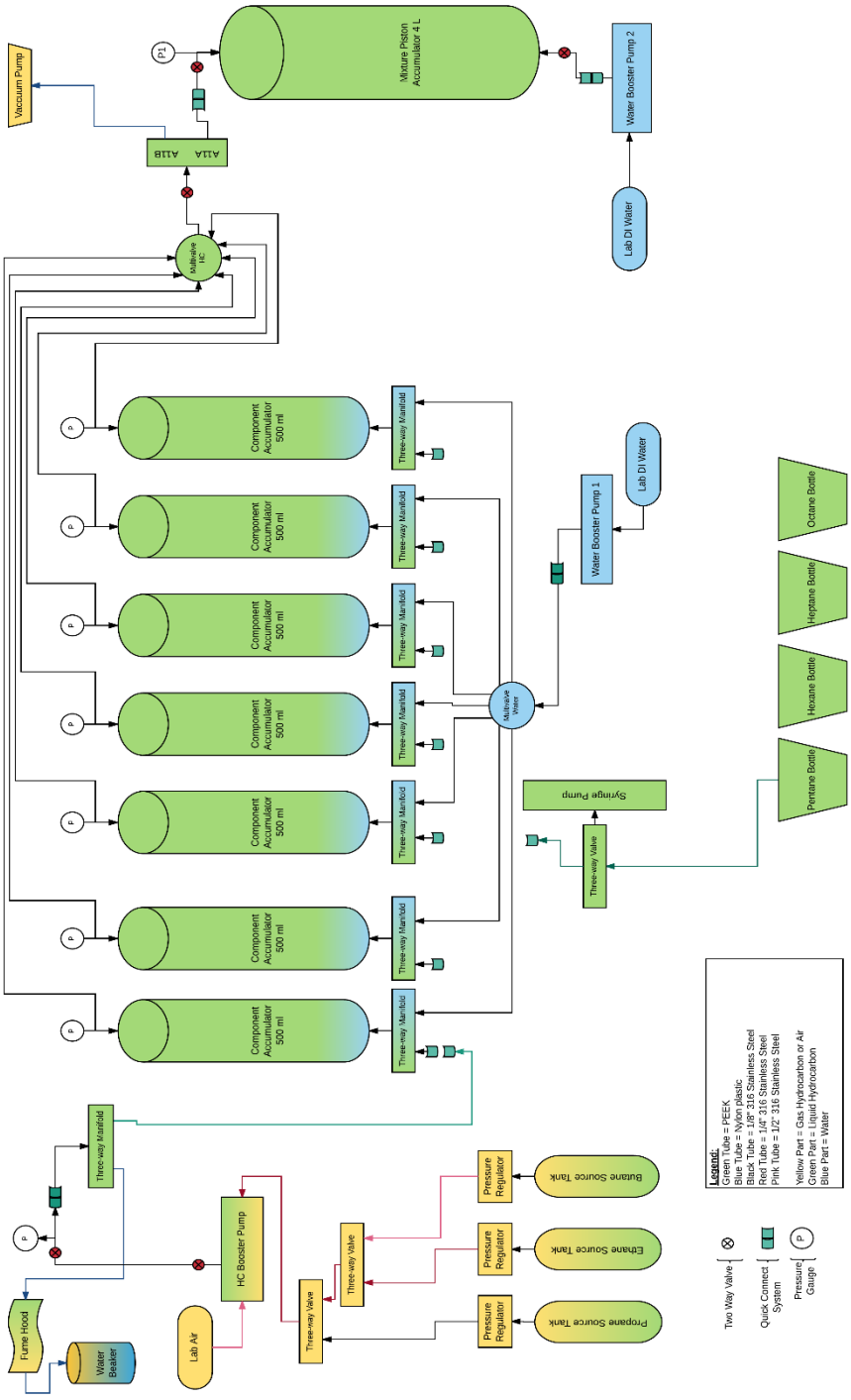

Figure 7.4: Synthesis Assembly schematic and schematic legend

7.2 MATERIALS AND PREPARATION

Several key components of the Synthesis Assembly led to an accurate and simple to use system. The majority of the valves used in the design were three-way manifolds supplied by Autoclave Engineers™. These manifolds were a combination of two needle valves that could be used separately or in tandem to combine two streams into one. For example, they were used at the bottom of each component accumulator so that either the alkane from its source tank or bottle or DI water could be injected through the same port while minimizing dead volume within the system. In addition, the fact that they were needle valves meant that they could be used as chokes anywhere within the system to decrease the flowrate. A schematic of the three-way manifold is shown in Figure 7.5

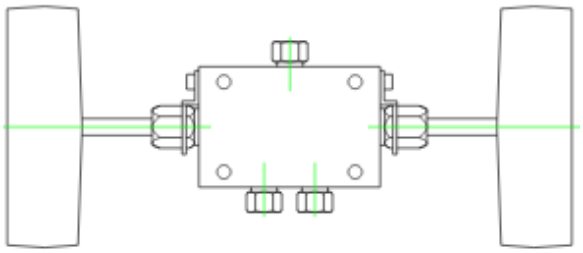

Figure 7.5: Autoclave Engineers three-way manifold schematic

The Synthesis Assembly used a considerable amount of pressure gauges to monitor each of the components as well as the blend within the Mixture Piston Accumulator. All pressure gauges used were Cecomp™ digital pressure gauges with a range of 0 to 1000 psi with an accuracy of +/-0.10% of the reading. These gauges allowed for precise measurements at higher pressures so that the components could be accurately monitored. A picture of one of the pressure gauges is shown in Figure 7.6.

Figure 7.6: Cecomp digital pressure gauge stock photo

The component accumulators were all 500 ml, stainless steel cylinders with two open ends. This accumulator is rated for pressures well over 1000 psi, and this particular size was a balance between being large enough to hold enough of the component while not being too large to mount effectively on a rack. The MPA was an older, 4 L accumulator with heavy, threaded end caps. Each endcap had a single outlet. The manufacturer of this piston accumulator was not known since the maker label had been worn off.

The two water pumps utilized to inject water into the component accumulators and to apply backpressure to the MPA are Quizix, QX6000 series water pumps. Each pump contained two pistons that worked in unison to apply a constant rate to the system. Also, each pump had its own external control panel where parameters such as injection rate, constant pressure applied, and safety pressure were set and system pressure for each piston was displayed. The Quizix pump also tracked total water injected or withdrawn which proved useful in operation. Both pumps had a maximum pressure rating of over 6000 psi and a maximum rate of 50 ml/min.

A Haskell refrigerant pump model 59025 was added to the system in order to completely drain the source tanks of the gaseous components and pump more gas into the component then what could be achieved with just the pressure from the source tank. The pump was connected to the lab air supply to function and was able to meet all of our pressure needs.

In order to select which component accumulator the injected water was being sent to and which component was being injected into the MPA, two multi-select valves from Valco Instruments Co. Inc. were utilized. These valves feature one inlet stream and eight outlet streams that can be selected one at a time by a manual knob. Since there were eight outlet streams available but only seven components that needed to be injected, the eighth outlet was sealed off and used as a neutral position where all of the component accumulators were shut off. These valves were rated up to 5000 psi. A schematic of one of the multi-select valves is shown in Figure 7.7.

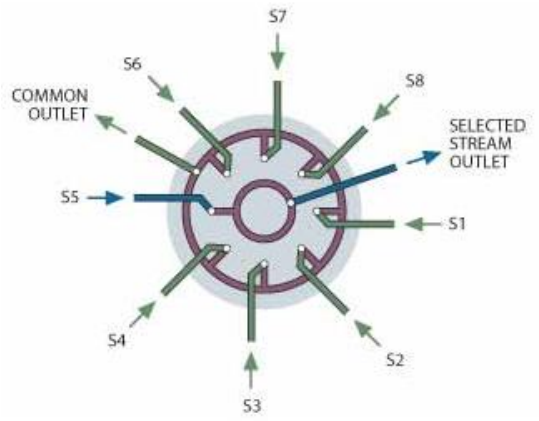

Figure 7.7: VICI multi-select valve diagram

Several additional parts were used in the construction of the Synthesis Assembly. All of the tubing was 0.125 inch stainless steel tubing with a 0.028 inch wall made by Swagelok. This tubing was rated up to 8500 psi. One segment of PEEK tubing was used between the gas tanks and the component accumulators to charge each. The tubing was rated up to 1000 psi. A quick connect system made by Swagelok was used in several places within the set up to allow one line to charge all of the components and to safely disconnect the MPA from the set up after it was filled with y-grade. Several Swagelok two-way ball valves were used throughout the system as safety check valves. All fittings were provided by Swagelok except those on the three-way manifolds provided by Autoclave Engineers.

Below are pictures of the final constructed Synthesis Assembly. Figure 7.8 shows the seven component accumulators with pressure gauges on top and three-way manifolds leading to either the alkane charging port in the front or the water injection port in the back. The PEEK tubing attached to the third charging port in the picture leads to another manifold where the gas components can either be sent to the component accumulator or out to the fume hood through a nylon line. The lines coming from the component accumulators going right lead to the two multi-select valves. The top multi-select valve leads to a three-way manifold that either goes out to a vacuum line or to the MPA. The bottom multi-select leads to the first Quizix water pump.

Figure 7.8: Synthesis Assembly component accumulators (center), multi-select valves (right), and inlet quick connects (bottom)

Figure 7.9 is a close up of the two multi-select valves, the vacuum port on the left side of the three-way manifold, and the outlet to the MPA on the right side of the manifold. The right side of the picture shows the first water pump leading to the component accumulators and half of the MPA. The MPA connects to the rest of the set up through a quick connect system, and a two-way ball valve prevents pressure from building up within the quick connect. A pressure gauge monitors the pressure within the y-grade side of the MPA.

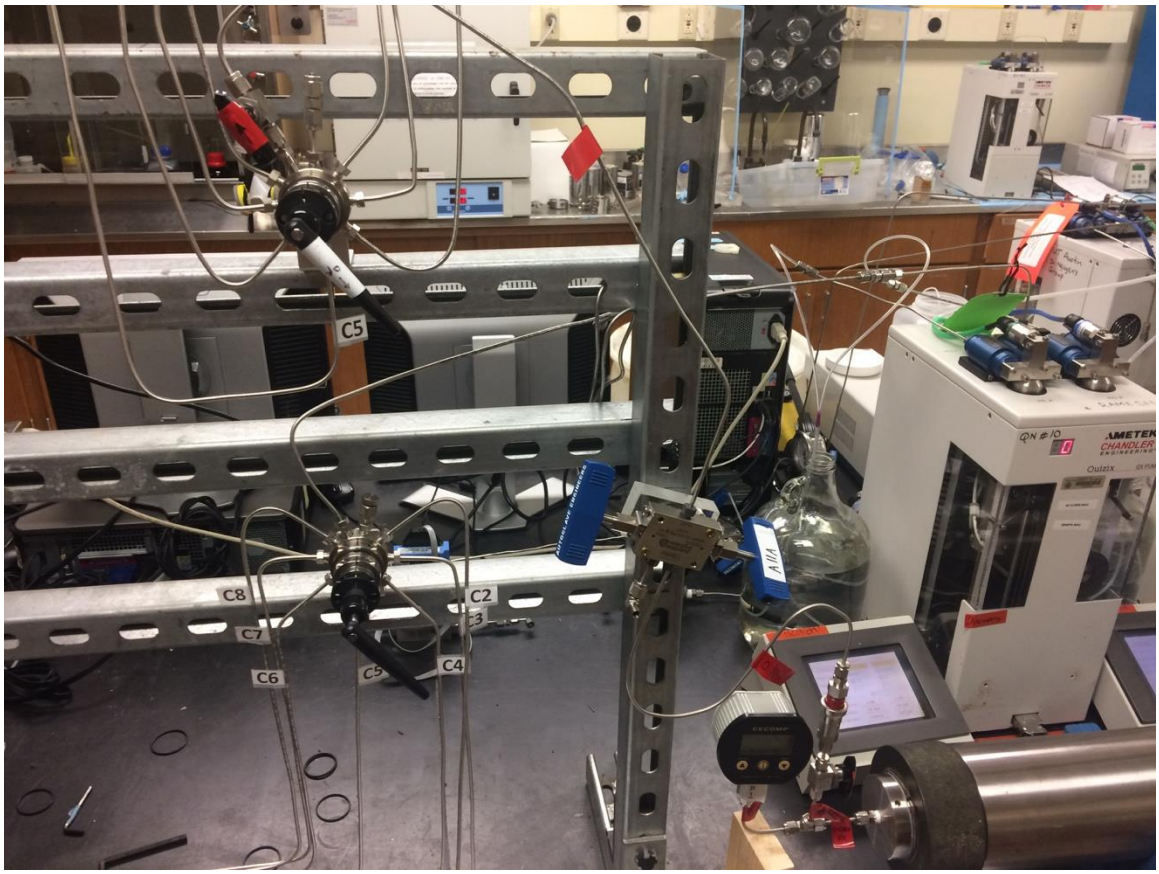

Figure 7.9: Synthesis Assembly close up view with multi-select valves (left), vacuum port (center), and outlet to Mixture Piston Accumulator (right)

Figure 7.10 is a close up of the manifolds below each of the component accumulators. Each manifold has a quick connect receiver to attach the PEEK tubing, shown disconnected on the table, to the source tanks or bottles. The lines to the back of the manifolds lead to the water multi-select valve. The labelling on each valve was for operational purposes and each communication between users.

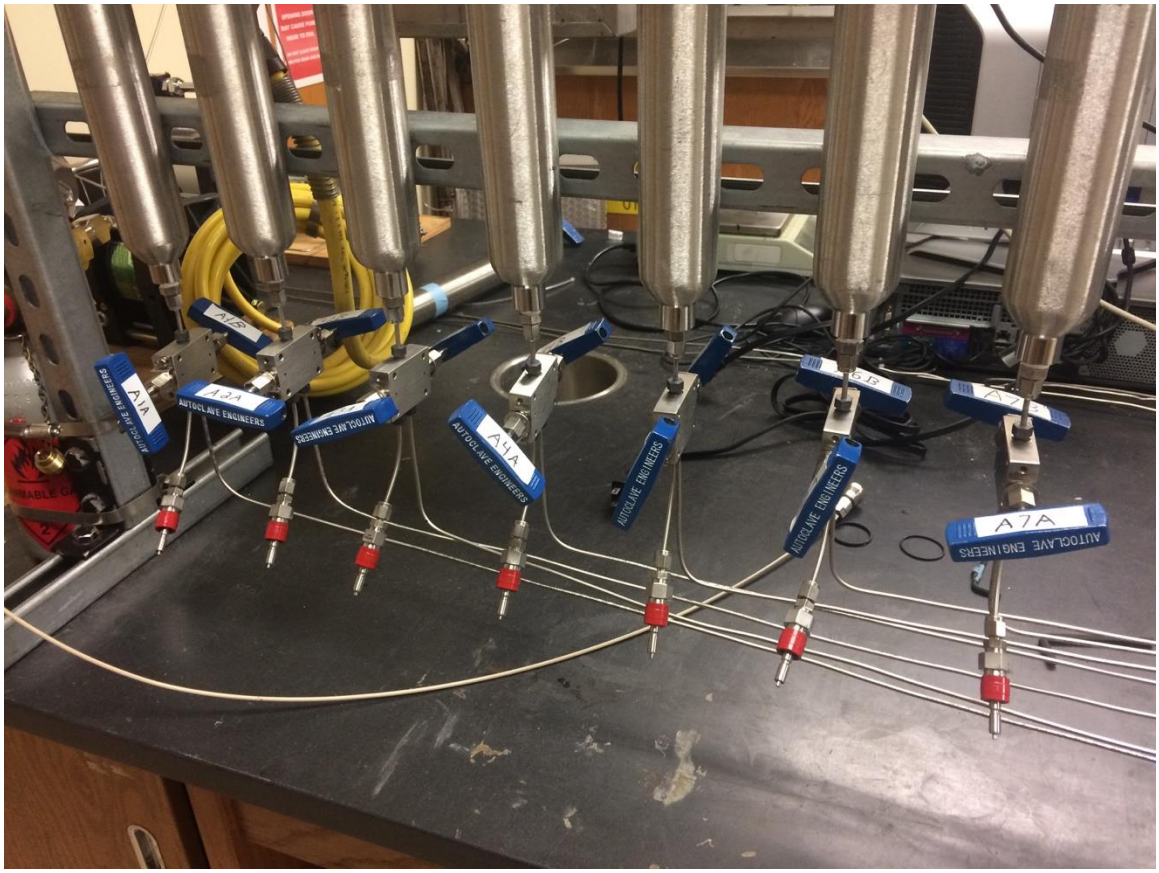

Figure 7.10: Close up of three-way manifolds allowing hydrocarbon or water injection

Figure 7.11 shows the MPA in the foreground and the two Quizix pumps in the back. The MPA is attached to the set up on the left side while the water side on the right is connected to the second water pump that provides back pressure. Next to each water pump is a jug of DI water to serve as a source reservoir and a control panel for the pump. The backs of the pumps are shown connected to the lab air outlet in order to have the gates within the pumps function.

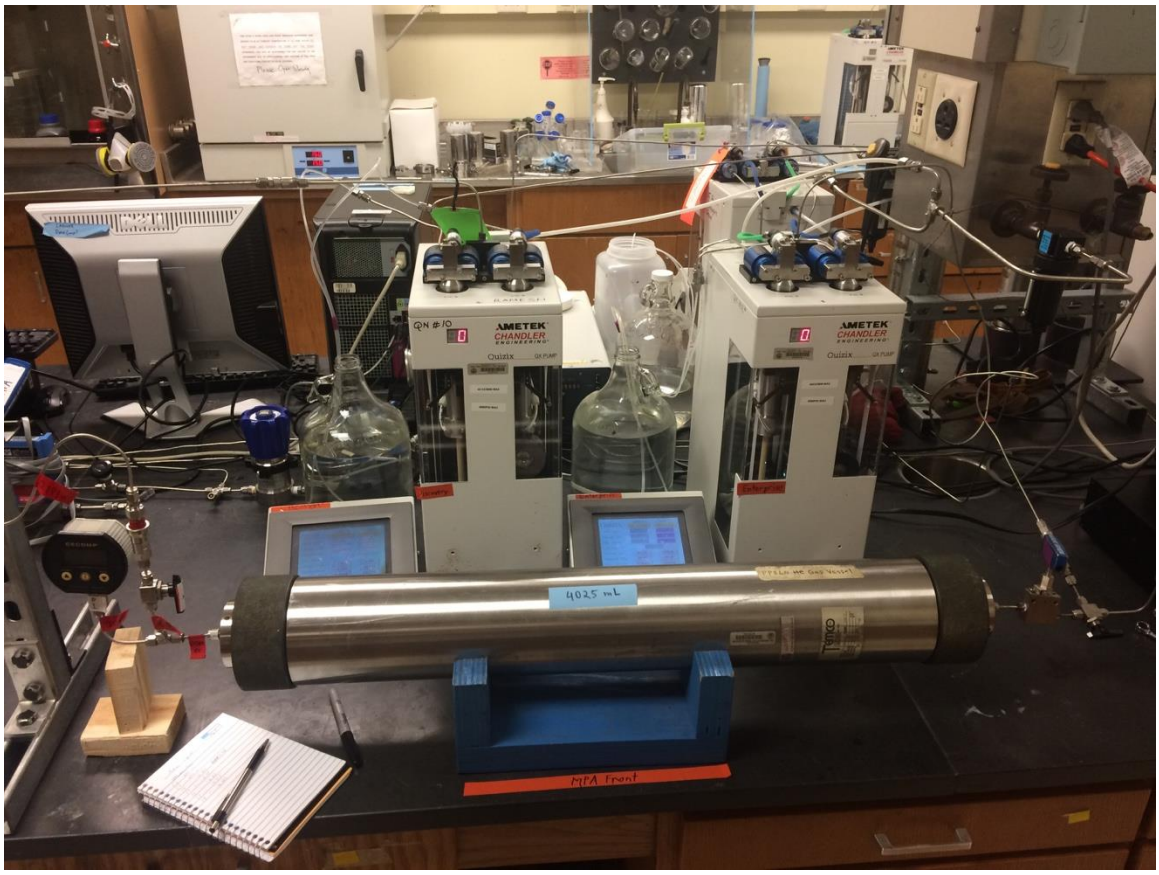

Figure 7.11: Mixture Piston Accumulator with two Quizix water pumps

The alkanes used in the formulation of the y-grade are shown in Table 7.1. It was prudent to order larger volumes of the gas-phase components since they comprised most of the y-grade. However, the propane had to be purchased in small vessels since the building's fire code prevented large amounts of propane being housed within the laboratories. Several small tanks of propane were purchased and kept off site until they were needed.

Table 7.1: Alkanes used for y-grade synthesis

Compound	Sales Weight/Volume	Sales Pressure	Min. Assay %	Supplier
Ethane	32 lbs	546 psi	99.50	Matheson
Propane	0.83 lbs	110 psi	99.88	Matheson
n-Butane	120 lbs	16 psi	99.85	Matheson
n-Pentane	2.5 liters	Atmospheric	99.00	Acros Organics
n-Hexane	2.5 liters	Atmospheric	99.00	Acros Organics
n-Heptane	2.5 liters	Atmospheric	99.50	Acros Organics
n-Octane	2.5 liters	Atmospheric	99.00	Acros Organics

7.3 PROCEDURE

The first phase in synthesizing the y-grade was to transfer the individual components from their storage vessels to the component accumulators. Separate procedures were used depending upon if the component was coming from a pressurized source tank or if the component was liquid at room conditions and could be pulled straight from the bottle. The second phase was the actual blending of the y-grade. Finally, if y-grade has been made previously and there is not enough of the components left in the component accumulator, it was necessary to drain the accumulators to recharge.

7.3.1 Gaseous Component Accumulator Charging

The first step in charging the component accumulators for the gaseous components is to consult with the data generated from the phase behavior analysis to determine a final operating pressure and initial pressures for each of the gas components before any water is injected. It is beneficial to have the pressure within each accumulator

as high as possible before any water is added so that the maximum amount of each component is transferred and more y-grade can be made without having to recharge. The post-water operating pressure of 650 psi was selected because it is higher than ethane's bubble point pressure at room temperature without being close to our 1000 psi safety limit. The real gas law for each component was used to determine starting pressures for ethane, propane, and butane such that a small amount of water would need to be injected to reach 650 psi. The pre-water filling pressures for the gaseous components are shown in Table 7.2

Table 7.2: Pre-water pressures for the three gaseous components

Component	Pressure [psig]
Ethane	600
Propane	150
Butane	100

Charging of the component accumulators happens individually, so the current accumulator being charged is referred to as the "active" accumulator. Once the goal pressures for the gas component charging were set, a vacuum pump was connected to the vacuum port on the right-hand side of the assembly. The PEEK tubing is attached to the bottom of the active accumulator and the entire flow line is open and vacuumed to remove air.

Vacuuming took several minutes until the pressure gauge attached to the vacuum read a constant -14.0 psig even when the pump was turned off. At this point, the multi-select valve connecting the component accumulators and the MPA (referred to as the alkane multi-select), was turned one position clockwise away from the active line essentially sealing off the accumulator to the vacuum port.

A series of valves upstream of the Haskell refrigerant pump are used to select the active component that will be charging the accumulator. Since all gaseous components are sent through the refrigerant pump, the line must be cleared of the previous component before charging. The manifold valve leading to the PEEK tubing and the accumulator is

closed, and the valve leading to the fume hood is opened. The tank is then opened and gas is allowed to flow freely out to the fume hood for 30 seconds to rid the line of unwanted alkanes. The line to the fume hood is then closed and the PEEK line reopened.

Initially, the refrigerant pump is not necessary because the pressure from the source tank will be regulated down to a low pressure and slowly brought up as high as the regulator would allow. The ethane was able to reach very close to the desired pre-water pressure, but propane and butane needed to be pumped in order to increase the pressure well above that of the source tank. Once the pressure within the component accumulator hits the goal pressure, close off the valve between the accumulator and the quick connect with the PEEK tubing. The quick connect ends should never be left under pressure when not together, so the fume hood line was again opened to decrease the pressure within the PEEK tubing down to atmospheric. The PEEK tubing can then be moved to the next component accumulator and the procedure is repeated until ethane, propane, and butane are all charged.

Once the three gaseous component accumulators were charged, water was injected into the bottom of all three individually to bring their pressures up to 650 psi. The initial injection rate was set to 5 ml/min and then decreased to 2 ml/min when the pressure got close to the target. The cumulative amount of water injected into each of the accumulators was tracked throughout the entire project. By knowing the amount of water present and the pressure of the component accumulator, the exact volume and mass of each component left within the system could be tracked to know when to recharge.

7.3.2 Liquid Component Accumulator Charging

Goal pressures before any water is injected for the components that are liquids at room conditions were determined in the same manner as for the gas components. The goal pressures are much lower since the liquid components are not as compressible as the gases and even a small amount of water injected could increase the pressure by a significant amount. The pre-water filling pressures for the liquid components are shown in Table 7.3.

Table 7.3: Pre-water pressures for the four liquid components

Component	Pressure [psig]
Pentane	50
Hexane	25
Heptane	25
Octane	25

The liquid components were injected into their respective accumulators using a standard syringe type pump. A line of nylon tubing was placed within the bottle of liquid components and wax paper was placed around the bottle's opening to prevent undue evaporation. The syringe pump was placed at the other end of the nylon tubing, piston is moved downward to draw in 500 ml of the liquid component into the syringe. The nylon tubing was then connected to the active accumulator through the quick connect system, and the piston was pushed upward to drive all of the air within the system and a slight amount of the liquid alkane into the accumulator.

The valve between the quick connect line and the accumulator was then closed to seal off the syringe pump, and the vacuum port was connected to a vacuum pump. The vacuum pump ran to remove all of the air in the system similar to the gas component accumulators before. After vacuuming was finished, what remained was a syringe line and component accumulator devoid of air. The vacuum line was sealed off and the bottom valve reopened slightly while injecting the remainder of the liquid component from the syringe pump. The pumping continued until the goal pressure was reached, at which point, the accumulator was sealed off, the pressure in the quick connect line was decreased, and the nylon line was detached. DI water was used to flush the syringe pump three times to remove any of the old liquid alkane and then was flushed with air to remove any residual water. This procedure for charging was repeated for all four liquid components.

Exactly like for the gas component accumulators, water was injected through the bottom by selecting an active accumulator and pumping with the Quizix pump. However,

since a small volume of water could have a high impact upon pressure, a low rate of 1 ml/min was used to increase the pressures up to 650 psi. Once all seven components were at a static 650 psi, y-grade was ready to be synthesized.

7.3.3 Component Mixing

The phase behavior modelling of y-grade as a whole rather than by individual component indicted that there would be some non-ideal mixing of the components due to electrostriction. The sum of the volumes of the individual components would not equal the total volume of the blended y-grade. This non-ideal mixing was important to understand since the Synthesis Assembly relied on mixing each component by a certain volume rather than a measured mass. To account for the differences between total component volume and blended y-grade volume, the amount of y-grade made in every batch was characterized by a mass quantity rather than a volume.

The analysis done in WinProp produced an anticipated density for each component and for blended y-grade at room temperature of 22.8^{o} C and the working pressure of 650 psi. Combining the density data with molar percentages and molar mass of each component determined the volume of each component that would need to be injected into the MPA to produce y-grade of a certain mass and composition. Since the mass is conserved, the produced mass is divided by simulated density to determine the produced volume of y-grade. This y-grade blend is composed primarily of butane and propane with smaller amounts of ethane, propane, and hexane. Very small volumes relative to the other components of heptane and octane were needed. Calculated and provided properties of each of the y-grade components are shown in Table 7.4. The blended y-grade was simulated to have a density of 0.5855 g/ml with a molar mass of 52.998 g/mol under the same conditions.

Table 7.4: Component properties at working conditions, 650 psig, 22.8° C

Component	Molar Mass [g/mol]	Density [g/ml]
Ethane	30.070	0.295
Propane	44.097	0.527
Butane	58.124	0.611
Pentane	72.151	0.649
Hexane	86.178	0.654
Heptane	96.000	0.736
Octane	107.000	0.747

Once the volume of each component that needs to be combined to create the y-grade, the blending process can begin. All component accumulators started at the working pressure of 650 psi. If there was deviation from this pressure since the last time the component accumulators were used due to slight temperature differences in the room, the pressure was adjusted with either injected or withdrawing a small amount of water accordingly. DI water was injected into the water half of the MPA until the internal pressure reached 650 psi. The other side was left open to the atmosphere allowing the piston to be pushed completely to the edge of the y-grade size yielding no initial volume within the accumulator for y-grade.

A vacuum pump was attached to the vacuum port above the MPA inlet point, and any air was removed from the system. Vacuuming continued until the pressure gauge read a constant -14.0 psig. After, the system was sealed off from the atmosphere and the vacuum pump was removed.

The injection order for the components started with butane and then moved up in molecular weight to pentane, hexane, heptane, and octane. The order then circled back to ethane and finished with propane. It was reasoned that the most amount of volumetric error would take place during the first and last components to be blended since the tubing volume between the component accumulator and the MPA needed to be taken into account. Since butane was the largest component by volume fraction followed by

propane, this sequence was used to reduce the percent error for y-grade synthesis. A factor of 0.374 ml/m was determined to account for the total tubing volume of 0.559 ml.

All lines connecting the active component with the MPA were opened except for a two-way valve above the alkane multi-select which was kept closed. The first water pump was set to a constant injection rate of 1 ml/min into the bottom of the component accumulator. At the same time, the second water pump was set to a constant pressure of 650 psi. Once the remaining valve was opened, the two pumps are essentially in communication with each other through the tubing network.

As alkane is displaced from the component accumulator into the MPA, water is ejected from the other side of the MPA allowing for the alkane to be transferred at a constant rate under near constant pressure. A low rate of injection was used to account for any compressibility between the two water pumps and to ensure an accurate synthesis. The first pump tracked water injected into each component accumulator which equaled the component volume added while the second pump measured cumulative water removed from the MPA which equaled the cumulative volume of y-grade as it was being produced.

Once the correct volume of the active component has been injected, the same two-way valve as before is closed and the amount of water injected into the component accumulator is tracked and added to any previously injected water for that accumulator to determine the amount of alkane left. The first water pump injecting is turned off, and the volume injected tracker is reset. Both multi-select valves are then shifted to the next active component, and the procedure is repeated until all components have been added to the MPA.

Once the last component, propane, has been added to the MPA in the correct amount, all open valves were closed to shut down the Synthesis Assembly. The vacuum port was attached to a nylon line leading to the fume hood to de-pressurize the quick connect system attaching the MPA to the rest of the assembly. The second water pump maintaining backpressure was turned off once two valves preventing flow out of the

water side of the MPA were closed, and the cumulative water ejected from the MPA was compared to the anticipated volume of y-grade that the blending would produce. At this point, the MPA can be completely disconnected from the assembly and the back pressure pump and moved to other laboratories for further experimentation.

7.4 RESULTS AND DISCUSSION

Initial runs at creating the y-grade only sought to produce 100 g or approximately 171 ml. This amount was enough for testing within the visual cells shown in Chapter 8, but the coreflood in Chapter 9 needed 250 g or 427 ml to be successful.

Since the second water pump tracked the cumulative water ejected from the MPA, this number could be compared with the theoretical volume of y-grade that would be produced from blending the 7 components. Initial runs when the assembly was just completed showed around a 5% error between the theoretical and experimental y-grade yield while later runs reduced this to around 2%. The reduction in error is attributed to the operator's proficiency in the process increasing and refining the procedure to reduce inaccuracies. A comparison of the theoretical and experimental volume of produced y-grade and associated percent error is shown in Table 7.5.

Table 7.5: Comparison between two theoretical and experimental results

Run Date	Goal Mass [g]	Theoretical Volume [ml]	Experimental Volume [ml]	Percent Error
17-Jan-17	100.00	170.79	179.12	4.88
10-May-17	250.00	426.97	436.54	2.24

The main limitation is the slow injection rate for each component and the time it takes to refill a component accumulator if not enough is left from the previous charge. Since the injection rate was only 1 ml/min to account for variability within the system, it would take an entire day to produce just one batch of y-grade. Having to recharge even one component added another day.

Chapter 8: Y-Grade Blending

Once the y-grade had been synthesized, another set-up, dubbed the Foam Assembly, was used to inject y-grade followed by nitrogen into vacuumed visual cells containing surfactant or some other additive for testing. The Foam Assembly consisted of the MPA containing some y-grade taken from the Synthesis Assembly, an accumulator charged with pure nitrogen, and a back pressure regulator (BPR) attached to the visual cell. Similar to how y-grade was synthesized, water would drive either the y-grade or nitrogen through the BPR into a vacuumed visual cell. Meanwhile the amount of water being added and pressure at various points in the system were monitored to ensure the right volumes were pushed through. In this manner, y-grade with nitrogen could be observed to see if assumptions made during the screening and secondary component tests were correct.

8.1 Design and Materials

The Foam Assembly was designed to utilize two water pumps to drive either the y-grade or pure nitrogen through a back pressure regulator and into a sapphire visual cell. Most of the components used in the construction were similar to those used in the Synthesis Assembly.

The MPA containing the y-grade was connected to the foam assembly, and a 500 ml Swagelok accumulator was filled with nitrogen from a source tank. The nitrogen accumulator was then mounted to a holding rack and a line allowing water to be injected into the bottom of the accumulator was added. The outlets of both the nitrogen accumulator and the MPA flowed to one three-way manifold where each could be selected to flow onward. A second three-way manifold provided an outlet for a vacuum line, and the other outlet lead to a pressure gauge and the BPR to hold everything upstream at a constant pressure while allowing fluid to flow through if the pressure was exceeded.

The BPR used was stainless steel, spring-loaded back pressure regulator manufactured by Swagelok. It contained a PEEK seal and was rated up to 500 psig. The spring-loaded type regulator was chosen to allow the operator to adjust the back-pressure at will in case a different operating pressure was required. Additionally, a pressure rating of only up to 500 psig was used to allow the most amount of sensitivity for the operator. The BPR is shown in Figure 8.1.

Figure 8.1: Swagelok spring-type back pressure regulator

Once through the BPR, the fluid was sent through another three-way manifold acting as a second vacuum port and then into a visual cell. Five visual cells with a volume of approximately 14 ml were available to be used for this project, and each contained a thick-walled, sapphire tube surrounded by a stainless steel enclosure. Each visual cell was attached to a pressure gauge, two-way needle valve from Autoclave Engineers, and a quick connect system to allow the cells to easily be attached and detached from the Foam Assembly. This ability to quickly swap visual cells meant that they could be lightly shaken to see if foam could be created, and it lead to easy cleaning for future use. These sapphire visual cells were rated at 5000 psi at room temperature. One of the cells is shown in Figure 8.2.

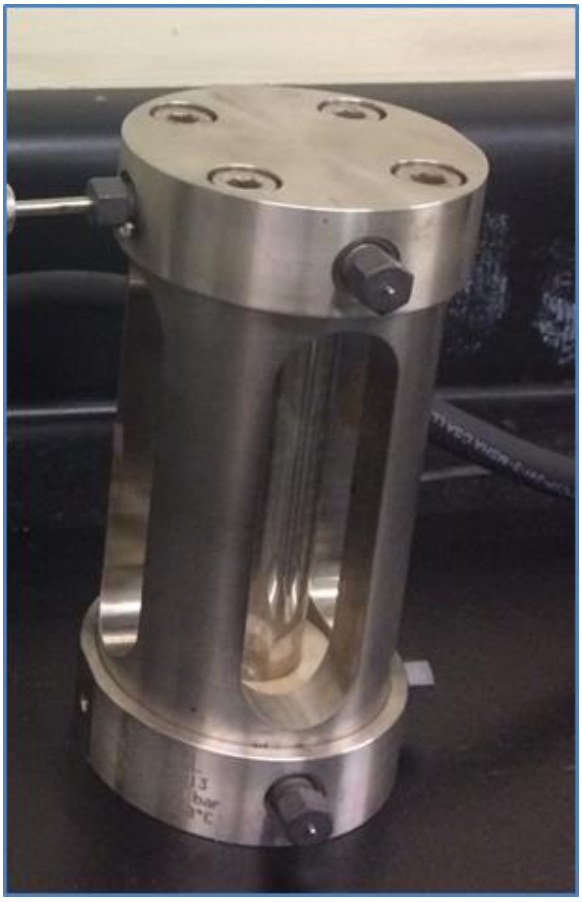

Figure 8.2: Visual cell with inlet tubing and high pressure sapphire chamber

Most of the other accessories to the Foam Assembly are the same as those used to construct the Synthesis Assembly. Similarities include Quizix water pumps, Swagelok tubing, Cecomp pressure gauges, Autoclave Engineers valves, Swagelok fittings, and Swagelok quick connect systems. A schematic of the Foam Assembly is shown in Figure 8.3, and a completed look of the assembly is shown in Figure 8.4.

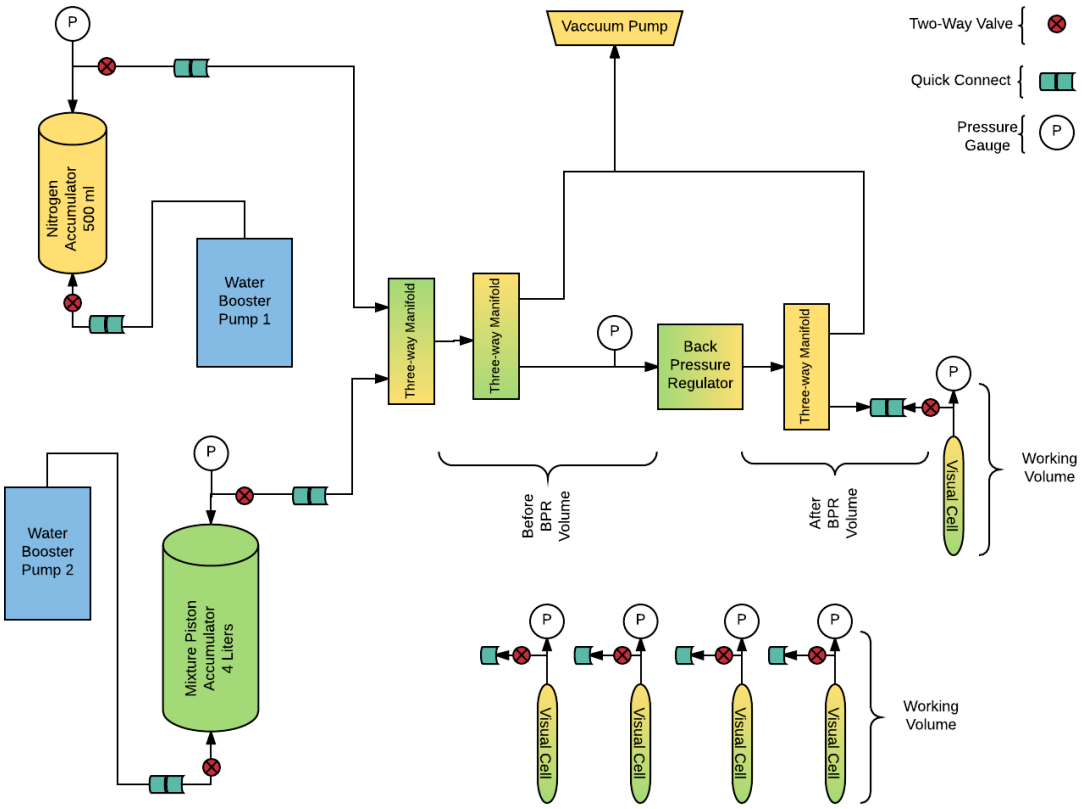

Figure 8.3: Foam Assembly schematic

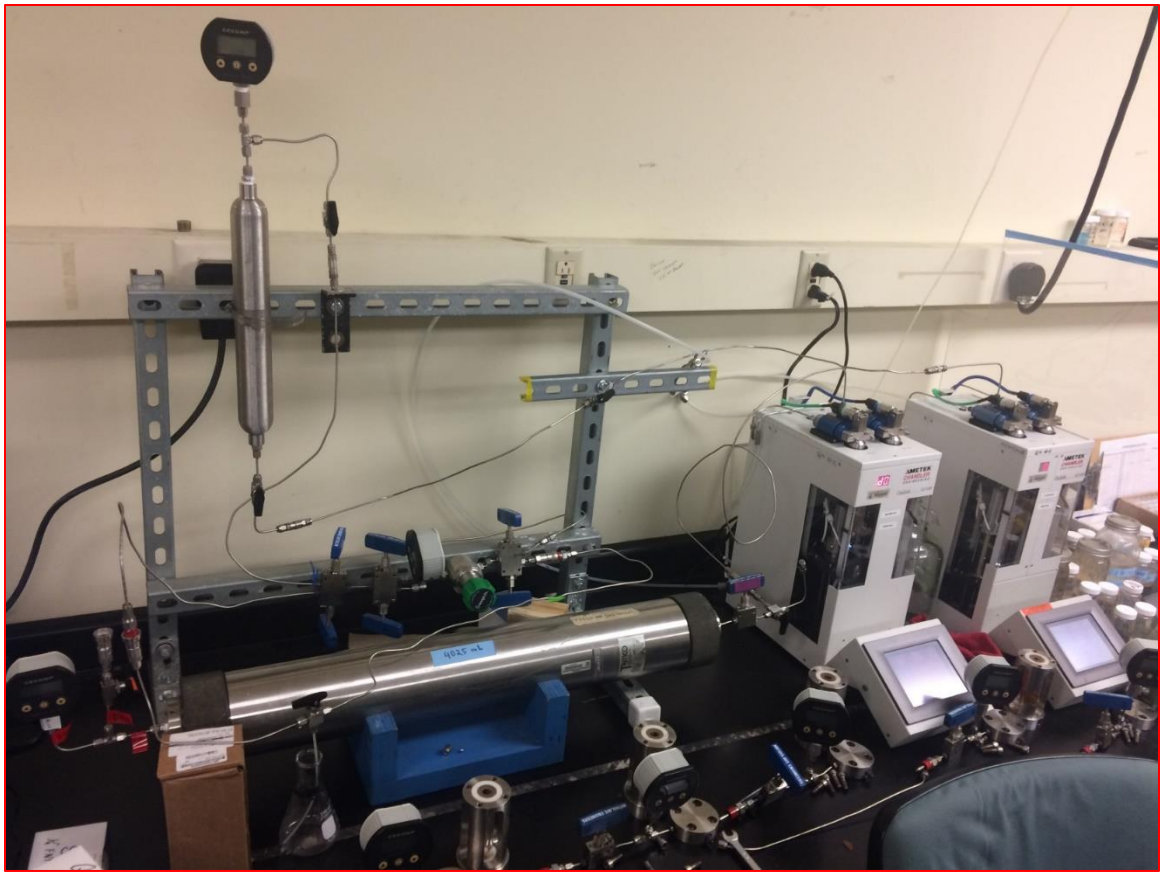

Figure 8.4: Foam Assembly set up

8.2 PROCEDURE

Previous phase behavior modelling for the y-grade was used to determine an operating pressure for this system. Since the y-grade is composed of multiple components with different critical pressures and temperatures, a pressure that would yield half the visual cell containing liquid y-grade, and half the visual cell containing gaseous y-grade was selected for the visual cells. The foaming abilities of y-grade with the lighter components comprising the internal gas phase, and the heavier components forming the liquid phase was explored. The operating pressure was kept the same, but DI water and pure nitrogen could be added if less y-grade was injected under the same conditions. While the ultimate goal pressure for the visual cells was 112 psig to allow the proper ratio of gas to liquid, the operating pressure of everything upstream of the BPR was 200 psig

to allow the y-grade to remain as a single phase in this area. The MPA is decreased from the 650 psig used in the Synthesis Assembly to 200 psig by allowing the attached water pump to withdraw a small amount of water.

The procedure to fill a visual cell with y-grade and nitrogen starts with adding any secondary component and additive to the visual cell prior to it being attached to the set up. The top of the cell is screwed off and the desired amount of additive and secondary component is added to the cell. The top is then tightened down and the cell is attached via quick connect to the rest of the Foam Assembly. All valves are opened except those leading directly to the y-grade and nitrogen accumulators and the system is vacuumed until the gauges read a constant -14.0 psig.

Once vacuuming is complete, the vacuum lines are closed and the BPR pressure is increased. There is no pressure indicator on the BPR, so it is initially set at a high pressure and slowly decreased to 200 psig. Opening the y-grade side of the three-way manifold allows the y-grade to flow up the BPR and the pressure gauge can then be used to manually adjust the upstream pressure down to 200 psig. The water pump pushing the y-grade out of the MPA was set at 1 ml/min to push the calculated volume of y-grade out through the BPR and into the downstream side of the assembly. If no nitrogen is being added, the calculated volume should yield a 50/50 gas to liquid ratio within the visual cell at 112 psig.

Once the proper amount of y-grade was pushed through the BPR, the y-grade water pump was turned off and the three-way manifold for the y-grade was closed. The manifold for the nitrogen is then opened and the water pump pushing the nitrogen is set to 1 ml/min. This nitrogen pushed the y-grade in the upstream line into the visual cell and then added nitrogen gas to the cell until 112 psig was hit. The nitrogen water pump is turned off, all valves are close, the vacuum line is open to depressurize the isolated quick connect holding the visual cell in place, and the visual cell is ready to be removed and replaced by a fresh cell. Once removed, the cell was gently shaken to see the foaming potential of the y-grade and whatever other compounds were present.

8.3 RESULTS

The visual cell experiments were all performed with Additive 1 and some combination of solvents including just y-grade, y-grade and nitrogen, and y-grade with nitrogen and DI water. Since the visual cell experiments were run either before or concurrently to the additive and secondary component screenings, the additives with the highest foaming potential were not used with the y-grade. Each of the three cases were at the same pressure of 112 psig, but since the composition of what was in the visual cell changed, each showed a different gas to liquid ratio with some disparity between what was anticipated and what the experiment actually showed. All three visual cells were filled with an early synthesis of y-grade showing roughly 5% error between theoretical and experimental volume produced.

The first visual cell contained only y-grade and 4 drops of Additive 1. This was mainly a test to see if the Foam Assembly could move the y-grade accurately into the visual cell and as a check to make sure the composition of the created y-grade was roughly accurate. If the y-grade synthesis was not successful, a ratio other than 50/50 gas to liquid would be observed. What resulted was a 55/45 ratio of gas to liquid which suggests that either the calculations to predict the ratio were slightly off, or the y-grade created in this batch was slightly lighter than ideal. While the ratio was not exactly as anticipated, the experiment was successful enough to add nitrogen to the next test. Visual Cell 1 is shown in Figure 8.3.

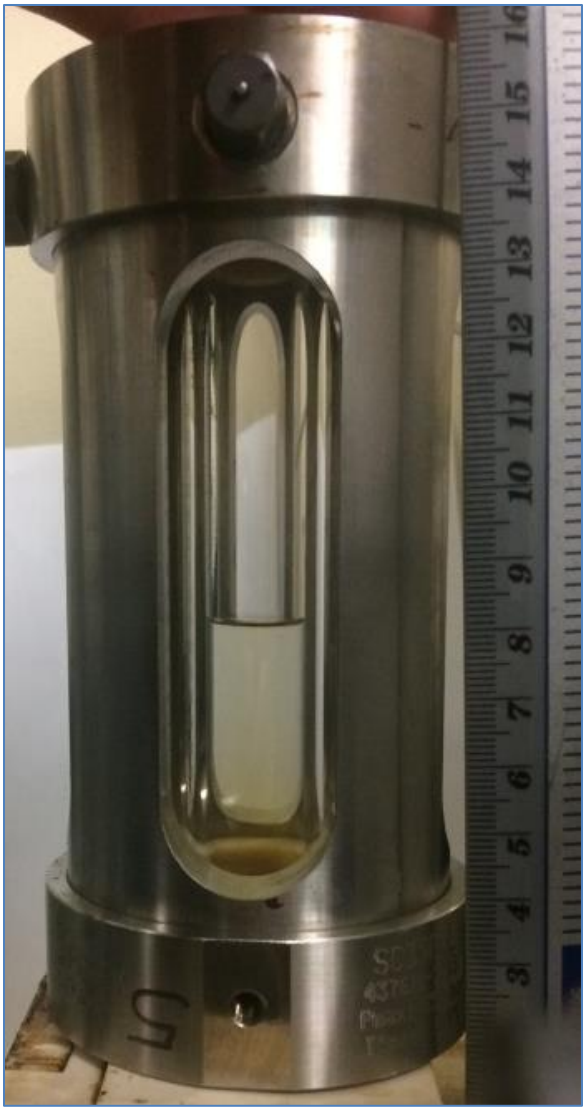

Figure 8.5: Visual Cell 1 with 4 drops of Additive 1 and y-grade

The second visual cell experiment contained the same amount of Additive 1, but nitrogen was added to the cell in addition to the y-grade. As a result, there was less y-grade by mass within the cell, and the expected gas to liquid ratio was closer to 60/40 since the nitrogen added was more volatile. However, the gas to liquid ratio was again different then expect, but in the opposite direction. Instead of there being more gas than liquid like in the previous test, there was more liquid leading to a 50/50 gas to liquid

ratio. This finding does not support the belief that there was something incorrect with the y-grade synthesis, but rather there may be some flaw to the calculations or Foam Assembly procedure. The cell was removed from the Foam Assembly and was lightly shaken. No foam or even bubbles were observed. Visual Cell 1 is shown in Figure 8.3.

Figure 8.6: Visual Cell 2 with 4 drops of Additive 1 and y-grade

The third visual cell experiment included 1.4 ml of water to the take up 10% of the visual cell volume with the additive before y-grade or nitrogen were added. The calculations treated the water as simply decreasing the volume of the cell, and the resulting calculations predicted a 54/46 gas to liquid ratio. Like in Visual Cell 2, a 50/50

split was actually observed. A clear separation of y-grade and water was seen within the cell, but is not visible within the picture, Figure 8.5

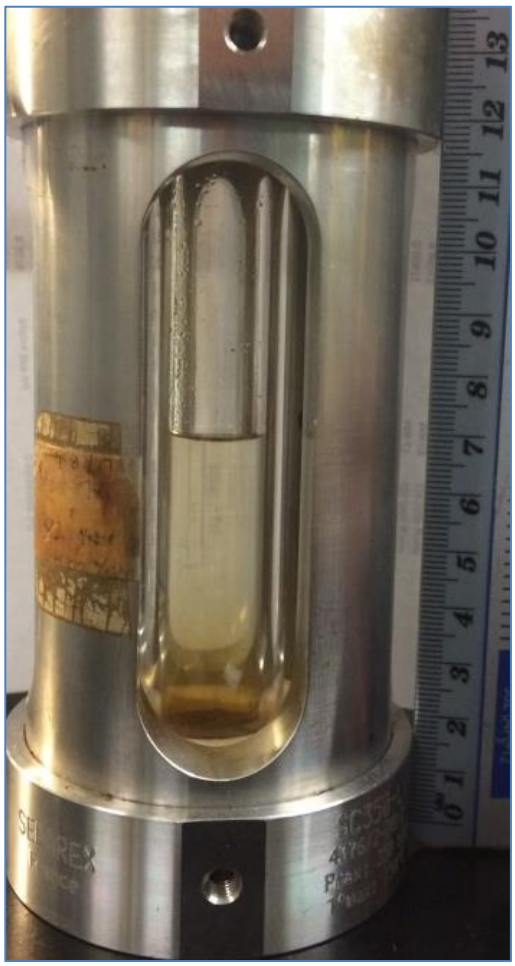

Figure 8.7: Visual Cell 3 with 4 drops of Additive 1 and y-grade, nitrogen, and DI water

Visual Cell 3 was removed from the Foam Assembly and shaken for 30 seconds. Towards the end of shaking, an emulsion gel very similar to that observed with pentane, water, and Additive 1 in the screening developed. This gel did not support a stable foam, but several trapped bubbles were observed indicating that it may be viscous enough to support foam if more shear was available. The visual cells were limited in how

vigorously they could be shaken do to safety concerns. Visual Cell 3 after 30 seconds of shaking is shown in Figure 8.6.

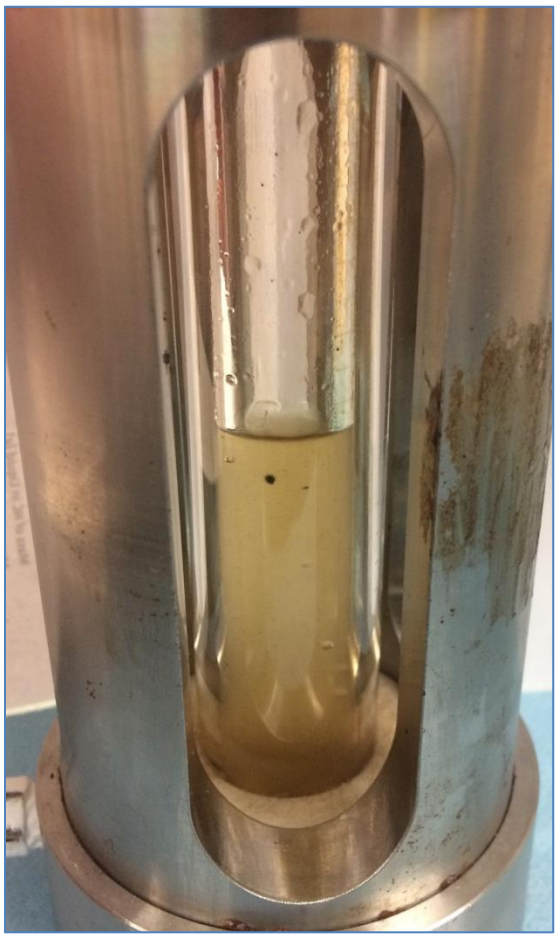

Figure 8.8: Visual Cell 3 after 30 seconds of light shaking

The simulated masses of each compound that went into the three visual cells as well as the gas to liquid ratios anticipated and observed are shown in Table 8.1. The simulation masses were used to determine the volume of each component to add through water injection.

Table 8.1: Theoretical masses added and gas/liquid ratio with actual gas/liquid ratio

	Visual Cell 1	Visual Cell 2	Visual Cell 3
Simulation Mass Y-Grade [g]	4.185	3.396	3.056
Simulation Mass Nitrogen [g]	0	0.119	0.107
Simulation Mass Water [g]	0	0	1.415
Simulation Gas/Liquid Vol.	50/50	60/40	54/46
Actual Gas/Liquid Vol.	55/45	50/50	50/50

8.4 CONCLUSIONS

The Foam Assembly works well to combine the synthetic y-grade with other component for testing purposes even if the anticipated gas to liquid ratios are slightly off from those observed. Based on the results, it seems most likely that this deviation is due to calculation error or user error in operating the set up rather than having an inherently incorrect y-grade blend.

In line with what was observed with Additive 1 and pentane in the screening tests, y-grade by itself and with nitrogen showed no response to the presence of the surfactant. However, when water was added, the same viscous, emulsion-based gel is seen that may lead to positive foaming results if the proper ratio of water, nitrogen, and y-grade is found.

Chapter 9: Y-Grade Coreflood

All the experiments up to this point have been investigations into how to create y-grade based bulk foam. Preforming a coreflood with the knowledge gained from previous work moves the focus to foam within a porous media. Thus, the Coreflood Assembly was created to test the assumptions about non-aqueous and semi-aqueous foam.

The purpose of the coreflood presented here and future corefloods was and will be to evaluate the performance of the y-grade foam on oil recovery under dynamic injection conditions. The coreflood presented here is a base case with only y-grade being injected into an oil-saturated core to evaluate its recovery potential without gas, secondary components, or foaming additive. Oil recovery and pressure drop measurements were the metrics to assess y-grade's performance of the coreflood.

9.1 MATERIALS

The focal point for the coreflood was the core holder. The core holder was placed in an oven to vary the temperature as needed while the rest of the Coreflood Assembly resided outside of the oven on a work bench. The coreholder was placed vertically within the oven to allow either a top-down or a bottom-up injection scheme depending upon the density of the injected fluid relative to the displaced fluid. Having the coreholder vertical and injecting correctly reduced gravity effects within the system and allows for a more piston-like displacement. The core, itself, was obtained by cutting a slab of Indiana Limestone into a 1.5-inch diameter, 12-inch long cylinder.

Outside of the oven, two Quizix water pumps were utilized to inject fluids into the core. The first water pump was used strictly for the y-grade while the second water pump could inject either brine or crude oil contained within two 500 ml piston accumulators made by the department's machine shop in house. These three components combined at a four-way join and then flowed into a three-way manifold. The manifold acted also as the connection for the vacuum line on either side of the coreholder.

The coreholder connected to three differential transducers at various points across the core and two absolute transducers at the inlet and outlet. This information was sent to a lab computer for tracking pressure through time. The coreholder was also connected to a hand hydraulic pump which was used to maintain confining pressure on the core and prevent fluid flow along the boundary of the core.

On the outlet of the coreholder was another three-way manifold sending the effluent to either a vacuum line or to a series of Mity Mite BPRs, supplied by Equilbar, LLC, to slowly step down the pressure of the fluid produced from the core. Passed the regulators, the produced fluid either travelled up into a line leading the gases to the fume hood or be sent downward bringing the liquids into a fraction collector to see how the produced composition changed through the injection. A schematic of the Coreflood Assembly is shown in Figure 9.1.

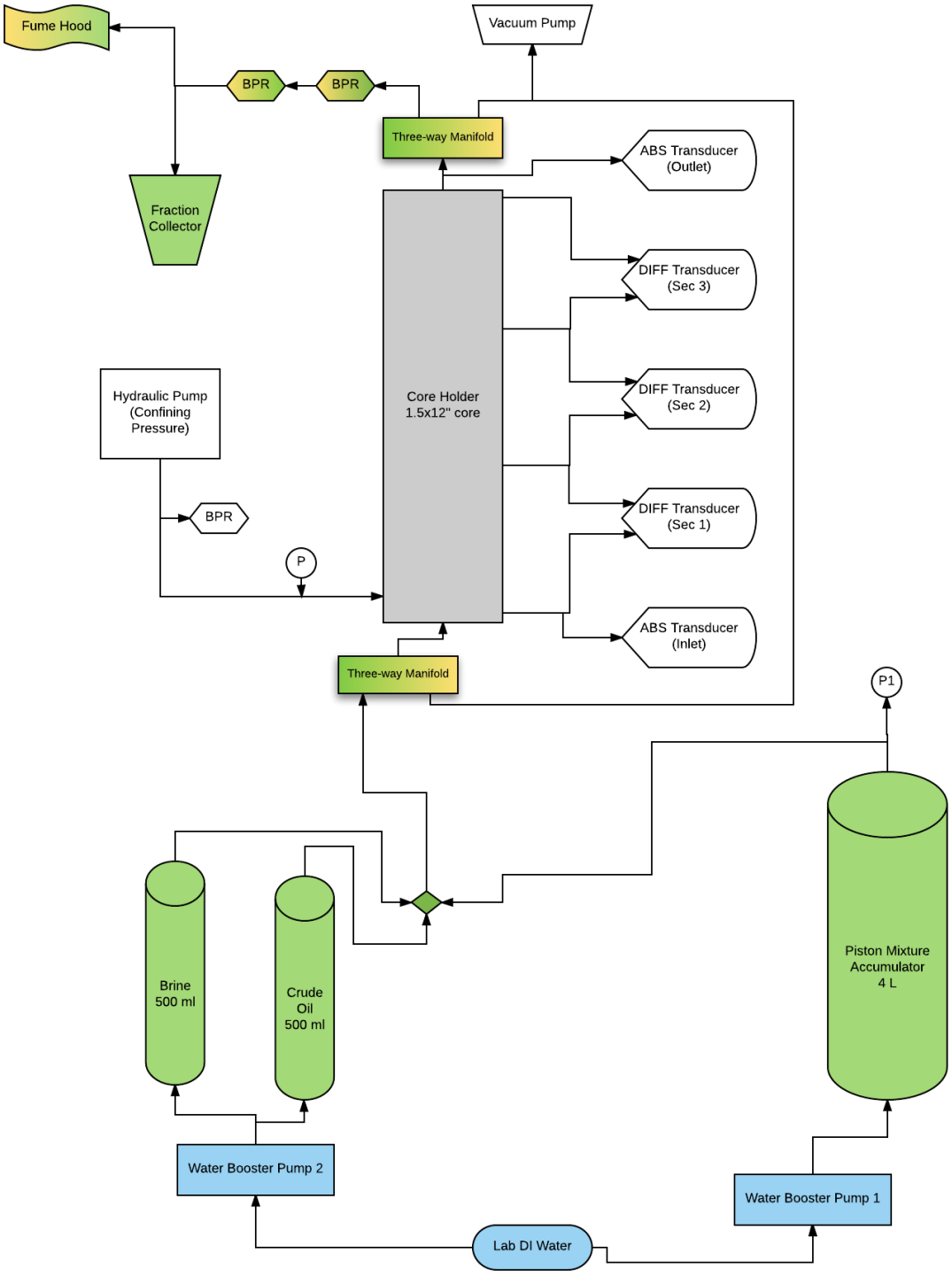

Figure 9.1: Coreflood Assembly schematic

9.2 PROCEDURE

The core sample needed to be prepped before being loaded into the coreholder. The sample was wrapped with Teflon to reduce flow around the core perimeter, two end pieces were affixed to the core. The core was then covered with 2 inch diameter shrinking tubing to protect the rubber sleeves within the coreholder since the rough surface of the core may cause damage. Two holes were drilled on the core at the location of pressure taps within the coreholder to allow communication with the pressure transducers.

The oven was kept at a constant 30° C to match reservoir conditions provided by the sponsoring company and the entire Coreflood Assembly was vacuumed for several hours. Carbon dioxide (CO_2) was then injected through the upstream vacuum line to displace any of the remaining air, and the system is again vacuumed for several hours to remove the CO_2.

After vacuuming, the core was completely saturated with brine made in house to the specifications of the brine found within the reservoir. Based upon the observed pressure drop across the core and flow rate, porosity and absolute permeability were determined using mass balance and Darcy's Law.

Brine injection was followed by injecting heated crude oil at the highest possible rate while keeping injection pressure below 100 psig. Mass balance was then used to calculate the residual water saturation, initial oil saturation, and relative permeability of oil at residual water saturation.

Previous analysis of the crude oil sample showed that it had an API gravity of 37.96 and average molecular weight of 211 g/mol. The oil sample was proven to be comprised of 63.9% of saturates, 28.0% of aromatics, and 8.1% of resins and asphaltenes by mass by SARA analysis outside the scope of this project.

The oil injection was followed by a second brine injection of the same salinity used previously until the water cut produced was 100%. This water cut indicated the core sample was at its residual oil saturation and ready for the y-grade injection to determine the recovery potential of the blend without gas or additive.

The y-grade was injected from top to bottom. Since the crude oil and water in place is denser than the injected fluid, a clean, piston-like displacement is created provided the difference between injected and displaced viscosities is not too large. The experimental properties of the brine, core, and injection scheme are shown in Table 9.1.

Table 9.1: Experimental properties

Rock Type	Indiana Limestone
Length	12 inches
Diameter	1.5 inches
Absolute Permeability	27.3 mD
Porosity	24%
Temperature	29 C
Back pressure	850 psi
Waterflood Inj. Rate	0.5 ft/day
Y-Grade Inj. Rate	0.5 ft/day
Brine Salinity	~4178 ppm
Waterflood Salinity	~4178 ppm

9.3 RESULTS AND DISCUSSION

Based upon the results of the second brine flood, the initial oil saturation was calculated to be around 58%. A relatively fast oil production response was observed with 61% ultimate oil recovery reached after 1.46 pore volumes of y-grade were injected. After this injection period, the oil recovery flattens out and the lack of mobility control with the injection scheme becomes evident in Figure 9.2. Residual oil saturation after the y-grade flood was determined to be 34%. The pressure profiles of the second brine injection and y-grade injection are shown in Figure 9.3 and show y-grades miscibility and lack of mobility control due to the low pressure drop through time.

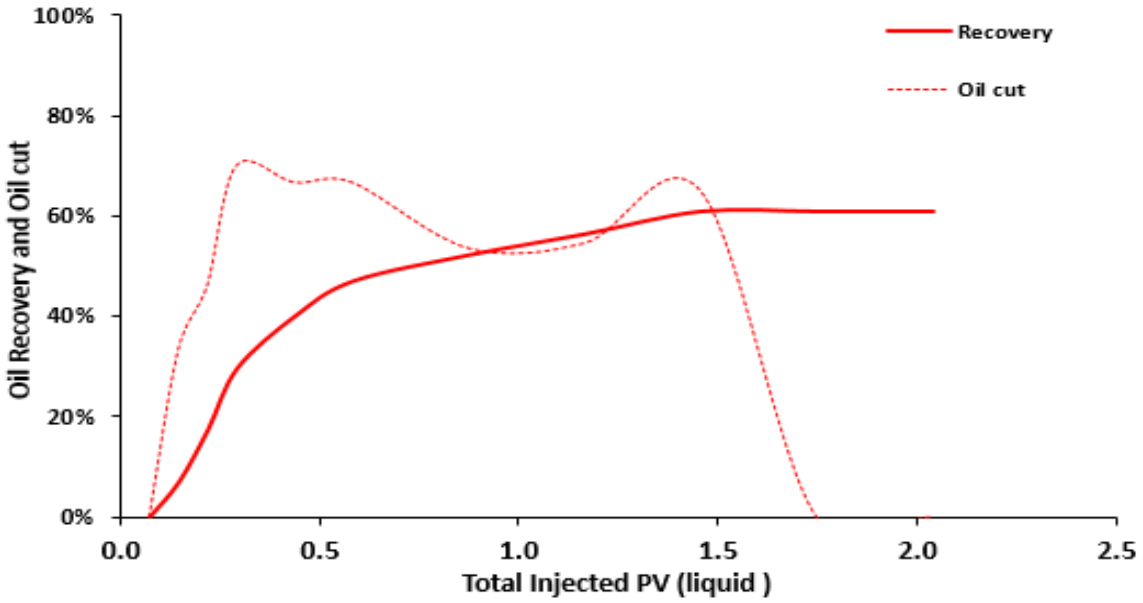

Figure 9.2: Tertiary recovery profile through y-grade injection

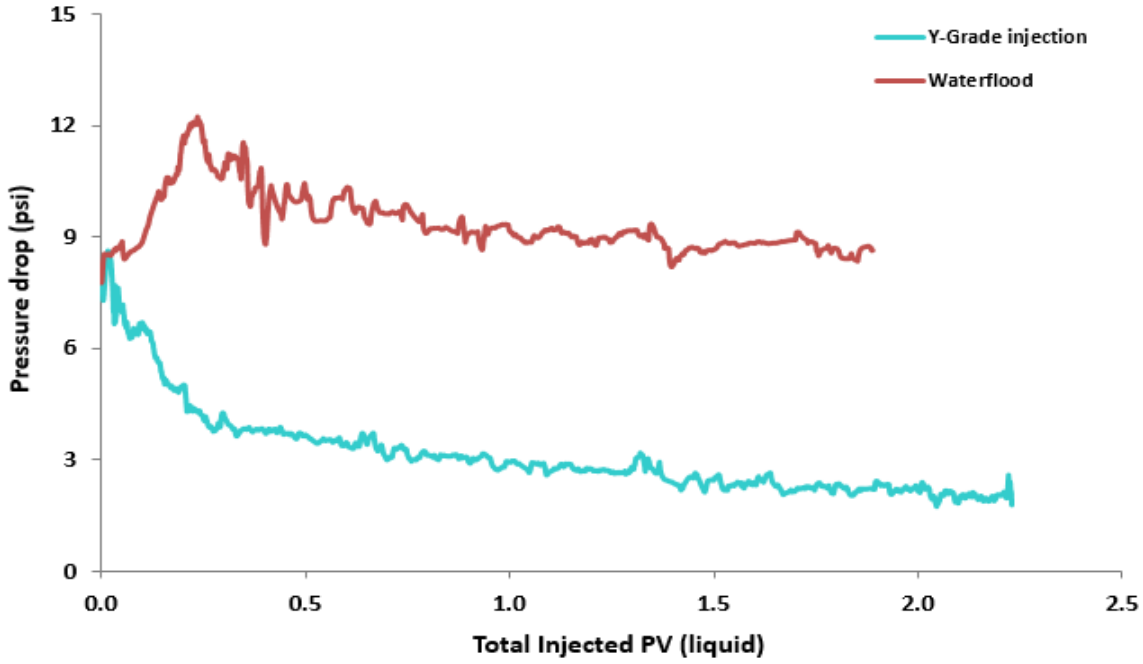

Figure 9.3: Pressure drop profile over y-grade injection

9.4 FUTURE COREFLOODS

As mentioned previously, this coreflood was only the first in a series designed to see how foamed y-grade effects the ultimate recovery in a coreflood. Y-grade was shown to be very miscible with the crude oil in place as expected, but the y-grade injection suffered from a lack of mobility control that did not hinder the flow of y-grade through the core.

The next two planned corefloods would follow the set up and procedure presented here, but with some additions. The first planned coreflood would see the y-grade be either coinjected or chased by a nitrogen drive to increase mobility control. The nitrogen would serve to decrease the relative permeability of the y-grade by taking up pore space.

The second planned coreflood would utilize the results from the additive and secondary component screenings. It has been shown that crude oil works very well as a secondary component to support non-aqueous foam with Additive 36. If the additive could be introduced during the injection within the y-grade or nitrogen phase, foam might be easily produced and stabilized by the crude oil already in place. The non-aqueous foam would act as a very strong mobility control agent and recovery factor is predicted to increase beyond that of a pure nitrogen drive or coinjection with y-grade.

Chapter 10: Conclusions and Recommendations

10.1 Conclusions

The purpose of this project was to investigate the potential use of y-grade-based foam in EOR processes. Initial screenings with pentane acting as a stand in for y-grade concluded that it was very unlikely that y-grade would be able to generate a stable foam with the available additives. These screenings also indicated that the presence of water and nonionic surfactants with long ethylene oxide chains created a strong emulsion-based foam, and the foaming potential of diesel fuel was greatly increased by several fluorosurfactants and one siloxane surfactant.

These six select additives were investigated further with a variety of polar and non-polar carbon-based solvents. Tests were done without pentane to understand the underlying foaming mechanisms and then with a volumetric fraction of pentane to see if the additional solvents could act as a secondary component to allow foam generation and stabilization. The tests showed that physical properties such as viscosity as well as chemical properties and polarity heavily influenced the foaming potential of the potential secondary components. Another large take away was that secondary components would help to create either non-aqueous or semi-aqueous foam still based around y-grade as the primary component.

Y-grade was proven to be able to be synthesized within a laboratory environment with an acceptable amount of experimental error. In addition, methods were demonstrated that combined the y-grade with nitrogen, secondary components, and additives in order to test the foaming potential of true y-grade systems. The same emulsion observed within pentane and water samples was also noticed with y-grade and water with the same additive. This observation supports the use of pentane as a y-grade substitute for large scale screening rather than creating a pressurized visual cell for each test.

Finally, a coreflood involving just y-grade as the displacing fluid showed decent recovery results but suffered from poor mobility control stemming from the fact that the

y-grade is very miscible with the oil in place. Future corefloods will hopefully show that adding nitrogen as a coinjection or as a drive will increase recovery, and adding a fluorosurfactants such as Additive 36 will increase recovery even more do to the better mobility control provided by the resulting foam.

10.2 RECOMMENDATIONS

- Effort should be made to expand the screening of both additives and secondary components. There remains a lot of work to be done with heavier aromatics and nanoparticles.
- Apparent viscosity for the foam outside of a coreflood would be beneficial to the project. Techniques laid out by Hirasaki (1985) can be used to calculate apparent viscosity for a foam within a capillary tube.
- Additional corefloods involving injected octanol with Additive 34 and light mineral oil with Additive 36 should be considered after just crude oil

References

Al-Anazi, B. D. (2007). Enhanced Oil Recovery Techniques and Nitrogen Injection. Recorder,32(8), 28-33.

Bergeron V., Hanssen J.E., & Shoghl F.N. (1997) Thin-film forces in hydrocarbon foam films and their application togas-blocking foams in enhanced oil recovery, Colloids and Surfaces A: Physicochemical and Engineering Aspects 123-124, 609-622.

Binks, B. P., Rocher, A., & Kirkland, M. (2011). Oil Foams Stabilized Solely By Particles. Soft Matter,7, 1800-1808.

Callaghan I.C., McKechnie A.L., & Ray J.E., Wainwright J.C. (1985) Identification of crude oil components responsible for foaming, Society of Petroleum Engineers Journal 25, 2, 171-175.

Cooperman, P. (2013). Opportunities and Pitfalls of Y-Grade. Oil & Gas Financial Journal,10(12).

Glaso, O. (1990, February 1). Miscible Displacement: Recovery Tests With Nitrogen. Society of Petroleum Engineers.

Gupta, D. V. S. (2003, January 1). Field Application of Unconventional Foam Technology: Extension of Liquid CO2 Technology. Society of Petroleum Engineers.

Heucke, U. (2015, September 14). Nitrogen Injection as IOR/EOR Solution For North African Oil Fields. Society of Petroleum Engineers.

Hirasaki, G. J., & Lawson, J. B. (1985, April 1). Mechanisms of Foam Flow in Porous Media: Apparent Viscosity in Smooth Capillaries. Society of Petroleum Engineers.

Egbogah, E. O. (1985, January 1). Research Into Enhanced Oil Recovery Technologies. Petroleum Society of Canada.

Koczo, K., Tselnik, O., & Falk, B. (2011, January 1). Silicon-Based Foamants For Foam Assisted Lift Of Aqueous-Hydrocarbon Mixtures. Society of Petroleum Engineers.

Lake, L. W., Johns, R. T., Rossen, W. R., & Pope, G. A. (2014). Fundamentals of Enhanced Oil Recovery. Richardson, TX: Society of Petroleum Engineers.

Murakami, R., & Bismarck, A. (2010). Particle-Stabilized Materials: Dry Oils and (Polymerized) Non-Aqueous Foams. Advanced Functional Materials, 20, 732-737.

Nasr-El-Din, H. A., & Al-Ghamdi, A. M. (1996, January 1). Effect of Acids and Stimulation Additives on the Cloud Point of Nonionic Surfactants. Society of Petroleum Engineers.

Owen M.J., Kendrick T.C., Kingston B.M., & Lloyd N.C. (1968). The Surface Chemistry of Polyurethane Foam Formation, Journal of Colloid and Interface Science, Volume 24, Issue 2, Pages 141-150

Sam Sarem, A. M. (1992). Waterflooding: Part 10. Reservoir Engineering Methods. In ME 10: Development Geology Reference Manual (pp. 523-526). Brea, CA: Unocal Science and Technology.

Schramm, L. L. (Ed.). (1994). Foams: Fundamentals and Applications in the Petroleum Industry(Vol. 242, Advances in Chemistry). American Chemical Society.

Shrestha, R. G., Shrestha, L. K., Solans, C., Gonzalez, C., & Aramaki, K. (2010). Nonaqueous Foam With Outstanding Stability in Diglycerol Monomyristate/Olive Oil System. Colloids and Surfaces A: Physicochemical and Engineering Aspects, 353, 157-165.

Slack, W. W., & Ehrlich, R. (1981, January 1). Immiscible Displacement Of Oil By Simultaneous Injection Of Water And Nitrogen. Society of Petroleum Engineers.

Zaki N.N., Poindexter M.K., & Kilpatrick P.K. (2002) Factors contributing to petroleum foaming. 2. Synthetic crude oil systems, Energy and Fuels 16, 711-717.

This thesis was typed by the author, Calvin M. Eberle.